Republic of Iraq

Ministry of Higher Education

and Scientific Research

University of Babylon

College of Engineering Mechanical

Engineering Department

Effect of Discrete and Alternative Heat Flux on Natural Convection in Annular Flow

A Thesis

Submitted to the College of Engineering University of Babylon in Partial Fulfillment of Requirements for the Degree of Master of Science in Mechanical Engineering/Power

By

Abrar Abdulkareem Saeed

Alhadad

(B.Sc., 2019)

Supervised By

Assist.Prof . Dr. Hussein Mahmood Jassim

2024A.D 1445A.H

بِسْمِ اللَّهِ الرَّحْمَنِ الرَّحِيمِ

يَرْفَعِ اللَّهُ الَّذِينَ آمَنُوا مِنْكُمْ وَالَّذِينَ أُوتُوا الْعِلْمَ دَرَجَاتٍ وَاللَّهُ بِمَا تَعْمَلُونَ خَبِيرٌ ﴿١١﴾

صدق الله العلي العظيم

سورة المجادلة (11)

DEDICATION

I dedicate this achievement to my father and my mother, who with love and support have accompanied me during my journey, without hesitating at any moment of seeing my dreams come true.

Supervisor's Certificate

I certify that this thesis entitled **"Effect of Discreet and Alternative Heat Flux on Natural Convection in Annular Flow"** was prepared by **Abrar Abdulkareem Saeed** under my supervision at the Mechanical Engineering Department, University of Babylon – Iraq, as a partial fulfillment of the requirements for the degree of Master of Science in Mechanical Engineering / Power.

Signature

Asst .Prof. Dr. Hussein Mahmood Jassim

(Supervisor)

/ / 2024

Examining Committee Certificate

We certify that we have read the thesis entitled "**Effect of Discreet and Alternative Heat Flux on Natural Convection in Annular Flow** " and as examining committee, examined the student **Abrar Abdulkareem Saeed** in its contents, and that in our opinion, it meets the standard of a thesis for the degree of Master in Engineering/ Mechanical Engineering/Power.

Signature:

Name: **Prof**

Dr. Hafidh H. Mohammed

(Chairman)

Date: / / 2024

Signature:

Name: **Asst. Prof**

Dr. Rafel Hekmet Hameed

(Member)

Date: / / 2024

Signature:

Name: **Asst. Prof**

Dr. Rehab Noor Al-kaby

(Member)

Date: / / 2024

Signature:

Name: **Asst. Prof**

Dr. Hussein Mahmood Jassim

(Supervisor)

Date: / / 2024

Approval of Head of Department

Signature:

Name: Asst. Prof Dr. Rehab Noor Al-kaby

Date: / / 2024

Approval of the Dean of College

Signature:

Name: Prof Dr. Laith Ali Abdul Rahaim

Date: / / 2024

Acknoledqments

First and foremost praise is to Allah, the Almighty, my creator, my strong pillar, and my source of inspiration, wisdom, knowledge, and understanding. He has been the source of my strength throughout this journey for giving me the opportunity, determination, ability, and strength to do my research and achieving my dream of obtaining a master's degree in mechanical engineering

I would like to express my deepest thanks and appreciation to my Supervisor **Assis. Prof. Dr. Hussein M. Jassim**, for his help, patience and support during the research period, The invaluable recommendations, unfailing and constructive comments, which greatly improved the structure and presentation of this thesis. It was a great privilege and honor to work and study under his guidance.

I would also extend my thanks and appreciation to all of my teachers in the department of Mechanical Engineering for their support and help, especially **Assis. Prof. Dr. Hameed K. Hamza** and **Assis. Prof. Dr. Rehab Noor**.

, I owe special thanks to **my father and mother** for their help understanding, and encouragement during the study period.

I am also thankful to everyone who helped me directly or indirectly to complete this work.

Abrar Abdulkareem Saeed

Abstract

A numerical and experimental investigations were done to study the convective thermal transmission through a vertical two concentric cylinders as well as to investigate the effect of the location and length of the heat source. Air (pr = 0.71) was chosen as a working fluid. The flow was two dimensional, steady, and laminar. The computational results were estimated using COMSOL 6.0 Multiphysics software package represented by isothermal lines circulation as well as velocity distribution. All the equations were inserted and parameters were substituted to estimate the computational results. Finite Element Method (FEM), Crank- Nicolson scheme was utilized to solve the differential equations. The considered values of Rayliegh number ($10^3 \leq Ra \leq 10^7$) and aspect ratio (Ar = 25.6).On the other hand, the same physical model was experimentally built in the fluid laboratory at university of Babylon. Both inner and outer cylinders are made of solid copper (thermal conductivity k=385 W/m.K) , the outer cylinder is 105 cm long, outer diameter of 76 mm and a wall thickness of 3.65 mm , while the inner cylinder is 160 cm long , outer diameter is 35 mm and a wall thickness of 2 mm . Heaters were attached to the external wall of the outer cylinder and the number of heaters was changed in three different cases. In case (I), five heaters with different lengths were used and in case (II), four heaters at the same length are used. In case (III) three heaters at different lengths are used. The resulting thermal flux from these sources was estimated. Furthermore, an insulating material was used to minimize the thermal losses. A control panel was constructed and connected to the heaters to control the operating process and to check and read the drawn voltage and current. A set of twenty thermocouples was attached in the annulus to measure the changes in temperature during the test time. Also a digital manometer was used to

measure the pressure readings during the experiments. The numerical results were presented in the form of the streamline and isotherms contours together with the local Nusselt number. Results showed that increasing the length of the heat source will increase the local Nusslet number and enhances the circulation of the flow. Furthermore, increasing the number of the heat sources will improve the overall heat transfer rate. Consequently, the highest thermal transmission rate was achieved in case(I) which includes the highest number of heat sources(five heaters) . Finally, the theoretical results were compared with the experimental ones to check the correspondence, case(I) achieved (82%), case(II) achieved (78%), and case (III) achieved (76%) .

Table of Contents

Terminology		
Symbol	**Description**	**Units**
A	Area	m^2
Ar	Aspect ratio	……
d	Dimensionless length of the heat source	……
g	Gravitational acceleration	$m.s^{-2}$
h	Convective heat transfer coefficient	$W/m^2.K$
k	Thermal conductivity	W/m .K
L	Length of the geometry	M
Nu_{avg}	Average Nusselt number	……
p	Pressure	$N.m^{-2}$
P	Dimensionless pressure	……..
Pr	Prandtl number	……
q	Heat flux	W/m^2
Ra	Rayliegh number , Ra = $\frac{g\beta\,(Th-Tc)\,L^3\,Pr}{v^2}$	……..
Gr	Grashouf number , Gr = $\frac{g\beta\,(Th-Tc)\,L^3}{v^2}$	……..
T	Dimensional temperature	K
U ,V	Non-Dimensional velocity components in (X,Y) directions, respectively	……
u ,v	Velocity component in (x ,y) – direction , respectively	m / s
W	Width of the geometry	
X	Non-dimensional coordinate in horizontal direction(x/l)	……
x	Cartesian coordinate in the horizontal direction	
Y	Non-dimensional coordinate in vertical direction(y/ l)	……
C_p	Specific heat	J/kg.ºC

Greek symbols		
Symbol	**Description**	**Units**
$\boldsymbol{\alpha}$	Thermal diffusivity, $\alpha=\frac{k}{\rho C_p}$	m^2/s
β	Thermal expansion coefficient	K^{-1}
μ	Dynamic viscosity	kg/m.s
ν	Kinematic viscosity	m^2/s
ρ	Fluid density	Kg/m^3
Ψ	Dimensionless stream function	------
ψ	Stream function	m^2/s
Θ	Dimensionless temperature distribution ($\Theta=\frac{T-T_c}{T_h-T_c}$)	--------

Subscripts	
avg	Average
calib	Calibrated
c	Cold
f	Fluid
h	hot
i	In
loc	Local
max	Maximum
min	Minimum
0	Out
re	Reading

ABBREVIATIONS	
Abbreviation	***Description***
BCs	Boundary conditions
CFD	Computational Fluid Dynamics
FDM	Finite Difference Method
FEM	Finite Element Method
FVM	Finite Volume Method
CHF	Constant heat flux
CWT	Constant wall temperature
KBS	Keller box scheme
PDE	Partial differential equations
SST	Series solution technique
TBC	Thermal boundary condition
TBL	Thermal boundary layer
FDA	Finite difference analysis

Chapter One

Introduction

Introduction

1.1General

Convection heat transfer deals with thermal interaction between a surface and an adjacent moving fluid, for example the flow of fluid over a cylinder. **[1].** In particular, free convection in an annulus that is resulting from the union of two concentric cylinders has been an important subject to study according to its wide applications in lots of fields. In the last few decades, different geometrical shapes has been studied to investigate the effect of the geometry and its dimensions on the process of free convective thermal transmission in the annulus region.**[2].** Almost every discipline of engineering encounters heat transfer in annular flow which necessitate study based on heat transfer principles.

1.2 Natural Convection(Free Convection)

Natural convection currents are generated within the fluid that urges it to flow as a result of the effects of the buoyancy force or what is called the flotation force. As this force results from the density gradient as a result of the presence of temperature difference and the gravity force**[3].**Natural convection fluid motion is generally imperceptible due to its low velocity, which is often less than 1 m/s. The amount of thermal exchange among a solid layer with a fluid per unit surface area per unit temperature difference is defined as the convective thermal transmission coefficient (h). Convection heat transfer coefficient is strongly related to speed, the greater the speed, the greater the convective thermal transmission coefficient**[4].** Free convective thermal transmission coefficients are substantially lower than forced convection heat transfer coefficients. It is worth noting that various kinds of thermal transmission supplies are constructed to function under free

convective rather than forced convective conditions, since free convection doesn't necessitate the employment of a fluid mover which makes it lower cost, as well as it is not noisy like forced convection**[5].**

1.3 Heat Transfer through Thermal Boundary Layer

The boundary layer is a thin layer of a flowing fluid in contact with a solid surface such as that of inside of a pipe**[6].** A velocity boundary layer develops when a fluid flows over a surface as a result of the fluid layer adjacent to the surface assuming the surface velocity (i.e., zero velocity relative to the surface). Also, we the velocity of the boundary layer can be defined as the region in which the fluid velocity varies from zero to 0.99V. Likewise, a thermal boundary layer develops when a fluid at a specified temperature flows over a surface that is at a different temperature, the fluid particles in the layer adjacent to the surface reach thermal equilibrium with the solid surface. These fluid particles then exchange energy with the particles in the adjoining-fluid layer, and so on. As a result, a temperature profile develops in the flow field that ranges from the solid surface temperature at the surface to the ambient temperature sufficiently far from the surface. The flow region over the surface in which the temperature variation in the direction normal to the surface is significant is the thermal boundary layer**[7].**

1.4 Applications of Free Convection in Annular Flow

The problem of the natural convection heat transfer in an annulus bounded by two vertical cylinders has received great attention due to its wide technological applications, such as ; removing thermal energy from auto electronic supplies like capacitors as well as computer chips, solar collectors, heat transfer in the tubing-casing annulus of oil Wells, removing excessive heat from nuclear reactors, design of heat exchangers, control of heating and ventilation in building design and thermal storage systems.**[8-11].**

1.5 View of the Present Work

- The aim of this work is to explore experimentally as well as computationally the natural convective heat transfer resultant from the discrete and alternative heat flux in an annulus generated from union of two vertical concentric cylinders.
- Furthermore, studying the impact of the location and the length of the heat source on the isothermal contours and regional Nu.
- The theoretical analysis was done using FEM (Crank–Nicolson).
- Theoretical results that presented in this work are obtained by COMSOL 6.0 Multiphysics software which solves the fluid circulation as well as thermal transmission problems by solving momentum, energy, and continuity equations subjected to laminar flow.In particular, temperature distribution, velocity profile, Rayleigh number, and overall heat transfer rate are obtained.
- In the experimental part, a physical model was built in the fluid laboratory at the university of Babylon, similar to the theoretical one.
- The results were attained experimentally and compared to the theoretical results to check the validity and applicability of the theoretical modeling.

Therefore, the aim of this work is to contribute in this field to improve the amount of transmitted thermal energy .

1.6 Outline of the Thesis

This thesis consists of six chapters, each chapter will be presented as follows:

- Chapter one: presents an introduction to the considered subject and the most important applications .

- Chapter two: is a literature review of the previous and most related studies.
- Chapter three: Shows the mathematical model, the governing equations , and the boundary conditions to analyze the temperature distribution in the annular flow .
- Chapter four: Displays the experimental apparatus and its auxiliaries, as well as shows the procedure of the experimental work.
- Chapter five: Shows the theoretical and experimental results .
- Chapter six: summarizes the conclusions and the suggestions for future work.

Chapter Two

Literature Review

Literature Review

2.1 Introduction

According to the variety of the applications of free convective thermal transmission in the annular flow, so many studies have been done on this subject to achieve more reliable results.

This chapter covers three aspects, the theoretical analysis, the experimental analysis, and both theoretical and experimental work.

2.2 Theoritical Studies

Silva et al.[12] studied The ideal placement of separate heaters cooled by laminar natural convection. When the overall thermal creation rate was established, the global goal was to optimize the overall conductance among the solid surface and the fluid, or to diminish T. The distances between thermal sources were not consistent and was varied. There were two situations studied: (i) a great number of little heaters added to a straight surface in front of a fluid reservoir, as well as (ii) a tiny number heaters embedded on the inner surface of a two-dimensional enclosure's side wall. The ideal distribution was demonstrated to be non-uniform (the heaters were not located at equal distances), and when the Rayleigh number increased, the heaters had no spacing. The ideal arrangement of the surface with separate heaters was developed in both (i) and (ii) by pursuing maximal global performance subject to global restrictions. The ratio of the heat source length was taken as H/L=1 and Pr=0.7. Results showed that the ideal distribution of heaters maximizes the inclusive performance. As well as ,the highest overall conductance increased as more heaters were embedded, however the average of the raise descended.

Al-Essa and **Al-Hussien [13]** investigated numerically the natural convection thermal removal from a horizontally installed rectangular fin. Square punctures in two directions were applied. The considered parameters in the investigation were the distancing as well as the directions of the puncture. A dimension specified fin with square puncture (b * b) was studied. To facilitate the study, the thermal circulation was hypothesized to be stable and 1-D thermal conduction with homogenous fin substance. The finite element technique was used to address the study's problem quantitatively. It was discovered that thermal removal increase from a fin with square puncture was greater than that from a fin with slanted square puncture. The results revealed that thicker fins caused more thermal transmission increase at any (b). It was also discovered that the inclined square puncture was favored for small fin thickness and heat conductivity, whereas the square puncture of equivalent kind was desirable for large k.

Dias Jr.and **Milanez [14]** studied numerically laminar natural convection in three-dimensional enclosures with a high aspect ratio. The enclosures were heated with a consistent thermal flux on one surface and chilled with a steady T on the other surface. The remaining walls were thought to be adiabatic. Except for the density variation with temperature on the buoyancy component, fluid characteristics were considered to be constant. FVM was employed to solve the PDE. The effects of the Ra and the aspect ratio on the Nusselt number were investigated for a Pr of 0.7. The results were estimated for modified Ra up to 10^6 and Aspect rati ranging from 1 to 20. Because the aspect ratio is a ratio of the enclosure's height and width, increasing it is comparable to decreasing the characteristic length (W), which leads in an increase in the dimensionless temperature and a drop in the average Nusselt number. A drop in W results in a decrease in the modified Rayleigh number.

Saha et al. [15] investigated numerically 2-D, laminar, incompressible and steady flow in a vee crimpy slanted enclosure. The two vertical vee-crimpy walls were kept at a fixed small temperature, while the heater with fixed thermal flux, with variable size, was directly inserted at the lower surface. The non-heated portions of the lower surface and the upper surface were considered adiabatic. The combined FEM was utilized to solve the governing equations with Grashouf $Gr=10^3,10^4,10^5,10^6$ with prandtle number of pr=0.71. Results revealed that at higher Grashouf $Gr=10^5,10^6$, when the intensity of convection increased significantly, there were small gradients in temperature at the central regime whereas a large stratification zone of temperature was observed at the vertical symmetry line due to stagnation of the flow.

Molla et al. [16] investigated in the presence of heat generation, free convective circulation through a horizontally assembled cylinder with a constant T_s. A non-dimensional formula was applied to transform the governing PDE . Two different numerical techniques were employed : (1) FDM in conjunction with the KBS, as well as (2) SST. τ_s in terms of C_f and the surface amount of thermal transmission in terms of regional Nu were calculated and shown in both tabular and graphical formats. The numerical findings demonstrated that for rising magnitudes Cf, the formula $Cf\ Gr^{1/4}$ raises while the formula $NuGr^{1/4}$ falls due to an increase in fluid temperature, even when the internal heat generation inside the non-solid field was set to 0. The influence of thermal creation increases the velocity and temperature distributions, as well as the thickness of the TBL.

Pullepu et al.[17] presented a computational estimation for laminar unsteady natural convective flow of an incompressible fluid past a straight cone with constant thermal flux. FDM was employed to solve the non-dimensional equations

of the flow which was efficient, accurate, and unconditionally stable. The velocity and temperature fields have been investigated for a variety of factors, including Prandtl number. The total Cf, as well as the Nusselt number, were also visually depicted and examined. Results showed that the time taken to reach a steady state increases with increasing Prandtle number, as well as the regional as well as total Nu were reduced with decreasing Prandtle number. It also revealed that reducing Pr leads to an increase in the Cf .

Jamal A. et al.[18] investigated numerically using a finite-difference approach the combined conductive-natural convective thermal transport in a straight annulus. The geometry was opened from each side end and sunken in a static Newtonian fluid . Natural convective circulation was created within the geometry by isothermally warming one surface of the cylinder while the other surface was kept at T_f of the entrance . With a constant speed's distribution , the constant laminar flow enters the eccentric annulus.

Results showed that the overall absorbed thermal energy by the fluid (Q) increases with eccentricity for a given channel height (L). Furthermore, eccentricity increases the fluctuation of T as well as the magnitudes of the total q on the boundaries. Lastly,, the computed outcomes revealed that for a specified required thermal transmission with full development attainment in the passage, an inherent greater eccentricity must be developed as opposed to one with a lower eccentricity.

DOGAN et al. [19] explored computationally the process of free convective thermal transmission through partly opened geometries with single heated surface . The exploration's goal was to investigate the steady-state thermal transmission inside the cavity under fixed thermal flux (q″). The PHOENICS code was used to solve the equations of conservation of mass, momentum, and energy utilizing

appropriate BC. With an accumulation in opening ratio and a drop in tilt angle, the total thermal transmission coefficient ascended, while the total surface temp. descended. The optimal thermal transmission was estimated with highest Aspect ratio of 0.75 and a tilt angle of -10 degrees.

Xu et al. [20] The natural convection heat transfer between various geometries of the inner cylinder (circular, square, rhombic, and triangular) positioned inside the triangular enclosure tilted for various inclination angles was numerically investigated. The inside cylinder was kept uniformly hot, while the triangle surround was kept cold. The governing equations were numerically solved utilizing finite volume technique and confirmed with earlier work along the bottom wall. The findings were critical, indicating that raising the Rayleigh numbers disrupted the symmetry of streamline contours and concentrated the isotherm contours to the top between the gaps. Furthermore, as the Rayleigh number increases, the flow intensity and overall heat transfer improve dramatically due to increased natural convection contribution. The overall heat transmission improves as the aspect ratio increases, but the flow intensity decreases.

Sivasankaran et al.[21] The influence of separate heating on free convective thermal transmission in a rectangular porous geometry containing a material that generates thermal energy was quantitatively explored. The enclosure's left wall featured two independent heaters, while the right wall was isothermally chilled at a low T. The upper as well as lower surfaces were adiabatic, as were the non-warmed parts of the left surface. An implicit finite difference method was used to solve the governing equations numerically.

The flow and heat transfer impacts of Aspect ratio, Darcy number, heater’s size, and modified Ra were investigated. The numerical results demonstrated that

raising the modified Rayleigh number and Darcy number enhanced the rate of heat transfer, but decreasing the aspect ratio. The average thermal transmission amount was noticed to be larger at the lower heat source than at the upper one in practically all parameter situations studied. In addition, the highest T was noticed at the top heat source. Furthermore, the computational outcomes demonstrated that the highest T was reduced when the Ra was adjusted and grew as the AR increased. Figure (2.1) displays the physical configuration of the considered case.

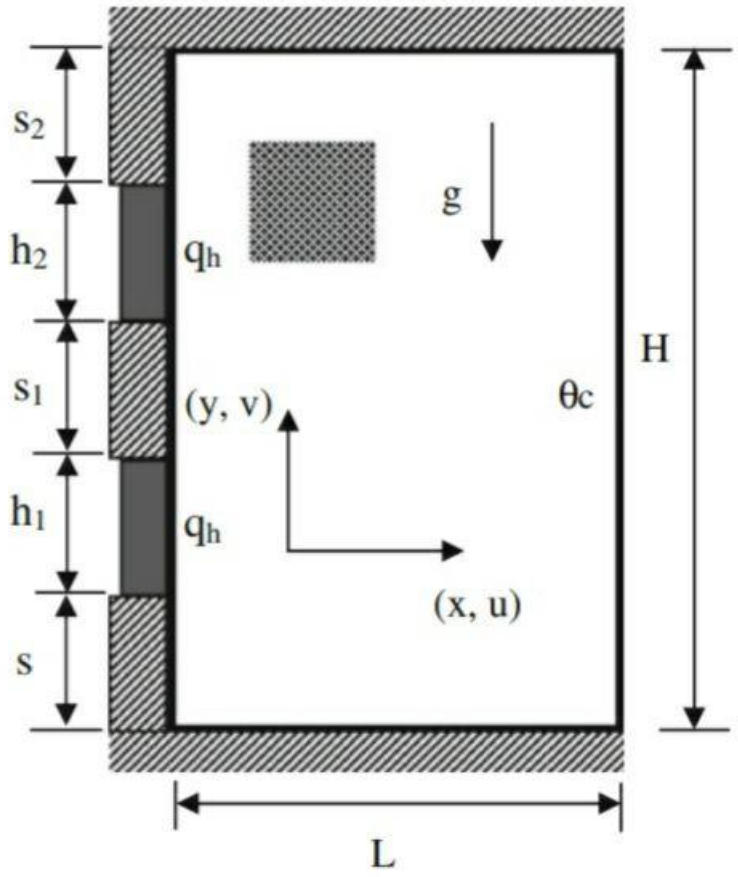

Figure (2.1): Physical configuration and boundary conditions of **Sivasankaran et al.[21]**

Sankar et al. [22] Free convective thermal transmission in a cylindrical velar geometry with separate heaters on the internal surface was studied numerically, while a smaller T was applied isothermally to the external surface. The upper,

lower, and non-warmed parts of the internal surface were presumed to be insulated. The influence of separate warming on free convective thermal transmission was studied. Mainly, two heaters near the upper and lower surfaces were explored, also the length as well as position of these distinct thermal sources in the geometry were adjusted. The PDE were numerically solved using an FDM approach. The influence of thermal source placement, size, Aspect ratio , Radius ratio, and modified Ra on circulation and thermal transmission in the annulus was investigated. The computational outcomes revealed that when the heater's length was reduced, the thermal transmission amount increased. Furthermore, it was discovered that thermal transmission in the physical domain increased with Radius ratio and adjusted Ra, and that it could be improved by positioning a thermal source with a shorter size towards the lower wall. Figure (2.2) demonstrates the concentric cylinders with the embedded heaters on the inner cylinder.

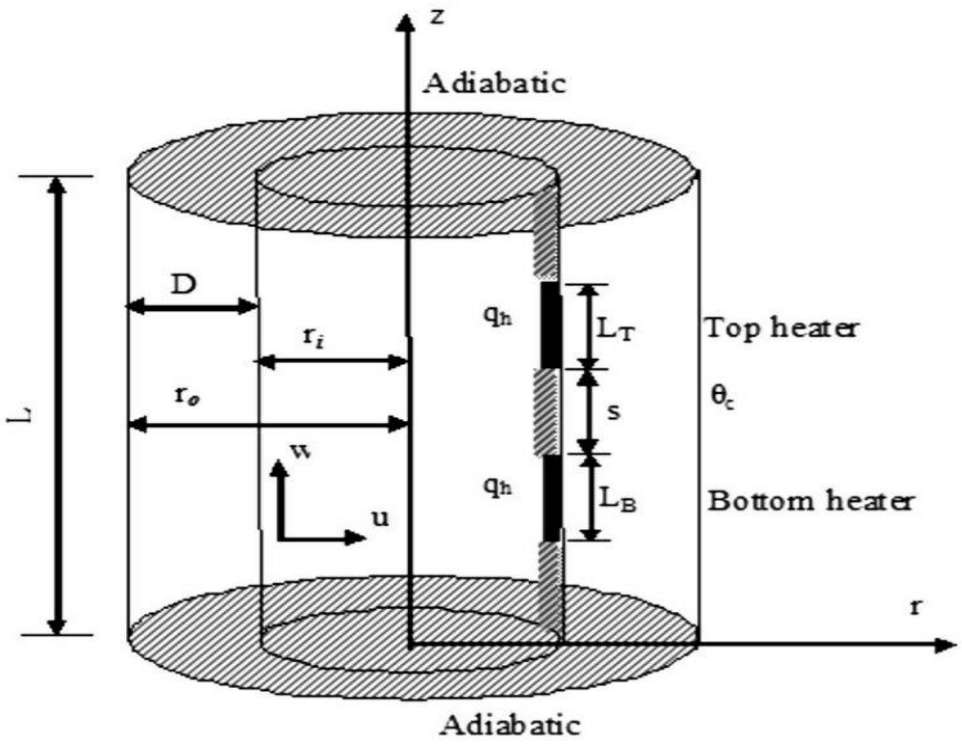

Figure(2.2): Tow concentric cylinders with heaters **Sankar et al. [22]**

Shoushtari et al.[23] investigated Radial heat transfer achieved by overcoming numerous resistances in sequence among the internal channel fluid circulation around the petroleum well. The oil well has a layered cylindrical wall. The main resistance is in the annular region between the wellbore tubing and the casing, so estimating the convection heat transfer coefficient in this location was critical. The flow is continuous, Newtonian, and compressible. This study looked at the nature of the annulus and projected the free convective thermal transmission coefficient, that is difficult to predict because the huge AR. In this work, analytical and numerical techniques were used to model natural convective heat transport. The study made use of vertical enclosure correlations. ANSYS-FLUENT - 12 software was used to model and simulate the flow field in this scenario for numerical analysis.

The Nusselt number was substantially smaller at the bottom of the wellbore than at the wellhead, according to the results based on 8.0 m high wellbore segments. The significant variation in Nusselt number with well depth was caused by the modest temperature difference between the outer temperature of the tubing and the inner temperature of the casing near the bottom hole. As a result, the Nusselt number at the deepest part of the oil well was reduced. Figure(2.3) shows the considered model under study.

Andreozzi et al. [24] Used the finite volume method to perform a computational study of an unsteady free convective flow using air as the working fluid, among two straight analogous plates (channel) warmed at constant thermal flux, with adiabatic analogous plates downward (chimney). The transient problem under consideration was laminar and two-dimensional. Overshoots and undershoots were seen in wall temperature profiles over time. When the maximum wall temperatures were compared, the simple channel was shown to be the most crucial arrangement

in steady state, however it was the optimum arrangement during the unsteady warming at the first overshoot. Profiles of total Nu throughout a period of discernment exhibited lowest and highest magnitudes as well as fluctuations before the steady state, as shown by the temperature profiles.

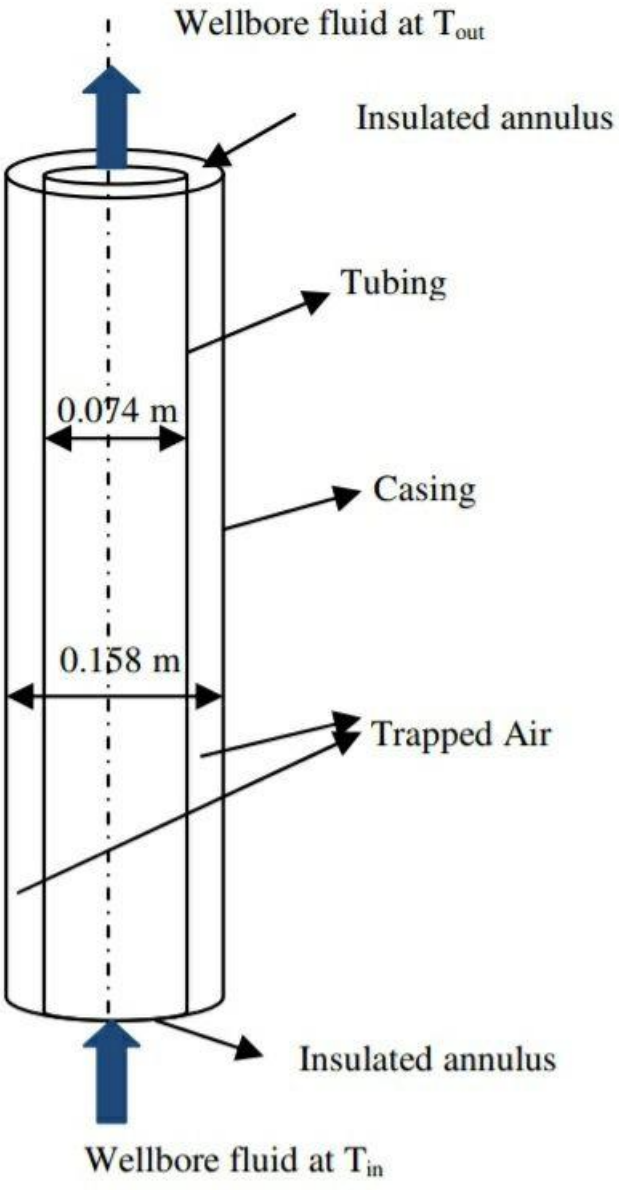

Figure (2.3): Model diagram of the considered annulus **Shoushtari et al.[23].**

Kusammanavar et al. [25] investigated the effect of heater's position on free convective circulation in a square geometry, natural convection in a closed square cavity was explored, with the influence of a heater on the thermal transmission taken into account. A parametric research on the location and strength of the heat source was considered. The source was divided into two halves. The ideal placement for the heater in the geometry was investigated so that it may be employed in the heat-generating electronic equipment. To determine the effective placement of the heat source in the enclosure, heat sources at various locations were investigated and analyzed for Rayleigh numbers 10^3, 10^4, and 10^5. A hot bottom wall existed in the cavity of length (L) and height (H). The top wall was supposed to be adiabatic, with gravity acting downwards. Because of the thermally produced density differential, a buoyant flow developed inside the hollow. Heat was transported from one wall to the other. Except for the heater in the lower surface and the whole top surface, the components were presumed to be adiabatic. A popular model, such as an air-cooled electronic gadget, was symbolized by the enclosure. The results showed that the Nusselt number grew at the margins due to convection while decreased in the center due to conduction. It was also discovered that when Ra reached 10^5, which is considered a large value of Ra, the temperature declined. As Ra increased, so did Nu, and convection took over.

Roslan et al. [26] The conjugated free convective thermal transmission in an unevenly warmed square enclosure involving a conductive polygon object was quantitatively investigated. The vertical walls were heated and cooled, while the horizontal surfaces were set adiabatic. The dimensionless governing equations were solved using the COMSOL Multiphysics program. The horizontal installation , $0.25 < X_0 < 0.75$, $0.1 < Kr < 10.0$, and 10^3 Ra 10^6 are the governing parameters evaluated. The amount of thermal transmission rose as the volume of the solid

polygon increased until it reached the highest magnitude. The volume of the solid polygon had achieved its crucial magnitude at this point. Furthermore, the heat transmission rate dropped beyond this crucial volume of the solid polygon. The amount of thermal transmission remained consistent for N=5 and polygons positioned in the core of the geometry, achieving the highest amount of thermal transmission.

Ahamad et al.[27] The effect of the viscous removal parameter (E) on the free convective thermal transmission mode was explored by delivering heat to the vertical annular cylinder immersed in porous medium at three distinct places. The viscous dissipation effect, which is a local production of thermal energy via the mechanism of viscous strains, is a common occurrence in both clear fluid viscous flow and fluid flow within porous media.

Finite element method was used to solve the governing equations. Partial differential equations were solved in order to predict the heat transfer behavior. Effect of Ar on Nu was investigated. The results showed that the average Nusselt number(Nu_{avg}) decreased with the increase in aspect ratio(Ar), It also demonstrated that the circulation of the fluid increased as the viscous dissipation parameter (E) increased, which is because of the fact that (E) is essentially a heat creation because of Cf among the moving fluid and the solid particles of the porous media.

Kumar et al.[28] studied numerically free convective thermal transmission in a 2-D transient revolving unevenly warmed geometry. The enclosed area was filled with air and rotated counterclockwise around the center of the enclosure. Boussinesq approximation was employed to solve the PDE subject to, a finite volume code on a staggered grid configuration using TDMA method was created and used. The computational exploration was applied utilizing constant Pr (0.71),

Ra ($1.1x10^5$) and Revolving Ra from $4.9x10^2$ to$3.1x10^3$.Results revealed a massive variation in thermal transmission amounts at large magnitudes of rotational speed specifically higher than 15 rpm.

Gupta et al.[29] carried out a simulation of natural convective thermal transmission in a variety of geometrical shapes . The problem was defined by fixed temperature on the downward as well as upper surfaces, whereas the side surfaces were set adiabatic. The investigation was carried out to determine the shape of enclosure with the highest heat transfer rate while taking into account various magnitudes for the AR as well as Gr. AR magnitudes range was (0.2- 0.5), while the Gr range ($10^4 – 10^{10}$). For the purpose of modulating the system ANSYS 14.0 was Utilized . It was concluded that heat transfer rate in triangular cavity was more than the rectangular and circular segmented cavity in both cases. Another statement was concluded that triangular cavity was having symmetry of air flow for the lower aspect ratio and low value of Grashof number, While for the higher values ($A \leq 0.3$) there would not be any symmetry. But for the circular segment cavity there was symmetry for all cases. In rectangular cavity, it was observed that as aspect ratio decreased , number of cycles increased as air particles reached cold surface early.

Seraji and **Khaleghi .[30]** A 3-D incompressible laminar circulation through a 270 angle curved velar conduit was quantitatively explored. In toroidal coordinates, the non-dimensional governing equations of continuity, momentum, and energy were driven. The projection algorithm was used to discretize the governing equations. The results were acquired using a three-dimensional computer code and a grid generating software written in toroidal coordinates. The solid core had a non-uniform heat source q = BeA, while the exterior wall was supposed to be adiabatic. Taking into account the influence of Re on

thermohydraulic parameters such as secondary circulation generation as well as axial speed, thermal transmission was raised by utilizing a varied thermal flux rather than constant. The computational outcomes showed that applying a varying thermal flux compared to an unvarying flux raised the average Nusselt number, given that each flux of them has the same value. Furthermore, the outcomes showed that as the aspect ratio was reduced, heat transfer increased.

Jamal and Mokheimer.[31] explored numerical laminar free convective thermal transmission in a vertical velar passages in steady state single phase. For ideal thermal conductivity ratio as well as ideal cylindrical surface thicknesses permitting highest rate of fluid circulation as well as thermal transmission under changing geometrical parameters such as Rr. Air was used as annular working fluid with Prandtl number 0.7 . The fluid was considered Newtonian. FDM approach was utilized to solve the computational PDE .

This problem consisted of a straight eccentric velar path. When the fluid enters the velar path , it circulates to the top by the free convective circulation caused by density difference which is created as a result of thermal BC decreed on the velar cylindrical surface.

Two examples were examined. Case I involves applying isothermal heating to the internal part of the inside channel while keeping the external part of the external channel adiabatic. Case II involves swapping these boundary conditions. A parted crooked double glass window contains air in the cavity among the doubled glass layer is a typical use of swappable boundary conditions.

The results were obtained using non-dimensional equations. During the computational study, convective thermal transmission as well as fluid circulation phenomena were explored for different values of non-dimensional eccentricity Rr

(0.1, 0.3, 0.5, 0.7). The results showed that the optimum conductivity ratio and the thickness of the cylinder walls grew nonlinearly with eccentricity and radius ratio.

2.3 Experimental Studies

Elsayed et al.[32] performed an experiment on air's natural convective thermal transmission around the outside wall of a fixed thermal flow elliptic tube. For different values of Ra and tube inclination angles, the local and average Nusselt number distributions were investigated. Based on the input heat flux, the test Rayleigh number ranged from 1.1×10^7 to 8×10^7. For the elliptic tube with vertical major axis, average Nusselt numbers was evaluated and associated with Rayleigh numbers. The convection characteristics of isothermal and constant heat flux elliptic tubes were compared. The influence of elliptic tube orientation on the average Nusselt number was also demonstrated. It was discovered that when the main axis of the tube was straight , the average Nusselt number increased.

2.4 Theoretical and Experimental Studies

ABD AL-SAADA[33] studied theoretically and experimentally natural convective thermal transmission among horizontal concentric pipes of constant internal as well as external pipes temperature, respectively where ($T_i > T_o$). The FEM was applied to attain results of the PDE. The computational results including the temperature as well as velocity fields within the annulus was estimated utilizing ANSYS . Rayleigh number values ranging from $Ra=7.12*10^2$ to $Ra=5.36*10^3$ were used. The results revealed that the total thermal transmission coefficient at the internal and external radii respectively raised with raising Ra and the ratio of outside to inside radius. Results also revealed that the conductive heat transfer takes place at Rayleigh number less than 10^3 and Nusselt number less than 1,while

the convective heat transfer occurs at Rayleigh number greater than 10^3 so that Nusselt number is greater than 1.

Bianco et al.[34] investigated experimentally and numerically free convective mode utilizing fluid of Pr equal to 0.71 as working fluid in straight pipes with wall constant thermal flux. Heat transfer in a convergent channel with two uniformly heated flat plates was studied. The passage way was constructed of two primary plates that were evenly warmed at constant q while the two plexiglass side walls were not heated. The channel was opened from each end. In the walls, a two-dimensional conduction model was used, and radiative heat transport was ignored. The physical domain was made up of two non-parallel plates that connected to produce a convergent channel. Both plates were conductive as well as warmed at the same rate (q_x). It was assumed that the flow through the channel was 2-D , laminar, and incompressible. The results revealed that the dimension from the intake at which the thermal domains could be deemed fully developed ascended with q . The recirculated domain caused a proportional ultimate temperature rise on the channel's core line.

2.5 Summary

All the presented studies in this chapter are summarized in Table (2.1)

Table(2.1): Summary of the previous studies.

Author	Model	Year	Method	Working fluid	Range of variables	Conclusion
Silva et al.[12]	Numerical	2003	FVM	Air	H/L=1 Pr = 0.7 $10^2 \leq Ra \leq 10^6$	The ideal distribution of heaters maximizes the inclusive performance. As well as ,the highest overall conductance increased as more heaters were embedded, however the average of the raise descended.
Al-Essa and Al-Hussien [13]	Numerical	2003	FEM	Air	$1 \leq b \leq 8$ $1 \leq t \leq 5$ Pr = 0.7	The heat dissipation enhancement from a fin with square perforation parallel to the fin base was more than that of fin with inclined square perforation.
Dias Jr.and Milanez [14]	Numerical	2004	FVM	Air	$10^3 \leq Ra \leq 10^6$ $1 \leq Ar \leq 20$ Pr = 0.7	The aspect ratio increases with the decrease of the characteristic length (W), resulting an increase in the non- dimensional T as well as a decrease in the average Nusselt number.
Saha et al. [15]	Numerical	2005	FEM	Air	Pr = 0.71 $10^3 \leq Gr \leq 10^6$	At higher Grashouf $Gr=10^5,10^6$, when the intensity of convection increased significantly.
Molla et al. [16]	Numerical	2006	FDM	Air	Pr = 0.7	The TBL thickness as well as Temp. and velocity distribution raises as a result of the heat generation .
Pullepu et al.[17]	Numerical	2008	FDM	Air	$0.71 \leq Pr \leq 0.72$	The local and average skin-frictions increased when the value of Pr is reduced.
Jamal A. et al.[18]	Numerical	2008	FDM	Air	Pr = 0.7 Ar = 0.5 Kr = 10	The total heat absorbed by the fluid (Q) is increased with eccentricity.

DOGAN et al.[19]	Numerical	2009	PHOENICS code	Air	$0.5 \leq AR \leq 1.0$ $40 \leq q'' \leq 480$ Pr = 0.7	The total thermal transmission coefficient ascended, while the total surface temp. descended. The optimal thermal transmission was estimated with highest AR of 0.75 and a tilt angle of -10 degrees.
Xu et al. [20]	Numerical	2009	FDM	Air	$10^3 \leq Ra \leq 10^7$ Pr = 0.71	As the Rayleigh number increases, the flow intensity and overall heat transfer improve dramatically due to increased natural convection contribution. The overall heat transmission improves as the aspect ratio increases.
Sivasankaran et al.[21]	Numerical	2010	FDM	Air	$10^3 \leq Ra \leq 10^6$ Pr = 0.7	The maximum temperature decreased with Ra* and increased with the Ar.
Sankar et al. [22]	Numerical	2011	FDM	Air	$10^3 \leq Ra^* \leq 10^7$ $0.1 \leq \varepsilon \leq 0.4$ $1 \leq A \leq 2$ Pr = 0.7	Thermal transmission through the annulus raised with Rr and Ra*, furthermore, it was improved by adding a shorter heat source close to the deepest part of the geometry.
Shoushtari et al.[23]	Numerical	2011	ANSYS-FLUENT – 12	Air	Pr = 0.71 $10^3 \leq Ra \leq 10^7$	The significant variation in Nusselt number with well depth was caused by the modest temperature difference between the outer temperature of the tubing and the inner temperature of the casing near the bottom hole. As a result, the Nusselt number at the deepest part of the oil well was reduced.
Andreozzi et al. [24]	Numerical	2012	FVM	Air	Pr = 0.71 $10^2 \leq Ra \leq 10^4$	Average Nusselt number profiles over a period of consideration showed minimum and maximum values and oscillations before the steady state.

Kusammanavar et al.[25]	Numerical	2012	FEM	Air	$10^3 \leq Ra \leq 10^5$ Pr = 0.71	Nusselt number at the edges increased due to convection while decreased at center due to conduction.
Roslan et al. [26]	Numerical	2014	COMSOL	Air	$0.25 \leq X_0 \leq 0.75$ $10^3 \leq Ra \leq 10^6$ $3 \leq N \leq \infty$ $0.1 \leq Kr \leq 10.0$	The heat transfer rate remained stable for $N \geq 5$ and polygons located at the center of the enclosure and this achieved the maximum heat transfer rate.
Ahamad et al.[27]	Numerical	2014	FEM	Air	$25 \leq Ra \leq 100$ $0 \leq \varepsilon \leq 0.01$ $0.5 \leq Ar \leq 1$	(Nu_{avg}) decreased with the increase in (Ar)and the circulation of the fluid increased with the increase in viscous dissipation parameter (E).
Kumar et al.[28]	Numerical	2015	FVC	Air	$Ra=1.1x10^5$ Pr = 0.71	There was considerable change in heat transfer rates beyond 15 rpm.
Gupta et al.[29]	Numerical	2015	ANSYS 14.0	Air	$10^4 \leq Gr \leq 10^{10}$ $0.2 \leq Ar \leq 0.5$ Pr = 0.7	In rectangular cavity, as aspect ratio decreased , number of cycles increased as air particles reached cold surface early that higher aspect ratio.
Seraji and Khaleghi .[30]	Numerical	2019	projection algorithm	Air	$50 \leq Re \leq 500$ $0.05 \leq Ar \leq 0.9$	Total Nu raised by applying constant thermal flux. Furthermore, thermal transmission was increased as Ar was minimized.
Jamal and Mokheimer.[31]	Numerical	2022	FDM	Air	Pr = 0.7 $0.1 \leq E \leq 0.7$	The optimum conductivity ratio and cylinder walls thicknesses increased nonlinearly with eccentricity and radius ratio.
Elsayed et al. [32]	Experimental	2003	FDM	Air	$1.1 \times 10^7 \leq Ra \leq 8 \times 10^7$ Pr = 0.7	A higher value of average Nusselt number was achieved when the major axis of the tube was vertical.

ABD AL-SAADA[33]	Experimental and Numerical	2006	ANSYS	Air	$7.12*10^2 \leq Ra \leq 5.36*10^3$ Pr = 0.71	Conductive heat transfer takes place at Rayleigh number less than 10^3 and Nusselt number less than 1,while the convective heat transfer occurs at Rayleigh number greater than 10^3 so that Nusselt number is greater than 1.
Bianco et al.[34]	Experimental and Numerical	2007	FDM	Air	Pr = 0.71 T_{amb} = 300 K	The recirculating zone induced a relative maximum raise of the temperature on the channel centerline.
Present work	Experimental and Numerical	2024	COMSOL	Air	Pr = 0.71	The local Nusslet number increased with increasing the length of the heater , which means a better thermal transmission was achieved when using a heat source of higher length.

2.6 Scope of the present work

Natural convective thermal transmission in the annulus region was investigated numerically and experimentally in this work.

For the theoretical work, a physical model was build using the model builder in COMSOL 6.0 software package. The fluid flow and thermal transmission were examined and the numerical results were plotted through isothermal contours, streamlines, and total Nusslet number. A comparison was done between the experimental and numerical results to test the applicability.

The experimental apparatus consisted of two concentric copper cylinders, installed vertically. Heaters were installed on the external wall of the outer cylinder to represent the heat flux source. Air was chosen as a working fluid (Pr = 0.71). Three cases were considered based on the number , the location , and the distance of heaters. Insulating material was added to the outer cylinder to achieve the discrete heating and to minimize the heat dissipation to the ambient environment.

Chapter Three

Numerical Computation

and

Mathematical Modeling

Numerical Computation and Mathematical Modeling

3-1. Introduction

The governing mathematical statements for laminar 2-D free convective flow in two concentric vertical cylinders, with non-dimensional parameters were characterized within this chapter. The physical model for the study cases as well as the related BCs are presented. The heat transfer efficiency was represented by the average Nusselt number.

3.2- Mathematical Model

In this study, two concentric cylinders in a vertical position with mounted heat sources on the external wall are studied depending on the heat flux coming from the heat sources. Also, the length and location of the heat source are considered in this study.

3.2.1 Geometrical representation for the case study

The geometry consists of two combined concentric cylinders opened from both ends. There are three basic heating modes studied depending on changing the location and the number of heat sources. Also, the effect of the length of the heat source is considered.

The front view of the two-dimensional external cylinder with the embedded heat source in this study is illustrated in **Figure (3.1)** and meshed section in **Figure (3.2).**

The length of the geometry is denoted by (L) and the and the width is denoted by (W). Also the non-dimensional length of the heated segment is denoted by (d) .The geometry was stabilized at angle of 90 degrees and the positioning is immovable. By changing the number of the heaters , different cases are considered:

- Case I : five heaters of different lengths.
- Case II : four heaters of equal length.
- Case III : three heaters of different lengths.

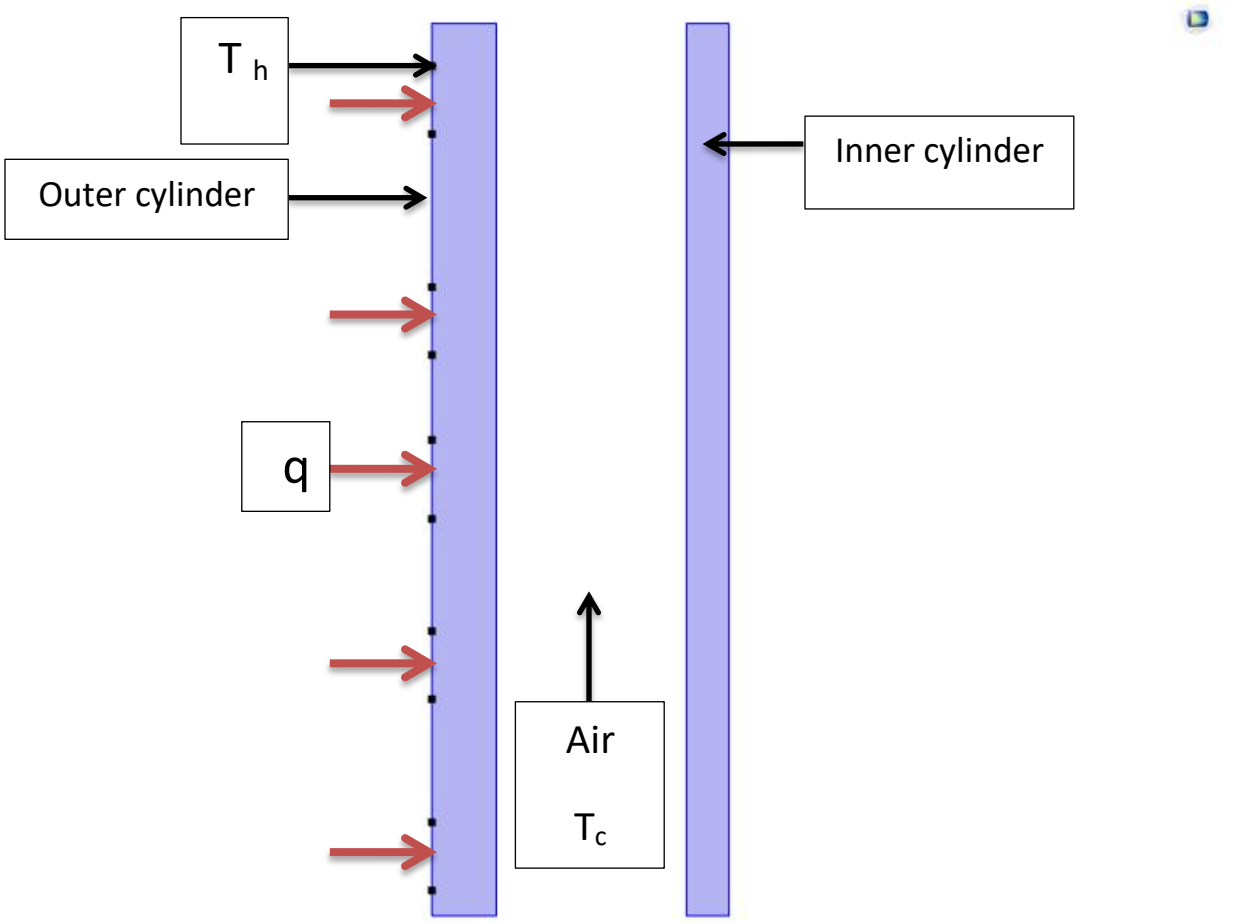

Figure(3.1): Geometrical representation of the physical model with boundary condition

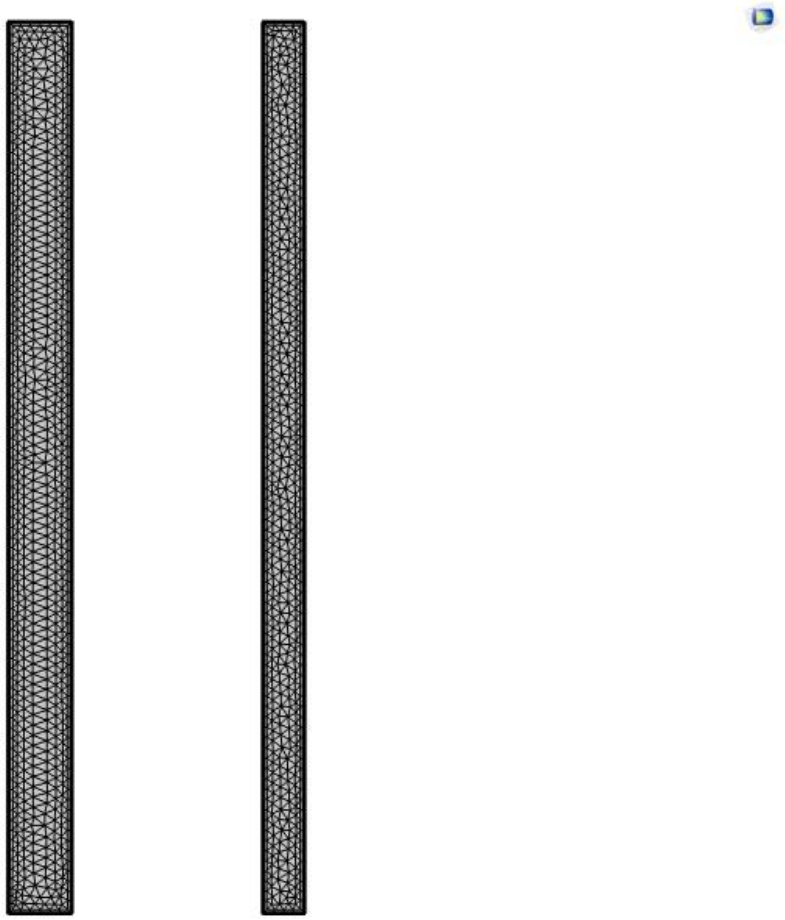

Figure(3.2): The meshed geometry is demonstrated in this figure.

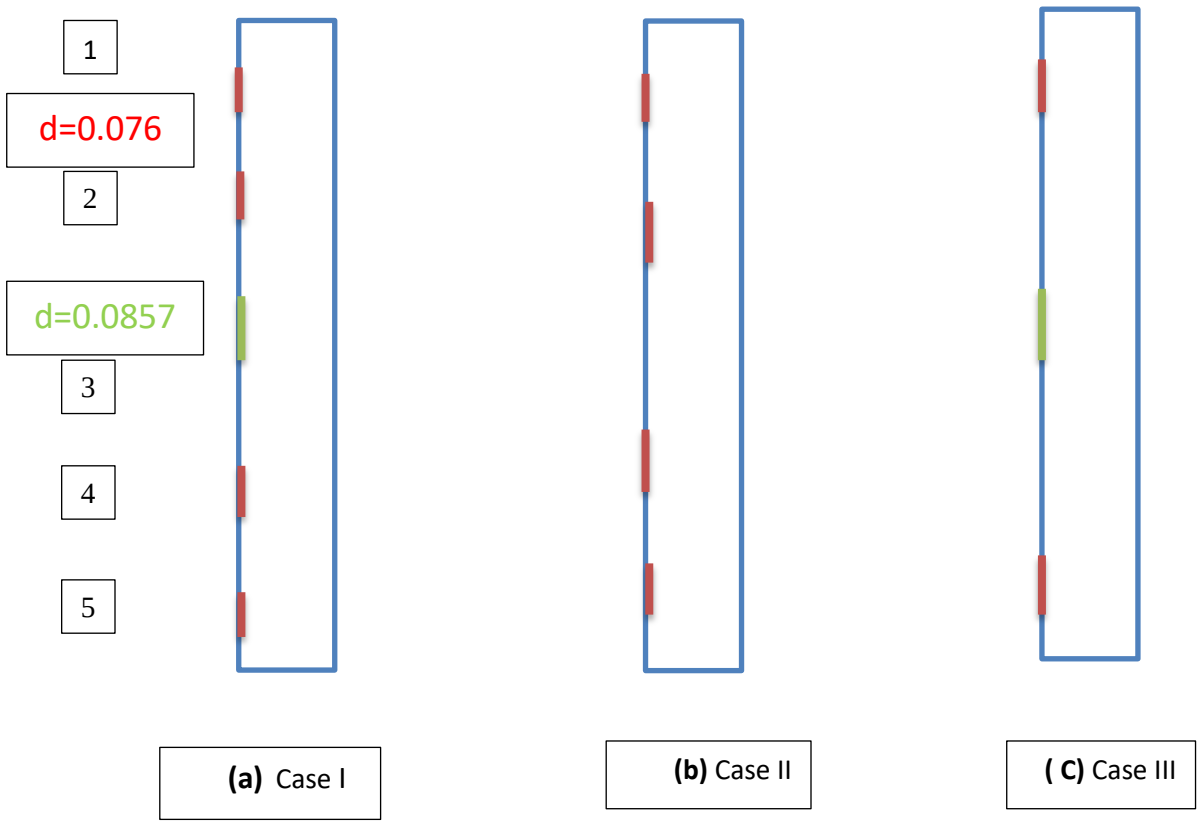

Figure (3.3) represents the three distinct cases, **(a)**:five heaters of different distance , **(b)**: four heaters of equal lengths, **(c)**: three heaters of different lengths.

3.2.2 Governing equations

The governing equations for a laminar free convection in two-dimension in Cartesian coordinates for the current work are illustrated in this section according to the next hypothesis:

- The circulation is regarded laminar, viscous ,two-dimensional, steady and compressible.
- Radiative heat transfer is so small (neglected).
- Heat generation inside the geometry is negligible.
- Working fluid is considered Newtonian fluid (air)
- Thermo-physical characteristics such as, thermal conductivity, specific heat, and thermal expansion are assumed constant except the density in the momentum equation, where the Boussinesq approximation is used to describe the flow that's driven by buoyancy forces (free convective circulation), which neglects changes in ρ except where they appear in terms multiplied by the gravitational acceleration g .

The Prandtl number was taken as Pr=0.71 for air as working fluid. The continuity, energy, and momentum equations in the dimensional formula are given by **Roslan et al. [26] .**

3.2.2.1Continuity Equation(Conservation of Mass)

In an Eulerian analysis, the continuity equation promotes mass conservation.

$$\frac{\partial u}{\partial x} + \frac{\partial V}{\partial y} = 0 \qquad (3.1)$$

3.2.2.2Momentum Equation

In open channel flow issues, to estimate the indiscernible forces operating on the boundaries of a control volume, the momentum equation is employed. The momentum equation deals with scalar as well as vector quantities , therefore it was created in the given directions (x-y) to utilize the components of force in each direction**[35].**

In the x-direction:-

$$u\frac{\partial u}{\partial x} + v\frac{\partial u}{\partial y} = -\frac{1}{\rho}\frac{\partial p}{\partial x} + \nu\left(\frac{\partial^2 u}{\partial x^2} + \frac{\partial^2 u}{\partial y^2}\right) \quad (3.2)$$

In the y-direction:-

$$u\frac{\partial v}{\partial x} + v\frac{\partial v}{\partial y} = -\frac{1}{\rho}\frac{\partial p}{\partial x} + \nu\left(\frac{\partial^2 v}{\partial x^2} + \frac{\partial^2 v}{\partial y^2}\right) + \beta g\,(Tf - Tc) \quad (3.3)$$

3.2.2.3 Energy equation

The fluids' energy equations are applied to various flow arrangements, yielding analytical formulae for calculating temperature changes**[36].**

$$u\frac{\partial T}{\partial x} + v\frac{\partial T}{\partial y} = \alpha\left(\frac{\partial^2 T}{\partial x^2} + \frac{\partial^2 T}{\partial y^2}\right) \quad (3.4)$$

3.2.3Dimensionless Analysis

To make the problem more general, all the parameters were considered non-dimensional. Dimensional analysis aids to relate the coefficients of heat transfer with fewer dimensional variables which are necessary to characterize the previous mentioned free convection problem, In fact , all the equations and boundary conditions are rendered non-dimensional by dividing all dependent and independent variables by compatible and consequential constant quantities.

The stated equations [(3.1) to (3.4)] can be transformed to the dimensionless formula by using the following non-dimensional parameters as demonstrated below:

-Dimensionless parameter

$X=\frac{x}{l}$; $Y=\frac{y}{l}$; $U=\frac{ul}{\alpha}$; $V=\frac{Vl}{\alpha}$; $Pr=\frac{v}{\alpha}$; $P=\frac{pl^2}{\alpha\rho}$; $\Theta f=\frac{Tf-Tc}{Th-Tc}$;

$Ra=\frac{g\beta\,(Th-Tc)\,\ell 3\,Pr}{v^2}$, $Ar=\frac{L}{ro-ri}$, $d=\frac{L_H}{L}$

Consequently, by using these dimensionless parameters, the resulting dimensionless dominant equations are stated below:

-Continuity Equation.

$$\frac{\partial U}{\partial X}+\frac{\partial V}{\partial Y}=0 \qquad (3.5)$$

-Momentum Equation in the x-direction.

$$U\frac{\partial U}{\partial X}+V\frac{\partial U}{\partial Y}=-\frac{\partial P}{\partial X}+Pr\left(\frac{\partial^2 U}{\partial X^2}+\frac{\partial^2 U}{\partial Y^2}\right) \qquad (3.6)$$

-Momentum Equation in the y-direction.

$$U\frac{\partial V}{\partial X}+V\frac{\partial V}{\partial Y}=-\frac{\partial P}{\partial X}+Pr\left(\frac{\partial^2 V}{\partial X^2}+\frac{\partial^2 V}{\partial Y^2}\right)+Ra\,Pr\,\Theta f \qquad (3.7)$$

-Energy Equation.

$$U\frac{\partial \Theta f}{\partial X}+V\frac{\partial \Theta f}{\partial Y}=\left(\frac{\partial^2 \Theta f}{\partial X^2}+\frac{\partial^2 \Theta f}{\partial Y^2}\right) \qquad (3.8)$$

$$\frac{\partial^2 \theta s}{\partial X^2} + \frac{\partial^2 \theta s}{\partial Y^2} = 0 \qquad (3.9)$$

The movement of fluid is described by utilizing Ψ calculated from speed elements U and V. The relation among Ψ with the velocity elements are U $= \frac{\partial \Psi}{\partial Y}$ and $V = -\frac{\partial \Psi}{\partial X}$, that gives an individual formula as:

$$\frac{\partial^2 \Psi}{\partial X^2} + \frac{\partial^2 \Psi}{\partial Y^2} = \frac{\partial U}{\partial Y} - \frac{\partial V}{\partial X} \qquad (3.10)$$

The above formula is known as Poisson's equation**[37].**

3.2.4 Boundary Conditions

In the numerical analysis of this problem , boundary conditions are essential to surround the domain. The objective of assuming boundary conditions is to simplify the process of solving the partial differential equations and make it easier.

In this work, the applied boundary condition that are surrounding the domain are illustrated in figure (3.3) given as the following:

Case I:

$\frac{\partial \theta_f}{\partial Y} = 0$ at Y = 0, Y = L (insulation)

$\theta_f = 0$ at X = W (right wall)

For left wall (heat flux):

$\frac{\partial \theta_f}{\partial X} = 1$ at $3 \leq Y \leq 11$, $25.5 \leq Y \leq 33.5$, $46.7 \leq Y \leq 56$, $66 \leq Y \leq 74$, $92.3 \leq Y \leq 100$

$\frac{\partial \theta_f}{\partial X} = 0$ at $0 \leq Y \leq 3$, $11 \leq Y \leq 25.5$, $33.5 \leq Y \leq 46.7$, $56 \leq Y \leq 66$, $74 \leq Y \leq 92.3$, $100 \leq Y \leq 105$

Case II:

$\frac{\partial \Theta_f}{\partial Y} = 0$ at Y = 0, Y = L (insulation)

$\Theta_f = 0$ at X = W (right wall)

$\frac{\partial \Theta_f}{\partial X} = 1$ at $3 \leq Y \leq 11, 25.5 \leq Y \leq 33.5, 66 \leq Y \leq 74, 92 \leq Y \leq 100$

$\frac{\partial \Theta_f}{\partial X} = 0$ at $0 \leq Y \leq 3, 11 \leq Y \leq 25.5, 33.5 \leq Y \leq 66, 74 \leq Y \leq 92, 100 \leq Y \leq 105$

Case III:

$\frac{\partial \Theta_f}{\partial Y} = 0$ at Y = 0, Y = L (insulation)

$\Theta_f = 0$ at X = W (right wall)

$\frac{\partial \Theta_f}{\partial X} = 1$ at $3 \leq Y \leq 11, 46.7 \leq Y \leq 56, 92 \leq Y \leq 100$

$\frac{\partial \Theta_f}{\partial X} = 0$ at $0 \leq Y \leq 3, 11 \leq Y \leq 46.7, 56 \leq Y \leq 92, 100 \leq Y \leq 105$

3.2.5 Nusslet number

Nusselt number is non-dimensional number which symbolizes the attribution of the convective to conductive thermal transmission across the domain.

It can be expressed as following**[38]:**

$$\mathrm{Nu} = \frac{h\,l}{k} \qquad (3.11)$$

Heat flux can be defined as:

$$\left(\frac{\partial \Theta_f}{\partial X}\right) = \frac{h\,l}{k} = \mathrm{Nu} \qquad (3.12)$$

The average Nusselt number is computed by integrating the local Nusselt number:

$$\overline{Nu}=\int_0^L \frac{\partial \theta_f}{\partial X}\, dY \qquad (3.13)$$

3.3 Numerical Computation

Generally, the most comprehensive modelling for natural convection systems would be CFD. **[39].** The computer is used to do the required computations to emulate free-stream circulation as well as the interaction of the fluid with surfaces which is determined using BC. The physical domain is divided into small cells, and the governing equations for each cell are solved. Superior results can be accomplished utilizing high-speed computers, which has higher efficiency to estimate the most complex problems. Many software applications, such as COMSOL, are used to simulate and solve these types of problems. Typically, experimental apparatus is used for first software validation. For ultimate confirmation , full scale testing is frequently used.

3.4 COMSOL Multiphysics

The Navier-Stokes equations are solved numerically using COMSOL 6.0 software package. In manufacturing processes , thermal transmission problems, designing procedures as well as scientific research purposes, COMSOL is used to modularize all these procedures. COMSOL is a simulative rostrum which accomplishes single-physics as well as completely attached multi-physics modelling. The model constructor contains all of the modelling workflow phases, like constructing the geometry , substance properties, executing computations as well as assessing the results. COMSOL Multiphysics solves and simulates mathematical models of given problems using finite element analysis. Meshes on the cylinder are generated

using triangular elements in this study**[40].** Many checks for grid sensitivity were carried out to establish if the mesh design was adequate as well as to confirm that the outcomes were independent. For predetermined mesh sizes, we use the COMSOL default values.

3.5 Finite Element Method

The FEM technique is an outstanding computational approach utilized to solve PDE **[41].** FEM divides a system into small and simple parts known as finite elements to solve a problem. Finite element analysis (FEA) is a word used to describe the process of researching or analyzing a phenomenon utilizing FEM.

Here are some aspects of FEM:

- This method is the perfect choice for complex shapes and geometries.
- It is well suited for complex boundary conditions.
- This technique can be applied where physical properties change with location.
- Both linear and nonlinear , as well as time-dependent boundary value problems can be solved.
- Software packages can be developed easily for FE calculations.
- It can be used to improve the accuracy of higher-order elements without complicity in boundary conditions ,unlike FDA of higher order.

3.6 Mesh Structure

A tinnier separate cell symbolization of a larger geometric domain is called mesh. For solving PDE, meshes are frequently utilized. A mesh splits up an area into

elements (cells) over which PDE can be solved, resulting in an approximation of the solution over a wider area **[42].**

There are two regularly employed varieties of two-dimensional cell shapes. The triangle and quadrilateral are examples of these shapes.

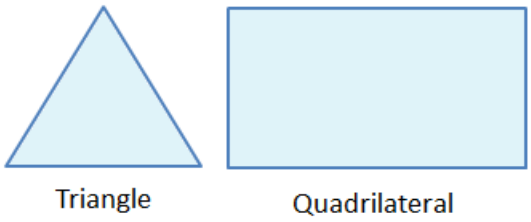

Figure (3.4): Types of two dimensional cells

The triangle cell form has three portions which is one of the most basic kinds of mesh. The triangle mesh is usually simple to make. It's commonly encountered in unstructured grids. The quadrilateral cell form, on the other hand, is a fundamental four-sided shape, as seen in figure (3.4), and it is most common in organized grids. Quadrilateral elements are typically not allowed to be or become concave.

It is worthy to mention that grids can be classified into three types:

- **structured grids** distinguishes regular connection. In 2D, the element options are quadrilaterals and hexahedral in 3D.
- **Unstructured** grids are distinguished by their uneven connectedness. It cannot be easily described in computer memory as a two-dimensional or three-dimensional array. This enables the use of any element that a solver may be able to utilize. In comparison to structured meshes, where neighborhood interactions are implicit, this model may be highly efficient. The storage requirements of a structured grid and an unstructured grid are

the same. In 2D, these grids are normally triangles, while in 3D, they are tetrahedral. **[43].**

- **Hybrid** grid consists of structured as well as unstructured sections. Merging unstructured as well as structured mesh in a functional method. Regular sections of the geometry can have structured grids, while complex parts can have unstructured grids.

As a result, a mesh is deemed to be of greater quality if a more exact solution is generated faster. Accuracy and speed are at odds. Reduced cell size always increases accuracy but also increases calculating time.

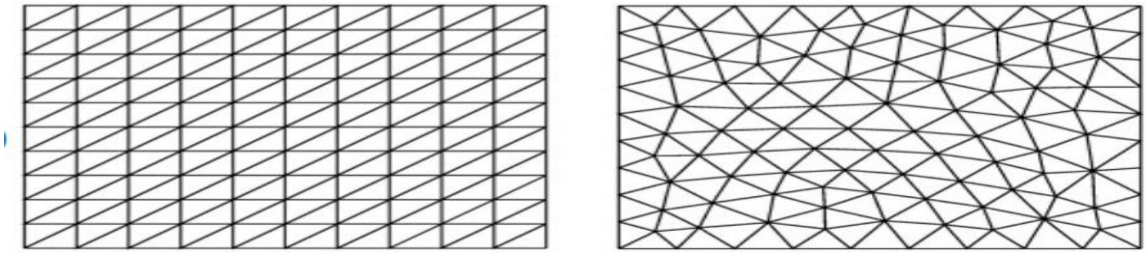

(a)Structured (b)Unstructured

Figure(3.5): illustrates the difference between the structured and unstructured grids.

Accuracy is determined by the total numbering of parts as well as the shape of every single part. Each iteration's speed increases (linearly) with the number of elements, and the number of essential iterations is determined by the shape and size of the elements.

Therefore, the triangular element in an unstructured grid is chosen in this study so that the temperature and velocity components (U,V) are computed at each node of the element.

3.7 Mesh Testing

In this work, in order to choose the appropriate grid size to the studied geometry, the influence of the grid resolution is tested.

To insure accurate results, a mesh independent test is performed using different element numbers and it was applied at Pr=0.71; the results are illustrated in this table:

Table (3.1) : Grid test at Pr = 0.71, Ra = 10^5 and A = 0.0798 m^2 .

Mesh size	Mesh element	Computation time (s)
Coarse	10373	34
Fine	29953	48
Finer	69778	62
Extra fine	162425	92
Extremely fine	315835	180

3.8 Procedures of the Numerical Solution

The stages of the numerical solution can be summarized as follows:

1. Illustrate the two-dimensional, steady and laminar flow by the governing equations of continuity, energy as well as momentum equations in the Cartesian form.
2. Build the geometry using the model builder.
3. Join the stream function and the velocity components.
4. Hypothesize boundary conditions and apply it.
5. Derive the average Nusslet number equation , since it represents the rate of the heat transfer.
6. Solve the governing equations using the FEM approach .
7. Compute the values of fundamental function spaces for the undefined quantities (U and V).

8. Plot the stream lines of the flow by solving the momentum equation, as well as plot the isothermal lines of the thermal domain by solving the energy equation.
9. For each state variable at each node , the criterion of the convergence is tested according to the given convergence condition $\left|\frac{\lambda^{i+1}+\lambda i}{\lambda i+1}\right| \leq 10^{-6}$ where i represents the number of iteration.

10. Evaluate the heat transfer rate.

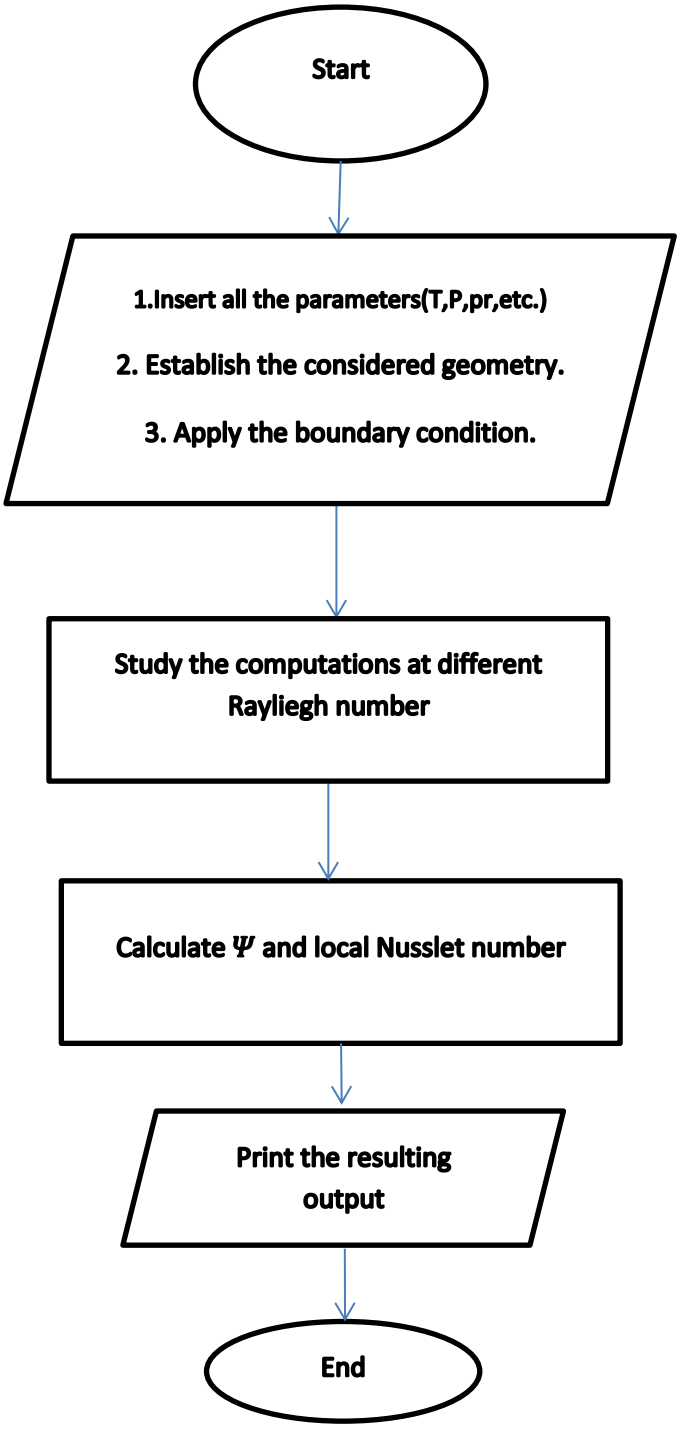

Figure(3.6): Flow chart of the solution steps

Chapter Four

Experimental work

Experimental Work

4.1- Introduction

The main objective of the experimental work that is accomplished in the present work is to validate the investigation of the correspondence between the theoretical and experimental results, in order to support the numerical (theoretical) results by the experimental results, to verify the theoretical cases with the real experimental ones. Moreover, the experimental work presents a clear idea and an essential information about the thermal behavior, flow pattern, and temperature distribution between two concentric cylinders when the outer cylinder is subjected to a high temperature and the inner cylinder of a low temperature.

This chapter displays a detailed description of the experimental apparatus (two concentric cylinders) and the utilized auxiliaries are demonstrated. In addition, a presentation to the procedures of the experimental cases .

4.2-Experimental Apparatus

The major objective of this experimental investigation is accomplishing a better case of temperature distribution , thermal conductivity and convection heat transfer coefficient (h) of the model (concentric cylinders). Therefore, all these properties are necessary to build a convenient experimental rig. The assembled apparatus and the devices that are used in the experimental work for wholly testing cases consist of :

1. Two vertical concentric cylinders.
2. Casing
3. Electric heaters, test section(annulus).
4. Electric board to control and supply power to the heaters
5. Thermocouples

6. Data recorder device connected to the thermocouples to measure temperatures in the test section.
7. Portable barometer
8. Insulation.

All these devices and equipment are clarified in the Figure (4.1) as well as Figure(4.2).

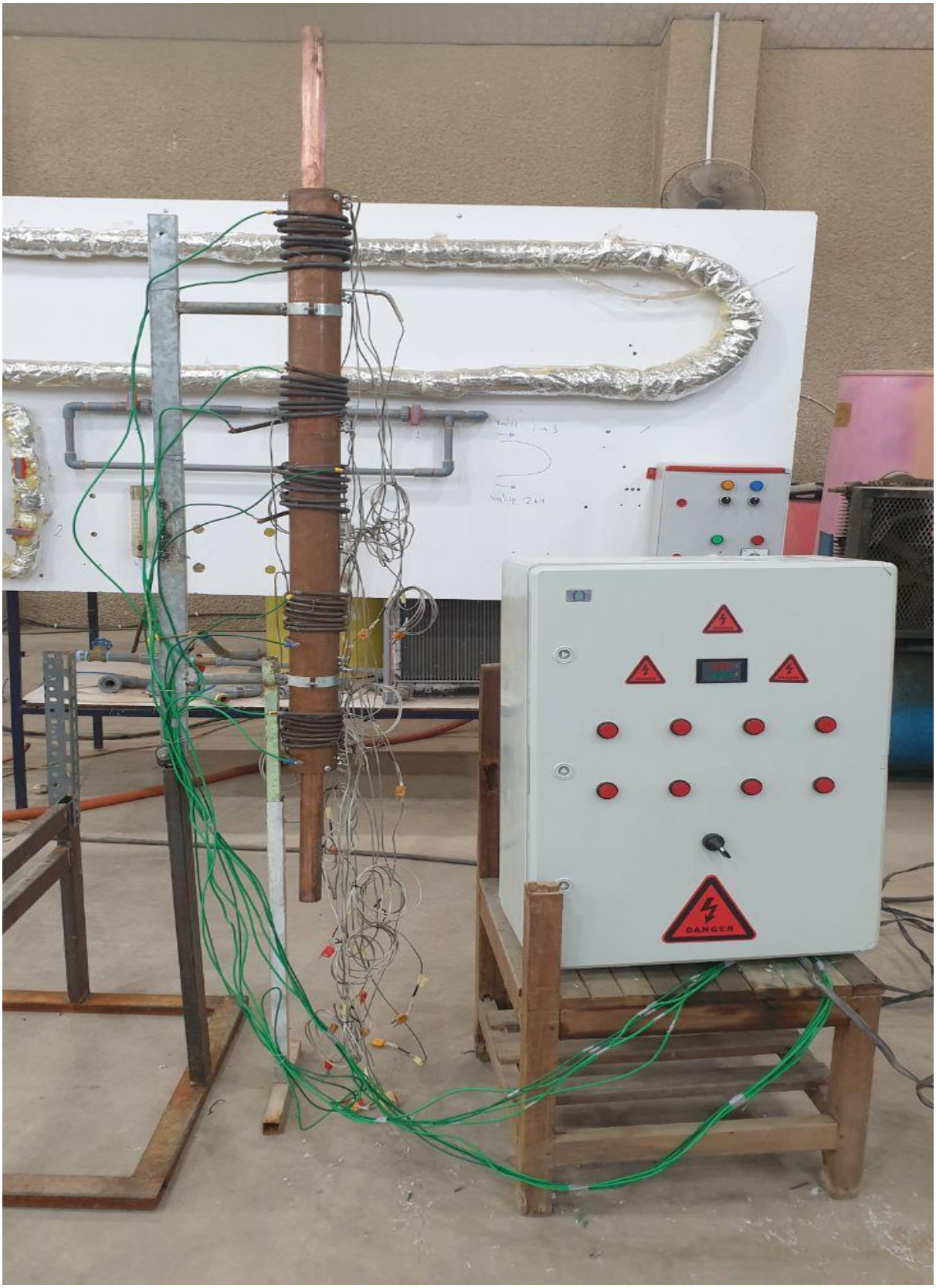

Figure (4.1) : The experimental apparatus connected to the electric board

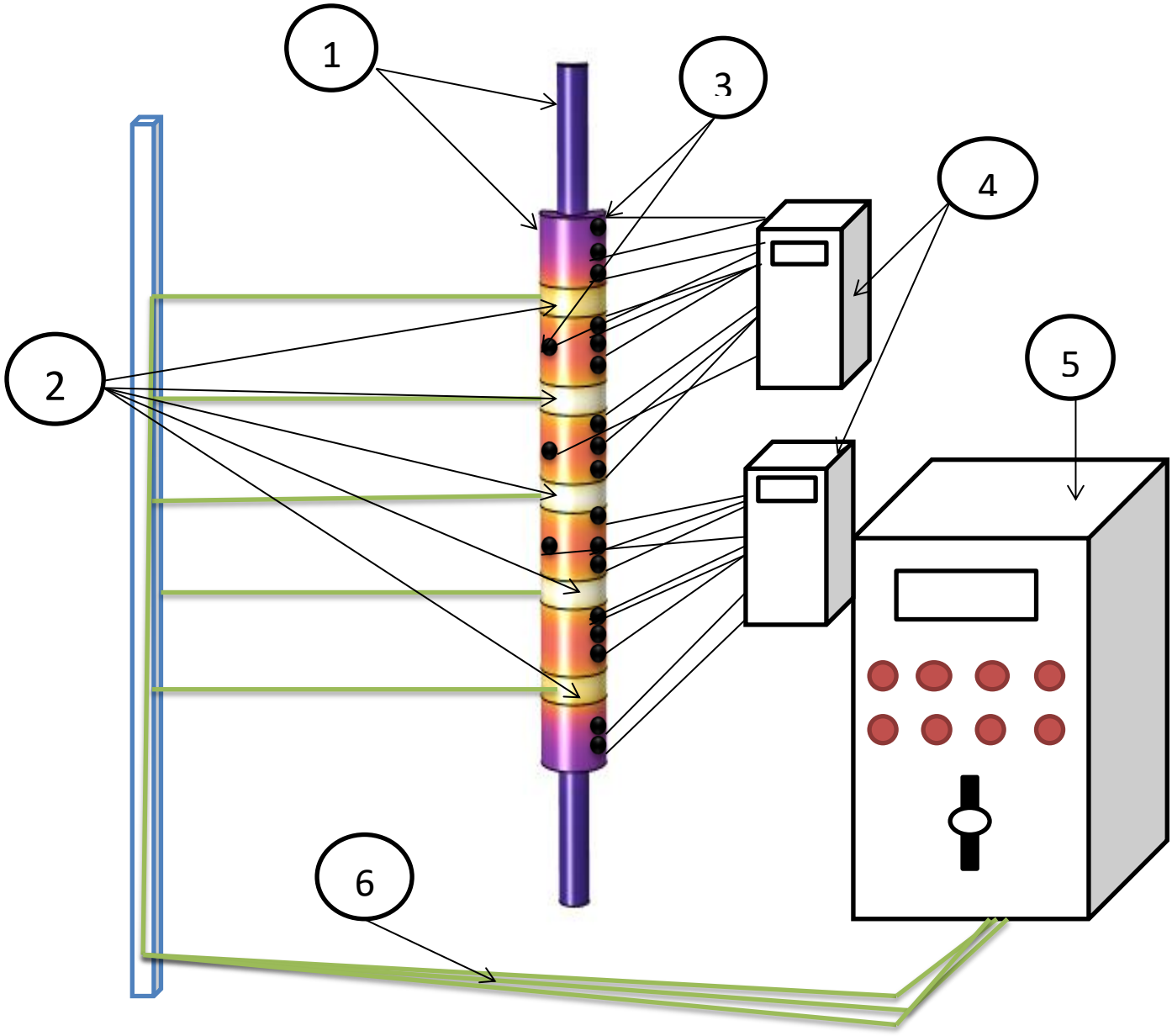

1-Two concentric cylinders	3-Thermocouples	5-Power and control board
2- Heaters	4- Two temperature recorders	6- Wires

Figure(4.2): Schematic arraignment of the experimental apparatus.

4.2.1 Experimental Model

The experimental model mainly consists of two vertically installed concentric cylinders. Both inner and outer cylinders are made of solid copper (thermal conductivity k=385 W/m.K) , the outer cylinder is 105 cm long, outer diameter of 76 mm and a wall thickness of 3.65 mm , while the inner cylinder is 160 cm long , outer diameter is 35 mm and a wall thickness of 2 mm . Three copper tubes were welded on the surface of the outer cylinder each of 3mm diameter to measure the pressure at three different positions in the test section during the experimental work. These tubes were connected later to a portable manometer to attain pressure readings. These tubes were mounted (23.2, 56.2, 82.2)cm respectively. A set of twenty thermocouples type-K is distributed in the test section(the annulus)at(5)mm depth and (1,2.2,3.4,20.4,21.6,17,22.8,43,44.2,45.4,52,65.6,66.8,68,88.2,72,,90.6,97.6,98.8,100)cm along the cylinder to measure the temperature distribution during the test. A number of tubular resistors (different number in each case), 2m long and 10 mm diameter are mounted around the outer cylinder and connected to an electric board to make them work alternatively by passing current of 9.8 A to each one and voltage of 210 V, consequently the resultant thermal flux is 7955 W/m^2. An insulation of Ceramic Fiber Bulk thickness of 6 cm is set all around the outer wall of the cylinder to minimize the heat loss to the atmosphere. The inner cylinder is held concentrically within the outer cylinder by using screws to make it fixed in the right position .

4.2.2The Insulation

A considerable portion of heat loss from typical residence occurs through vertical heat pipe. Insulation is used in order to conserve energy. An examination of the

thermal conductivities of the insulating materials reveals that Rosewool ceramic fiber blanket (see figure (4.3)) has excellent specialties, therefore it makes sense to insulate the outer cylinder with this type of insulation and some characteristics of this insulation are shown in Table (4.1).

Figure(4.3): Ceramic fiber blanket insulation

Table (4.1) features of insulation**[44].**

Characteristics of Ceramic Fiber Blanket	
Features	low (k) , good thermal insulation and thermal shock resistance .
temperature level	1100-1430℃ (2012℉-2600℉)
Density	200-250 kg/m³ (13-16 lb/ft³),
raw materials	100% non- asbestos
Thickness	6 cm
Function	heat Insulation

Therefore, this type of insulation was the best choice for this case according to the characteristics mentioned above.

The outer cylinder is insulated using Ceramic Fiber Bulk to assure the best insulation from the outside and to minimize the thermal loss.

4.2.3 The Heat Source (Heaters)

Five Tubular heaters of 2 meters long and 10 mm diameter model (1515A) were embedded around the outer cylinder (see Figure (4.4)) and connected to an electric board to achieve alternative operation to the heaters. Consequently, by measuring the drawn current and voltage we can calculate the resulting heat flux from each heater.

It is worthy to mention that the number of heaters changes in each one of the three cases mentioned in the previous chapter.

Figure(4.4): Five tubular heaters embedded on the outer cylinder.

4.2.4 Portable Manometer

UT366A Digital portable Manometer (accuracy ± 0.5% FS @ 25° C)**[45]** is connected to the annulus in three different locations during the experiments through the welded narrow tubes to achieve an accurate pressure readings. The manometer is shown in figure (4.5).

Figure(4.5): Portable manometer

4.2.5 Calibration of Digital Manometer

The digital portable manometer was calibrated by connecting U-tube manometer between two points one on the section No.1 and the other on the section No.2 , measuring the difference pressure between two points with different temperatures. Figure (4.6) represents the calibration data for the pressure taken from digital manometer and U-tube manometer at the same condition . Relation between U-tube manometer readings and that evaluated by digital manometer was described using an equation to rectify the digital manometer .

$$P_{calib}=0.5+0.1357\ P_{re}-0.3421\ P_{re}^{-2}-0.0221\ P_{re}^{-3} \qquad ....(4.1)$$

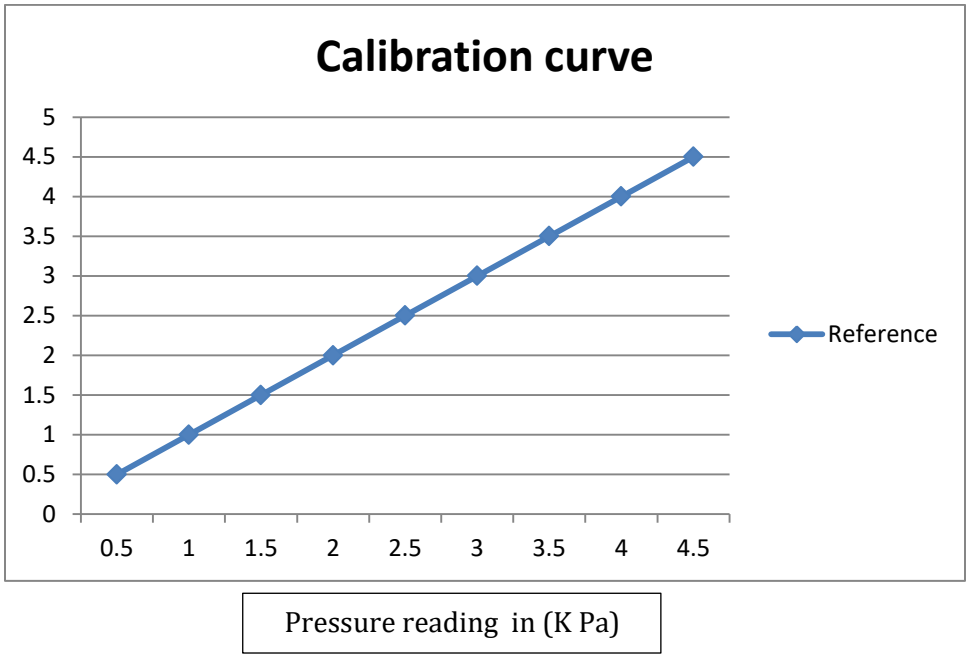

Figure (4.6): Calibration curve of digital manometer.

4.2.5 Thermocouple set

Thermocouple sets type **K** (0.27) mm Chromel-Alumel thermocouple wires are used, range (0°C to 1200°C) as listed in Table (4-2) are used. In all experiments (20) thermocouples were distributed along the external wall in the air gap between the two cylinders and through their surfaces to determine the temperature distribution through this region. Thermocouple type K is illustrated in figure (4.7) below.

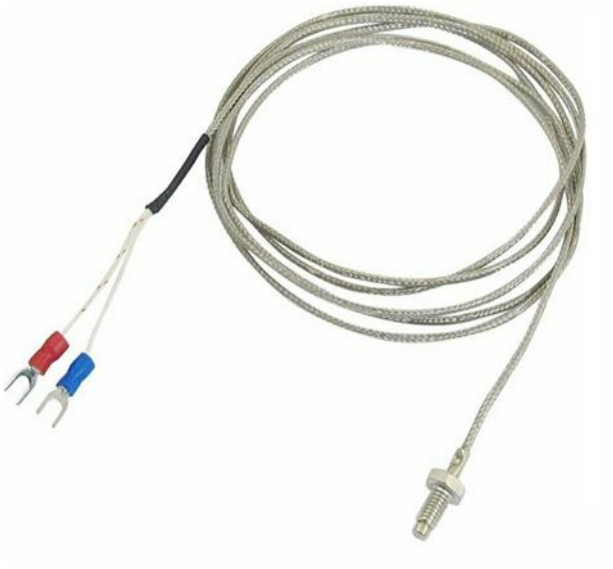

Figure(4.7): Thermocouple type K.

Type-K was specifically chosen due to its reliability, accuracy , and low cost**[46].**

Table(4.2): Thermocouples information**[47].**

Detector type	Resolution	Domain	Precision
Type K	0.1°C	(-50.1°C to -100°C)	±(0.4 % +1°C)
		(-50.0°C to -999.9°C)	±(0.4 % +0.5°C)
	1°C	(0°C to - 1200°C)	±(0.4 % +1°C)

4.2.6 The Electric Board

To change and control the temperature for the outer cylinder, all heaters are connected to an electric board . The electric board consists of 12 Relay , 8 Flash-timer , 7 timers , conductor(Ampere) , current transformer and miniature circuit breaker .

The heaters are connected to a set of relay ,the purpose of each relay is to achieve an alternative operation for the heaters, in addition each relay is connected to a Flash-timer and each Flash-timer is connected to a Timer to achieve a better control to the operation time.

The CT(current transformer) measures the input voltage and current that is shown on a digital screen embedded at the interface of the board, consequently the power can be calculated from the drawn current and voltage , hence the heat flux can be estimated.

The purpose of the conductor is to control and operate the load. It is connected to a Miniature Circuit Breaker (MCB), single phase , two poles for safety purposes. The board is shown in figure (4.8).

Figure(4.8): The electric board

4.2.7 Data Recorder

All thermocouples are connected to data recorder device. Two devices have been used since we used 20 thermocouples. Each device has 12 channel for

measuring temperature. It measures temperature in Celsius and shows it on a digital screen an addition to recording the data on a RAM 2GB memory card.

The RAM is inserted in a laptop computer later to show the recorded data through an Excel worksheet. It is shown in figure (4.9).

Figure(4.9): Temperature recorder.

4.2.8Calibration of temperature measurement

The temperature recorder was calibrated with thermometer where the temperature was measured with varying temperature of water by using the temperature recorder device for the range temperature (0°C to 100°C). Then compared with the readings of the thermometer as shown in figure (4.10). Relevance among thermometer reading and that estimated using temperature recorder was an equation which used to debug the temperature recorder reading .

$$T_{calib}=1.2033+1.0273\ T_{re}-0.0002123\ T_{re}^{2}+2.43211\times10^{-4}\ T_{re}^{3} \quad ....(4.2)$$

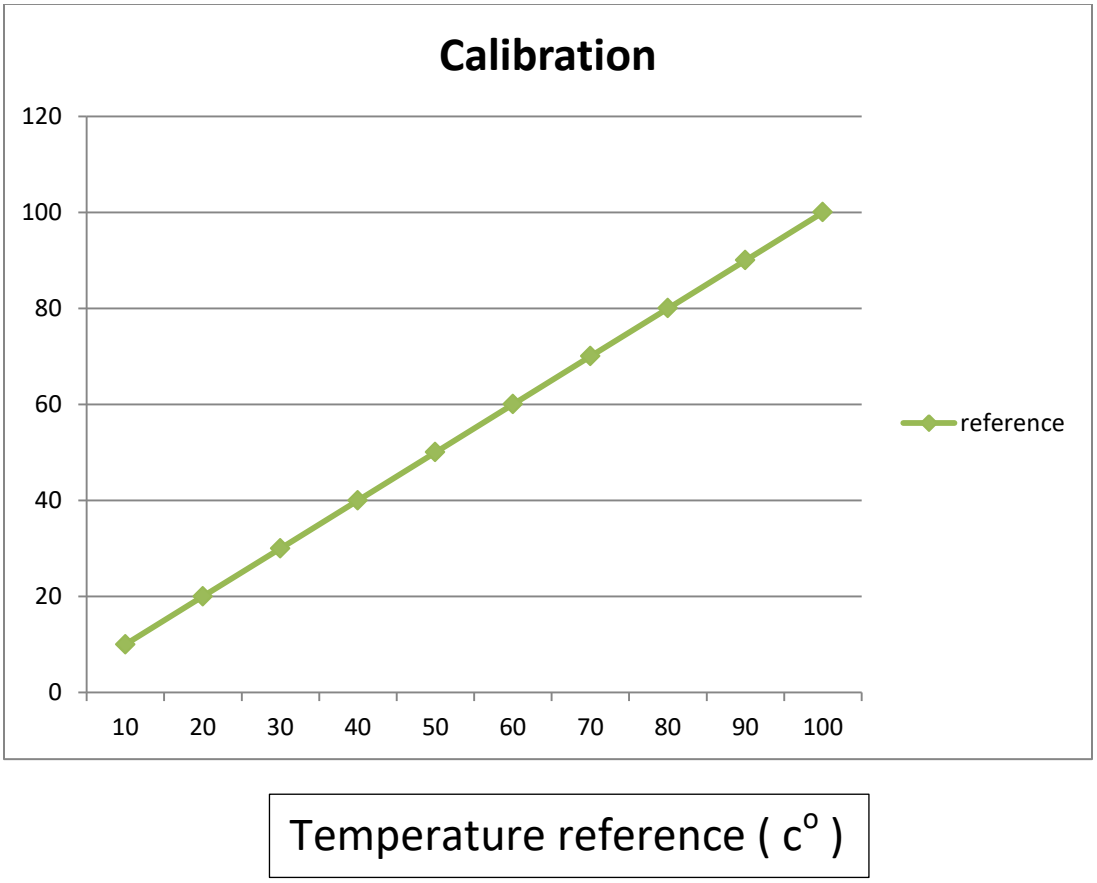

Figure(4.10): Calibration curve of temperature recorder

4.3 Experimental Procedures

To start the experimental work an important feature must be satisfied, this feature is the calibration process for measurement devices to assure the accuracy of each reading. The procedures are illustrated below:

1- The ambient temperature was measured before starting the heating process.

2- The power was supplied to the (Control-Power) board and the starting switch was turned on.
3- The temperature recorders have started recording the measured temperatures at each channel during the test period.
4- The heaters began to operate alternatively.
5- Pressure was measured during the operation time by the digital manometer.
6- The value of the drawn power by each heater is estimated by using a CT to control , read the voltage and current, and display it on a digital screen.
7- The heat flux resulting from each heater is dependent on the consumed power. The time period of the operation was (60 minutes) for the first case, (45 minutes) for the second case, and (30 minutes) for the third case.
8- The experimental procedure was repeated for all the cases.

4.4 Experimental Analysis

To calculate the amount of thermal transmission and other parameters such as Nu and Ra from the experimentally recorded temperatures for the annulus, they are listed as follows:

1- Consumed power**:**

$$P = V \times I \cos\theta \qquad (4.3)$$

Where $\cos\theta$ is the ability factor and equals 0.92 **[48].**

2- Heat flux:

$$q = \frac{P}{A} \ W/m^2 \qquad (4.4)$$

Where $A = \pi D$

3- Convective heat transfer coefficient (h) by dividing the heat flux to the temperature difference:

$$h = \frac{q}{\Delta T} \qquad (4.5)$$

where $\Delta T = T_h - T_c$

4- Nusslet number**:**

$$Nu = \frac{h\ l}{k} \qquad (4.6)$$

The average Nusslet number can be estimated as follows**[49]:**

$$Nu_{avg} = \frac{1}{L} \int_0^L Nu_L \ dY \qquad (4.7)$$

5- Rayliegh number:

$$Ra = \frac{g\beta\ (Th - Tc)\ L^3\ Pr}{v^2} \qquad (4.8)$$

Chapter Five

Results and Discussion

Results and Discussion

5.1 Introduction

The physical model of two concentric cylinders with alternative and discrete heat sources attached on the outer wall have been analyzed numerically using the computational software package COMSOL 6.0 Multiphysics. The top as well as bottom surfaces of the cylinder are insulated while the right wall is subjected to a constant temperature. An alternative and discrete heat flux is applied to the right wall. A computational validation was done to verify the numerical results .The numerical results are used to support the experimental design.

5.2. Validation of the Computational Results

Numerical solution validation is the process of checking the accuracy and reliability of a numerical solution obtained from a mathematical model or algorithm. Numerical solution validation is an important stage in the numerical modeling process since, it contributes to assure that the outcomes of the model are trustworthy as well as precise. The numerical model that was used in the current study was verified by solving some cases that the researcher used. **Sankar et al. [22]** studied numerically free convective thermal transmission through a cylindrical annulus . Separated heaters were added on the internal surface, however the external surface was isothermally cooled at a smaller temperature, the upper surface, the underneath surface, as well as unheated parts of the internal surface were presumed to be insulated. The influence of separate heating on the free convective thermal transmission was investigated. Basically, the two heaters situated near the peaked as well as lower s urfaces were analyzed, as well as the

length and location of these separate heat sources were changed in the enclosure. Demonstrating the hydrodynamic circulation through isothermal lines as well as stream lines which shows the hydrodynamic flow and the thermal domains inside the separately heated annulus for two various magnitudes of Ra, Ra = 10^3 as well as 10^7 , for three distinct heat source lengths (H_B = H_T = 0.2, 0.3, and 0.4) were validated.

Sankar et al. [22]	Present work
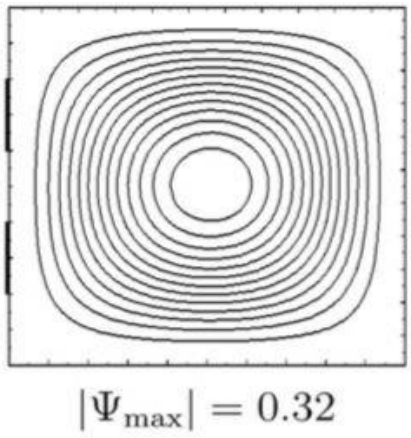 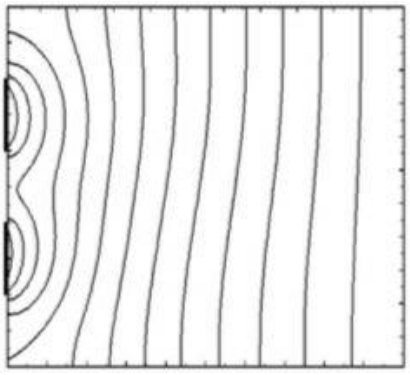 Ra = 10^3	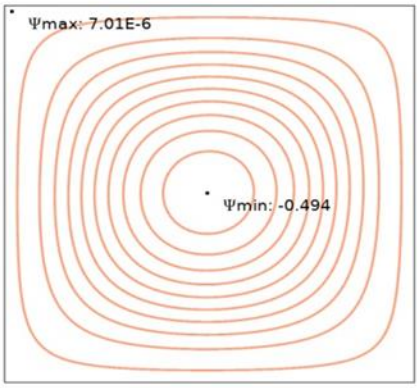 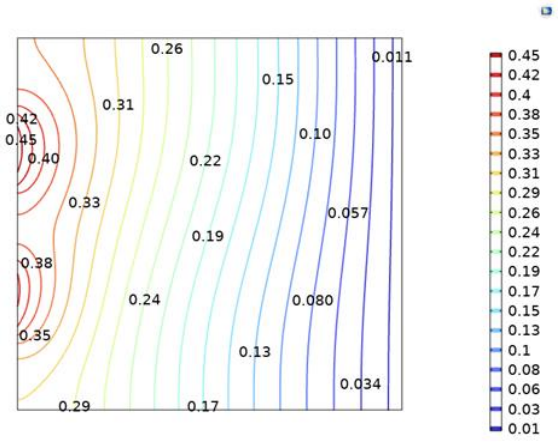

Figure(5.1): The streamlines and the isotherms when H_B = H_T = 0.2,Ra = 10^3.

Sankar et al. [22]	Present work
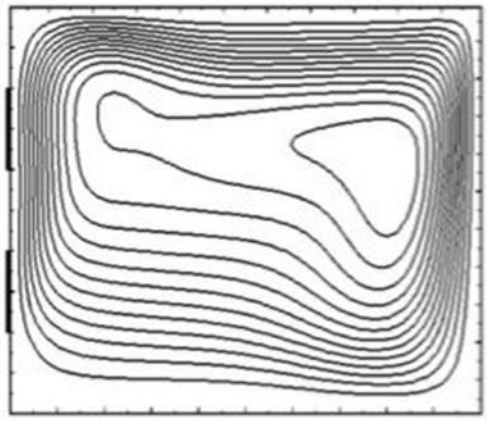 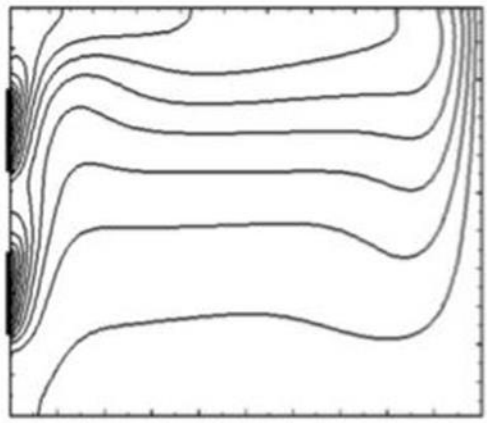 Ra = 10^7	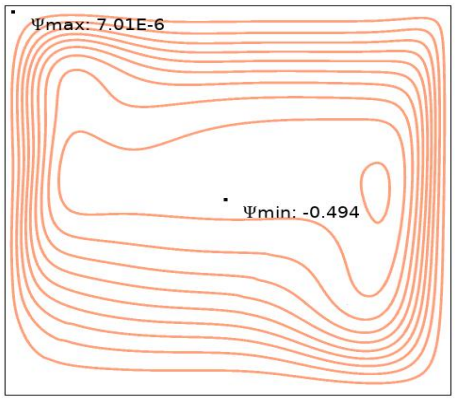 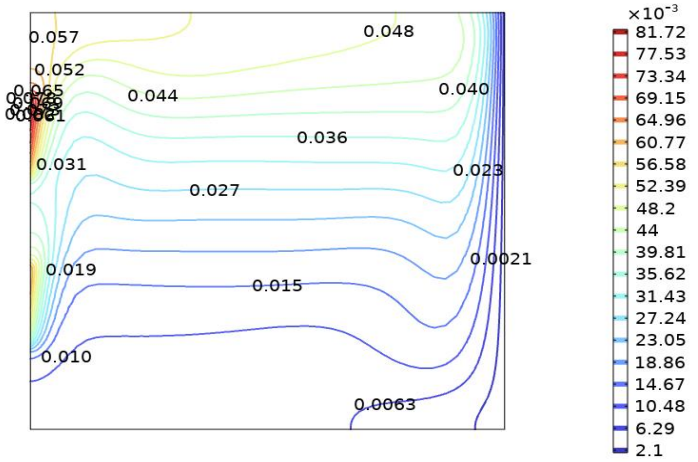

Figure(5.2): The streamlines and the isotherms when $H_B = H_T = 0.2$, Ra = 10^7.

Sankar et al. [22]	Present work
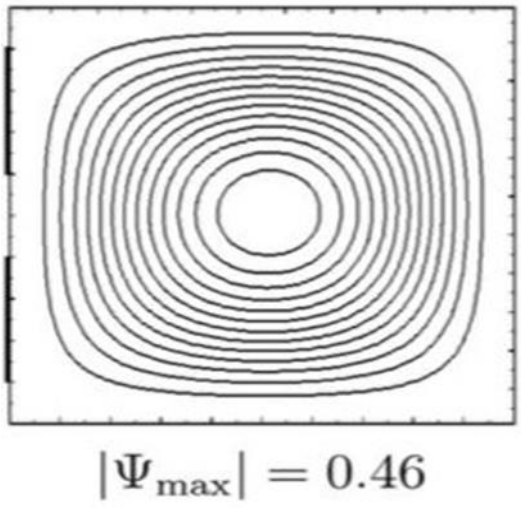 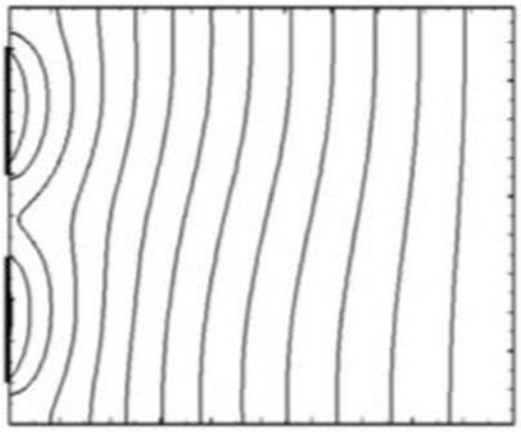 Ra = 10^3	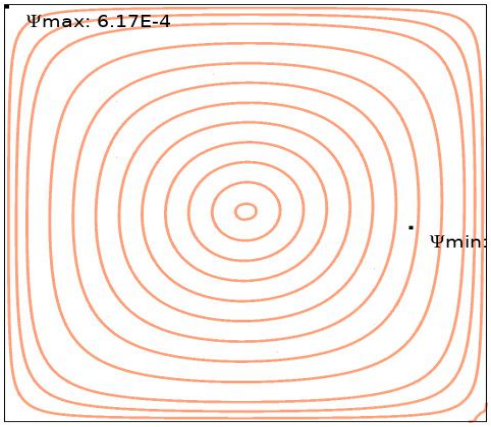 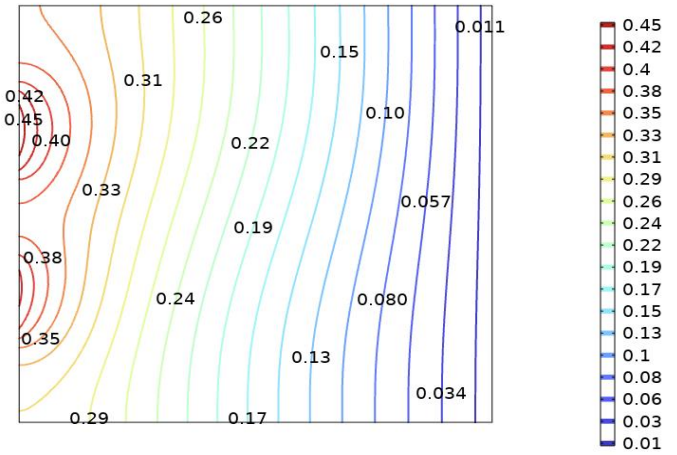

Figure(5.3): The streamlines and the isotherms when $H_B = H_T = 0.3$, Ra = 10^3.

Sankar et al. [22]	Present work
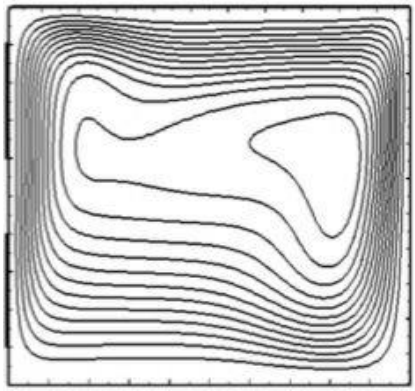 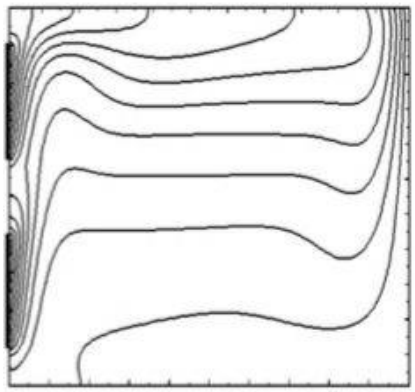 Ra = 10^7	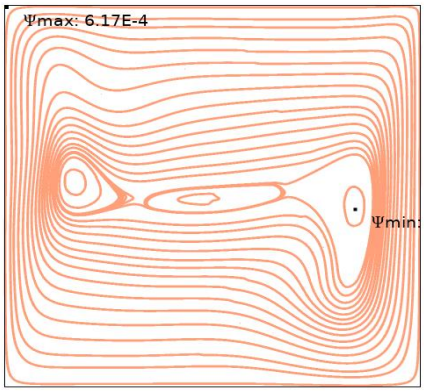 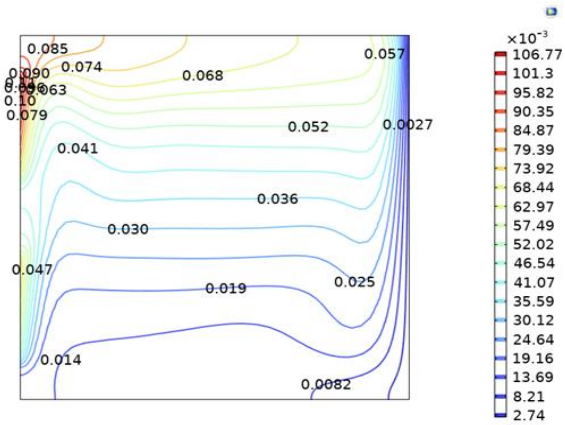

Figure(5.4): The streamlines and the isotherms when $H_B = H_T = 0.3$, Ra = 10^7.

Sankar et al. [22]	Present work
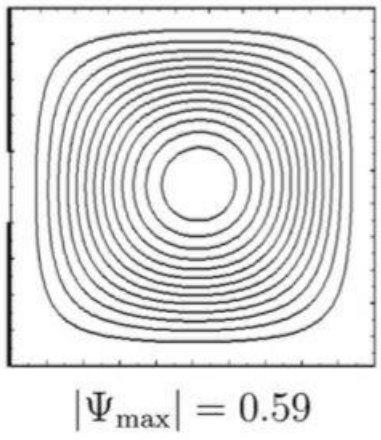 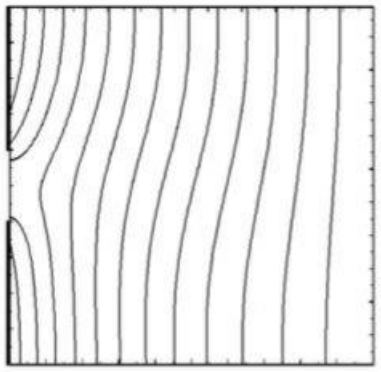 Ra = 10^3	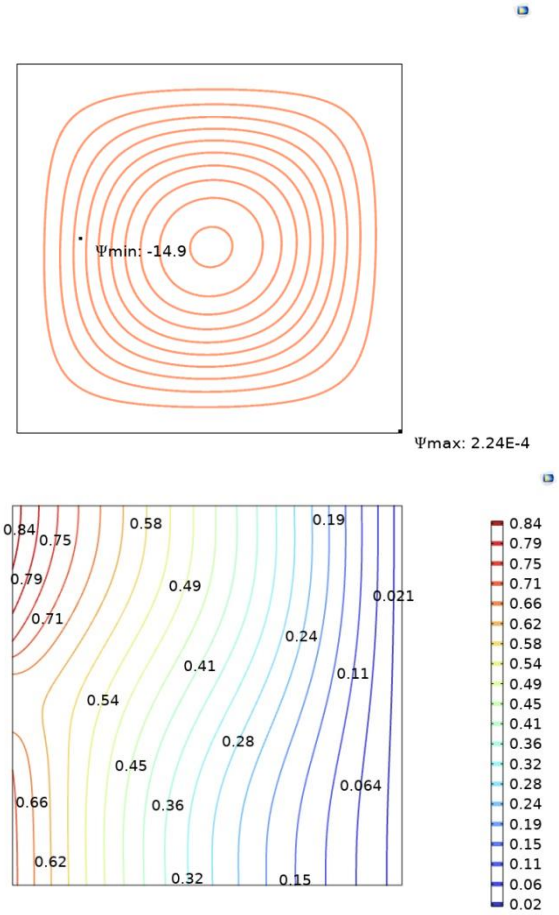

Figure(5.5): The streamlines and the isotherms when $H_B = H_T = 0.4$, Ra = 10^3.

Sankar et al. [22]	Present work
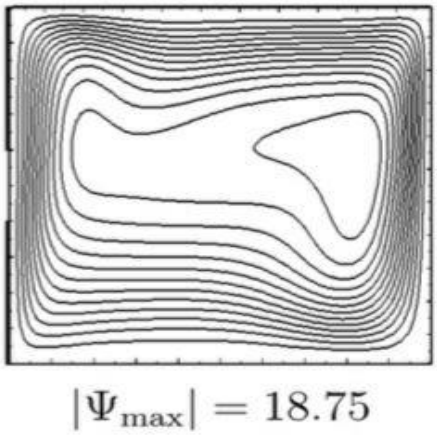 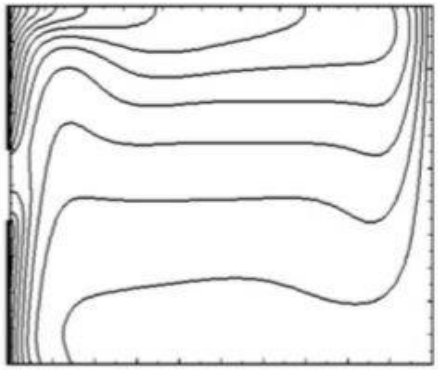 Ra = 10^7	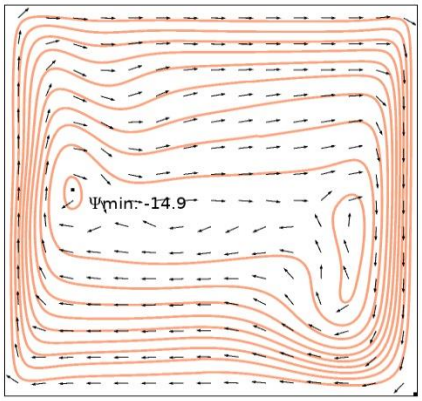 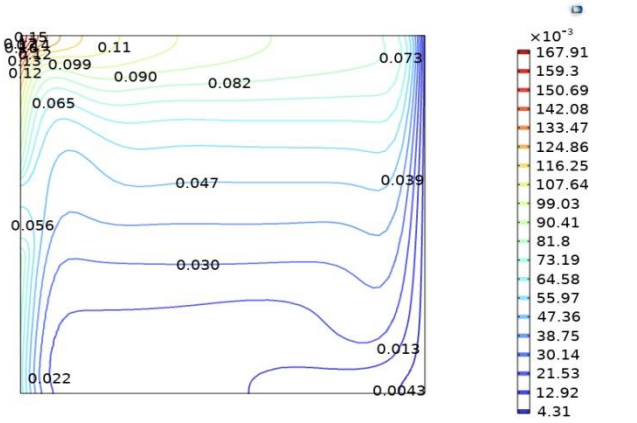

Figure(5.6): The streamlines and the isotherms when $H_B = H_T = 0.4$, Ra = 10^7.

The comparison among the previously attained results and recent results at (Ra =10^3 as well as Ra =10^7) has showed a good agreement .

5.3 Numerical Results of the Studied Cases

Results are obtained for the physical model resulting from the union of the heat sources with vertical geometry. Three cases are presented according to the number and location of heaters. The flow pattern, temperature distribution, as well as velocity distribution are determined and shown here for Pr =0.71 at different values of Ra considering the steady state laminar flow. The final results showed the variation of the Nusselt number with Rayleigh number for different number and length of heaters.

5.3.1 Case I (Five heaters at different lengths)

In this case, the middle heater(third heater) has the largest length (d = 0.0857), while the remaining four heaters are at the same length(d = 0.076). An accumulation of the isothermal lines in front of each heater is noticeable which seems to be very intensive near the heater and starts to diminish when getting away from the heater. It was observed that there was a huge difference in contours at the lowest value of Ra = 10^3 versus Ra =10^7 as shown in figures(5.7),(5.8) , and (5.9), where the streamlines contours become more intensive at a greater magnitudes of Ra . For smaller value of Ra , (Figure(5.7)), the thermal transmission from the separated heat sources is majorly controlled by the conductive technique, which is noticed by the approximately not deformed isotherms for all the heat source sizes , moreover a circulation manner is circulating around the core of the annulus can be observed. The buoyancy forces drives the fluid upraised , on the other hand the lower temperature drives it downward. By increasing Ra to 10^7 ,it was observed that the stream lines exhibited an improving circulation model and higher intensity of vortices as well as isotherms exhibited stratified temperature layers in the annular space. Vortices corresponding to each heat source were observed which

formalizes the flow pattern. It is obvious that the circulation as well as thermal domains are majorly affected by Ra as well as the size of heat sources.

Isotherms	Stream lines
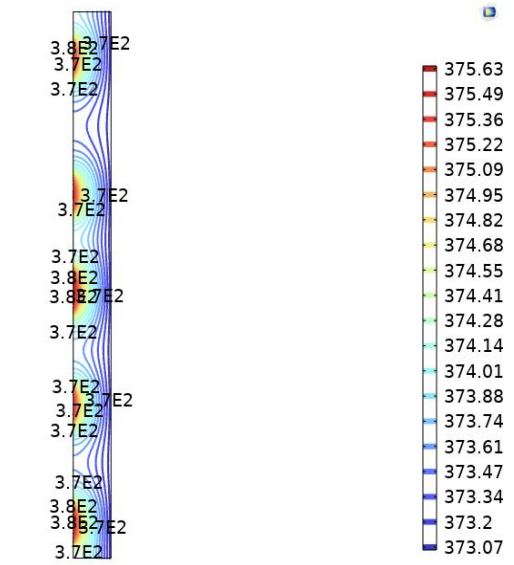 Ra = 10^3	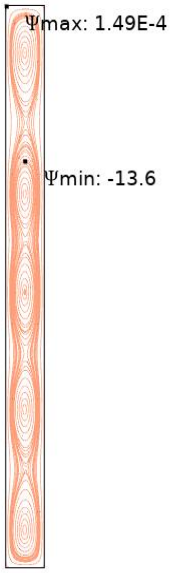 Ra = 10^3
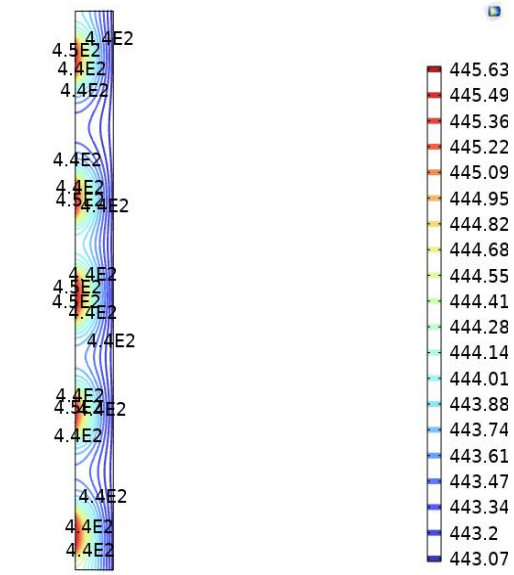 Ra = 10^4	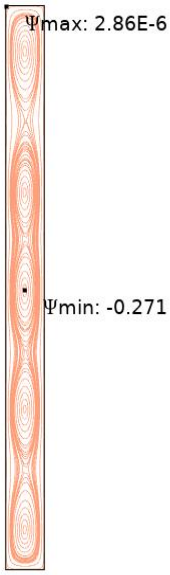 Ra = 10^4

Figure(5.7): The streamlines and the isotherms case I(five heaters, different lengths) at Ar = 25.6 for Ra = 10^3and10^4.

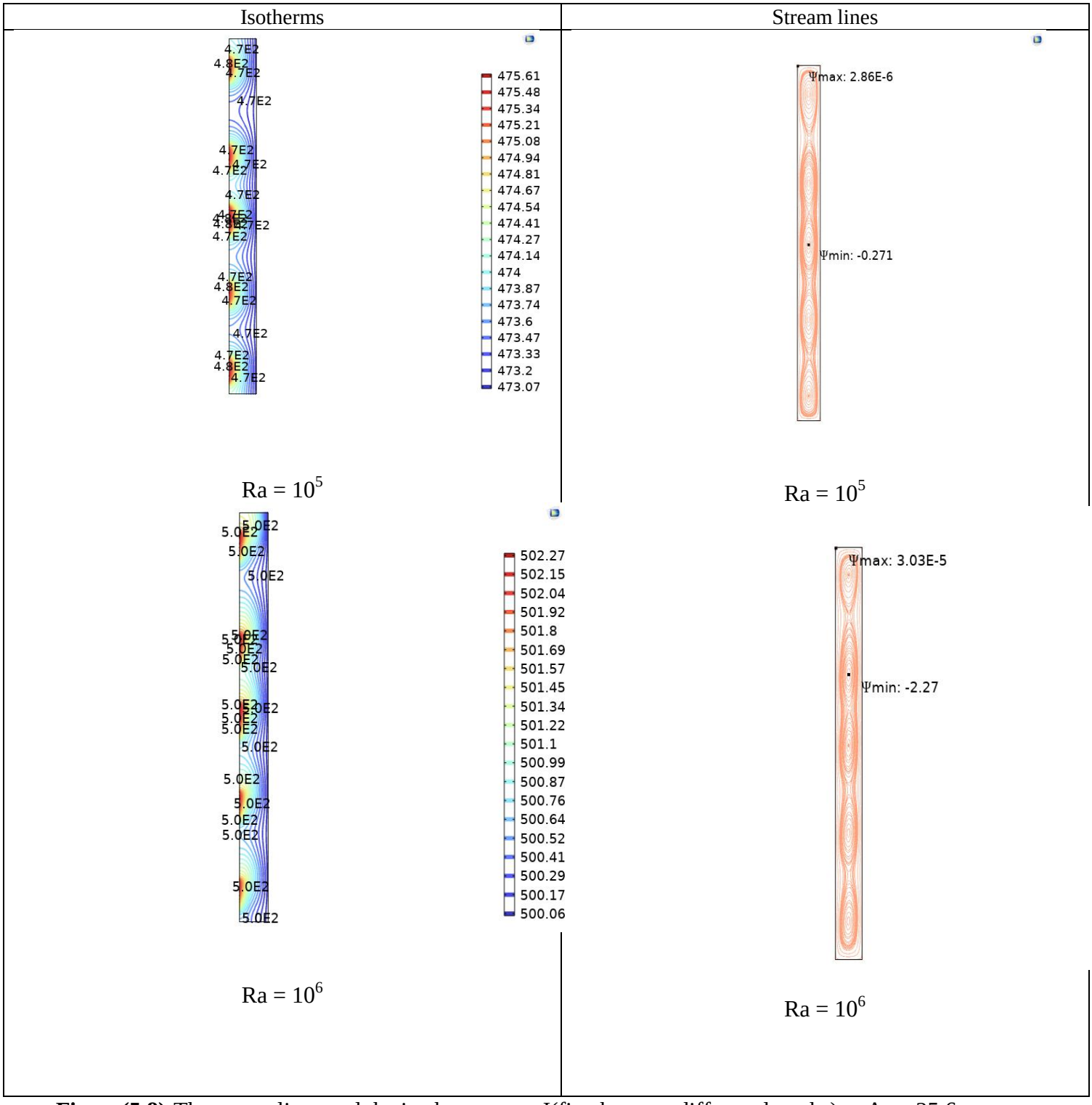

Figure(5.8): The streamlines and the isotherms case I(five heaters, different lengths) at Ar = 25.6 for Ra = 10^5and10^6.

Isotherms	Stream lines
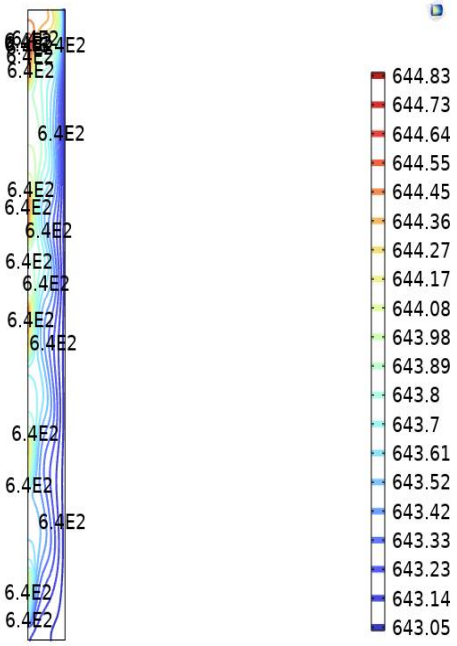 Ra = 10^7	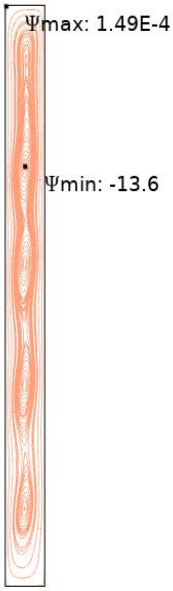 Ra = 10^7

Figure(5.9): The streamlines and the isotherms case I(five heaters, different lengths) at Ar = 25.6 for Ra = 10^7.

5.3.2 Case II (Four heaters of equal lengths)

In this case four heaters a of equal lengths (d= 0.076) were used, the results are demonstrated in figures(5.10), (5.11), and(5.12), Stream lines as well as isothermal lines at various magnitudes of Ra.

An accumulation of the isothermal lines in front of the location of each heater was very obvious which means that the temperature gradients are very large at this location. Furthermore, a formation of streamline swirls is seen which are adjacent to each heater's location. It was observed that the intensity of the streamlines and isotherms reached the highest level at the highest value of Ra = 10^7, furthermore at this value there was an integration between the two upper swirls and the two lower swirls of streamlines as well as the intensity of the stream lines reached the highest.

On the other hand, the swirls were separated with a space in the middle of the annuli at lower Ra =10^3,10^4. Also there was a noticeable gap in the middle space among the upper and lower heat sources in the isotherms at these low values of Ra. At the highest value of Ra figure (5.12), an accumulation of the isotherms was noticed at the top of the domain. This accumulation is due to the buoyancy forces which lifts up the hottest layer of air upward. Moreover, the velocity contours expanded to fill the whole area and to form two large vortices where the upper vortex was noticed to be larger than the lower one. Generally, the different magnitudes of the stream function in various locations results from the differences in the temperatures in each location, the negative sign represents the opposite direction.

Isotherms	Streamlines
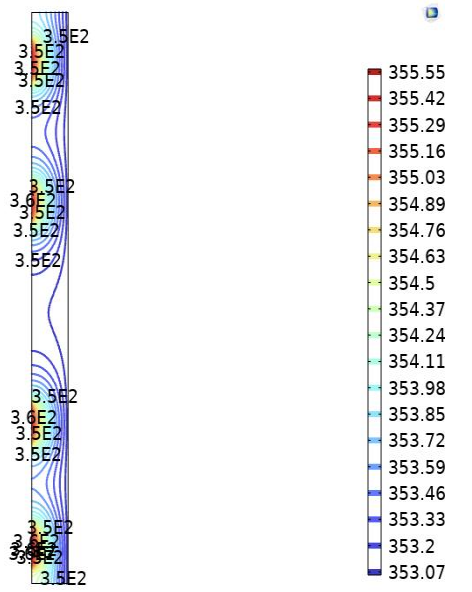 Ra = 10^3	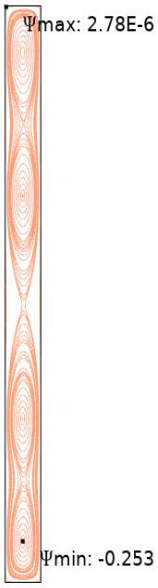 Ra = 10^3
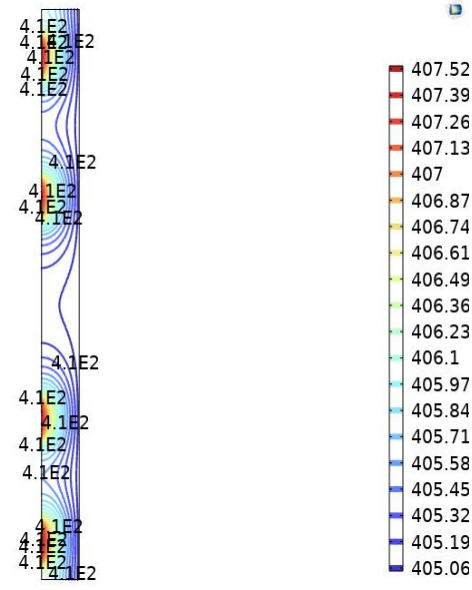 Ra = 10^4	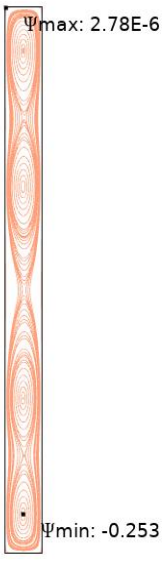

Figure(5.10):The streamlines and the isotherms case II(four heaters, equal lengths) at Ar = 25.6 for Ra= $10^3$and 10^4.

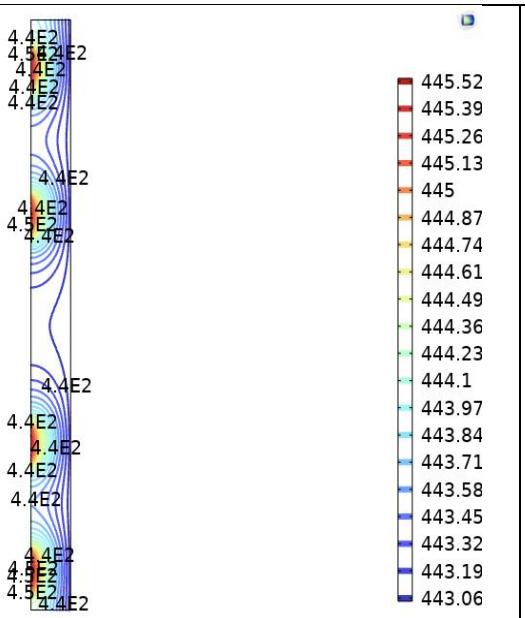

Ra = 10^5

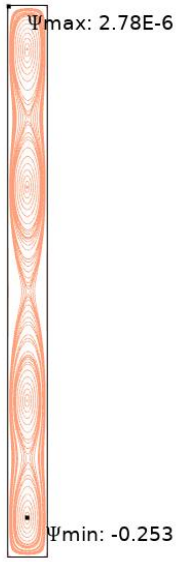

Ra = 10^5

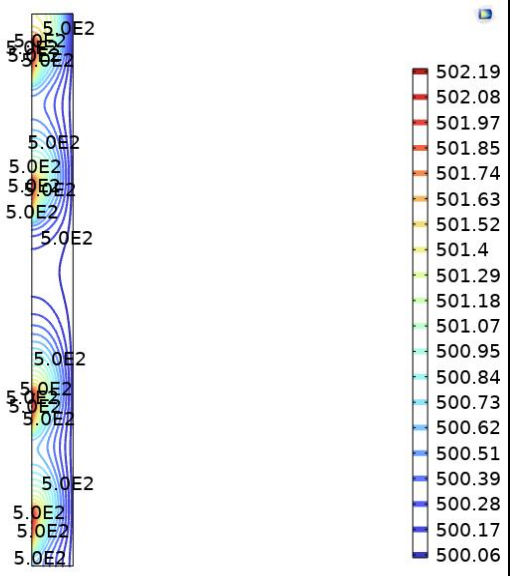

Ra = 10^6

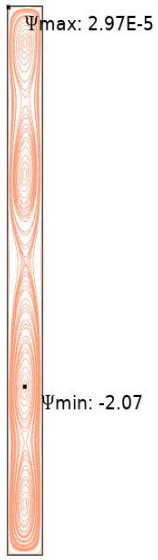

Ra = 10^6

Figure(5.11):The streamlines and the isotherms case II(four heaters, equal lengths) at Ar = 25.6 for Ra= $10^5$and 10^6

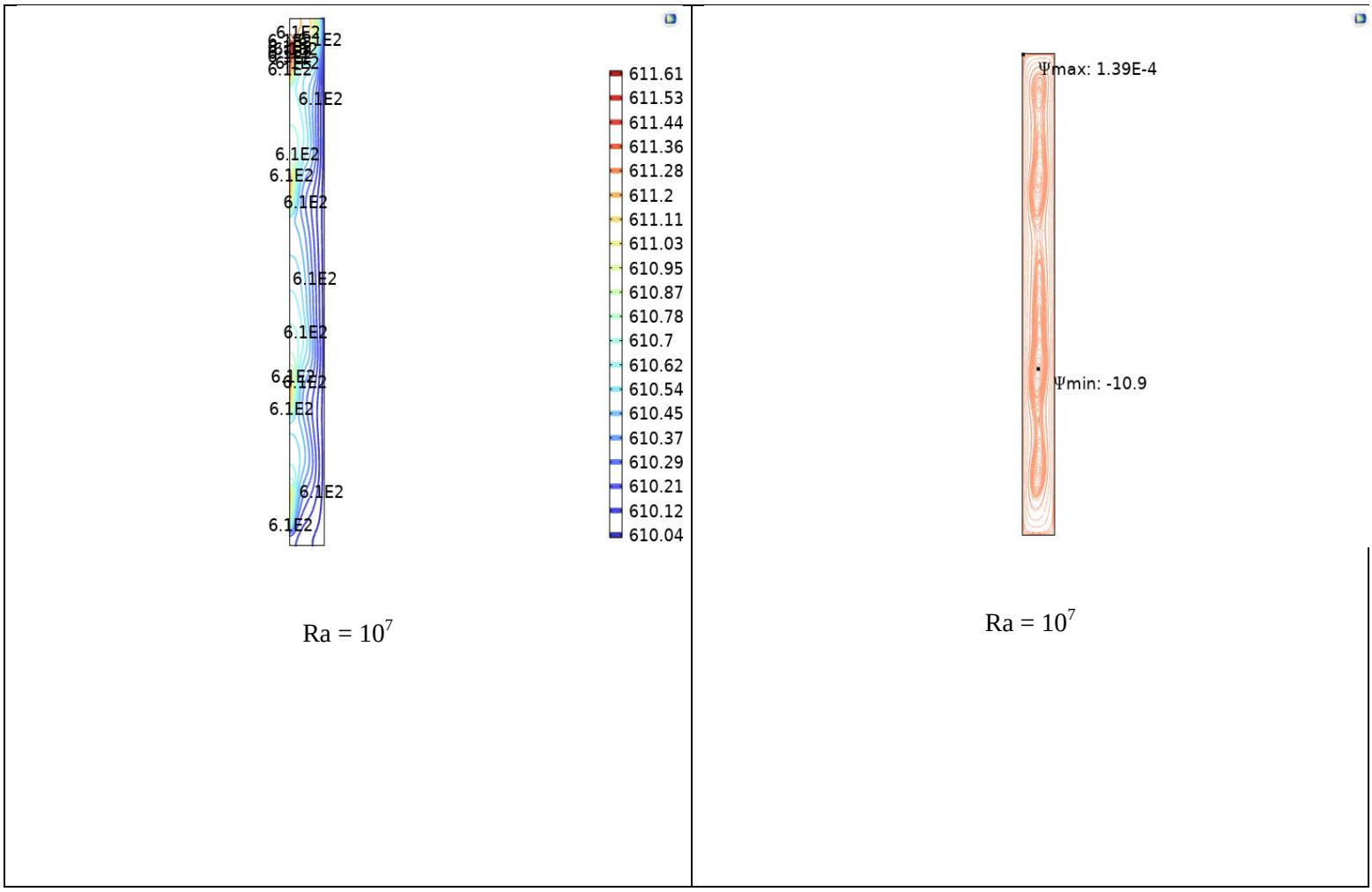

Ra = 10^7 Ra = 10^7

Figure(5.12): The streamlines and the isotherms case II(four heaters, equal lengths) at Ar = 25.6 for Ra = 10^7.

5.3.3 Case III (Three heaters at different lengths)

Three heaters at different lengths were used, figures (5.13),(5.14), and (5.15) illustrates the streamlines as well as isothermal lines for this case at different values of Ra. The warmed fluid starts to raise upward according to its low density due to the buoyancy forces, while the cooler fluid drops down due to its large density, this represents the mechanism of the natural convective flow.

The major and largest swirl in the middle of the enclosure can be obviously observed in figure (5.13). In this case (three heaters) a large space can be noticed in the isothermal contours between the top and middle heater as well as between the bottom and muddle heater leaving a stagnant region at this gap. Nevertheless, this static area vanishes and the intensity of the isothermal lines is boosted when reaching the upper heat source. Moreover, figure (5.15) clearly shows that the creation of TBL along each heat source, as well as stratified temperature in the central domain become increasingly evident, indicating the ascendancy of a convective thermal transmission technique in cooling the separated heat sources. For varying Ra, changing the temperature along the separately warmed outer surface of the annulus is demonstrated in all three distinct cases of heating. The influences of various types of separate warming on the thermal fields at the heated wall of the annulus is very obvious.

Isotherms	Stream lines
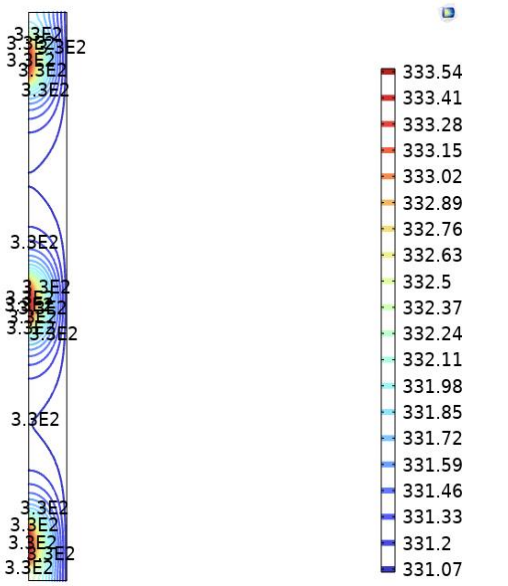 Ra = 10^3	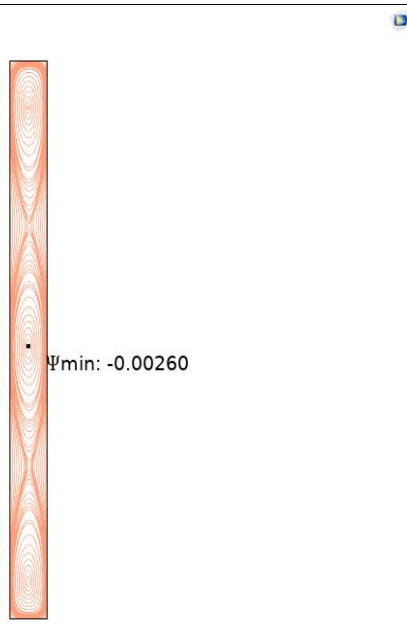 Ra = 10^3
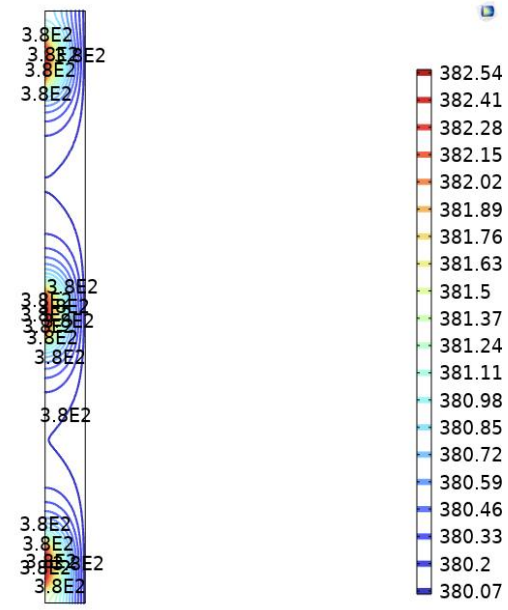 Ra = 10^4	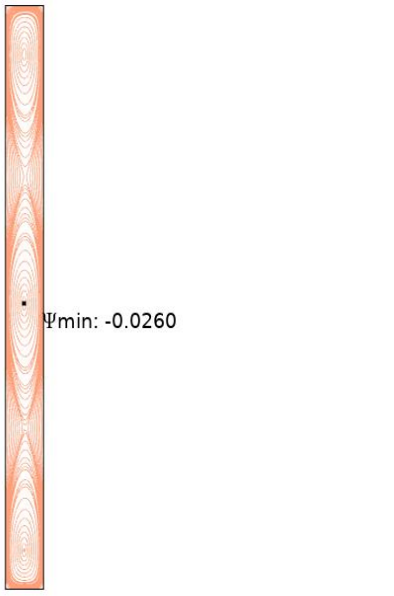 Ra = 10^4

Figure(5.1**3**): The streamlines and the isotherms case III(three heaters, different lengths) at Ar = 25.6 for Ra =$10^3$and 10^4

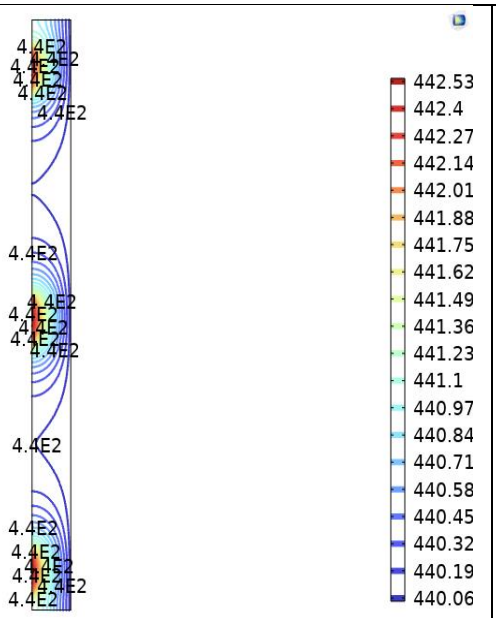

Ra = 10^5

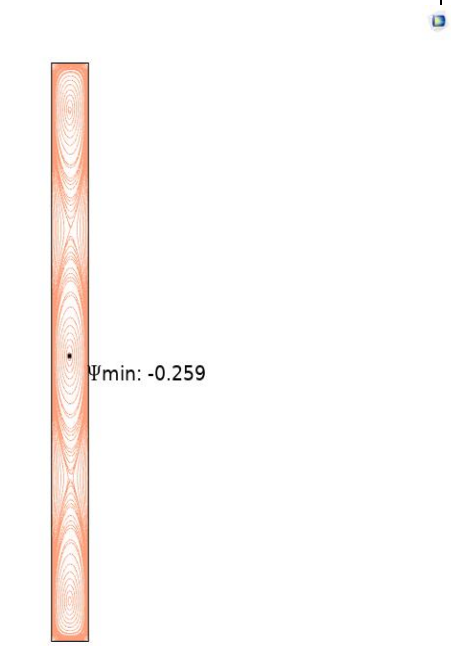

Ra = 10^5

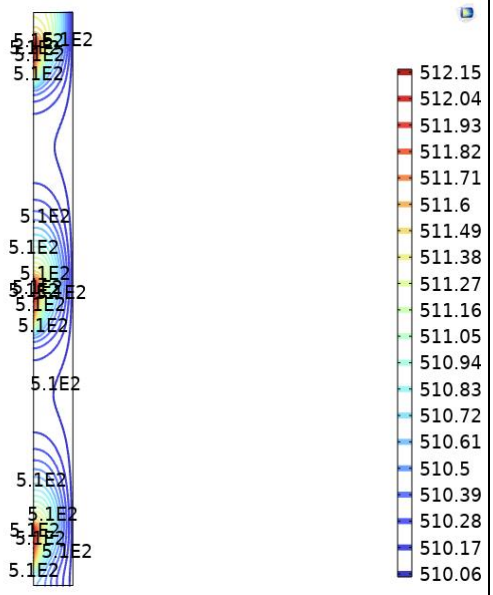

Ra = 10^6

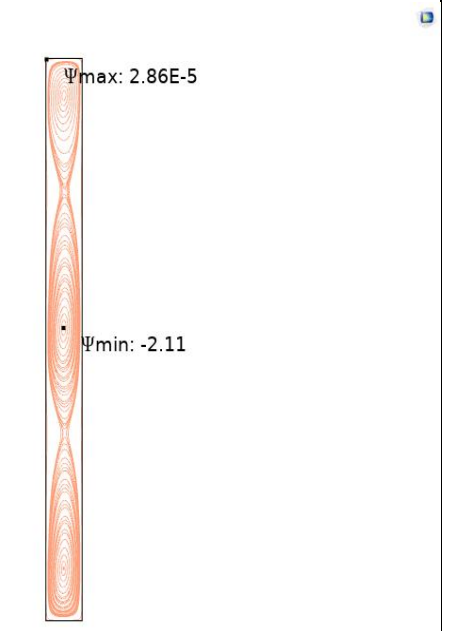

Ra = 10^6

Figure(5.14): The streamlines and the isotherms case III(three heaters, different lengths) at Ar = 25.6 for Ra =$10^5$and 10^6

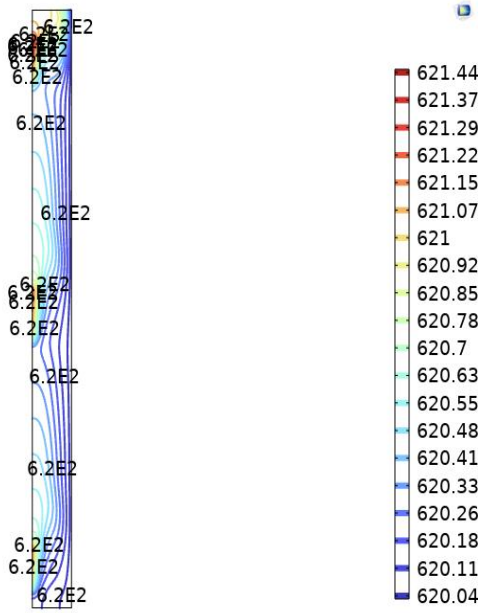

Ra = 10^7

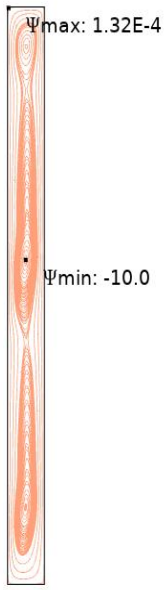

Ra = 10^7

Figure(5.15): The streamlines and the isotherms caseIII(Three heaters, different lengths) at Ar = 25.6 for Ra = 10^7.

5.3.4 Nusslet Number

The local Nu is estimated for five different locations of the heat sources as shown in figures below.

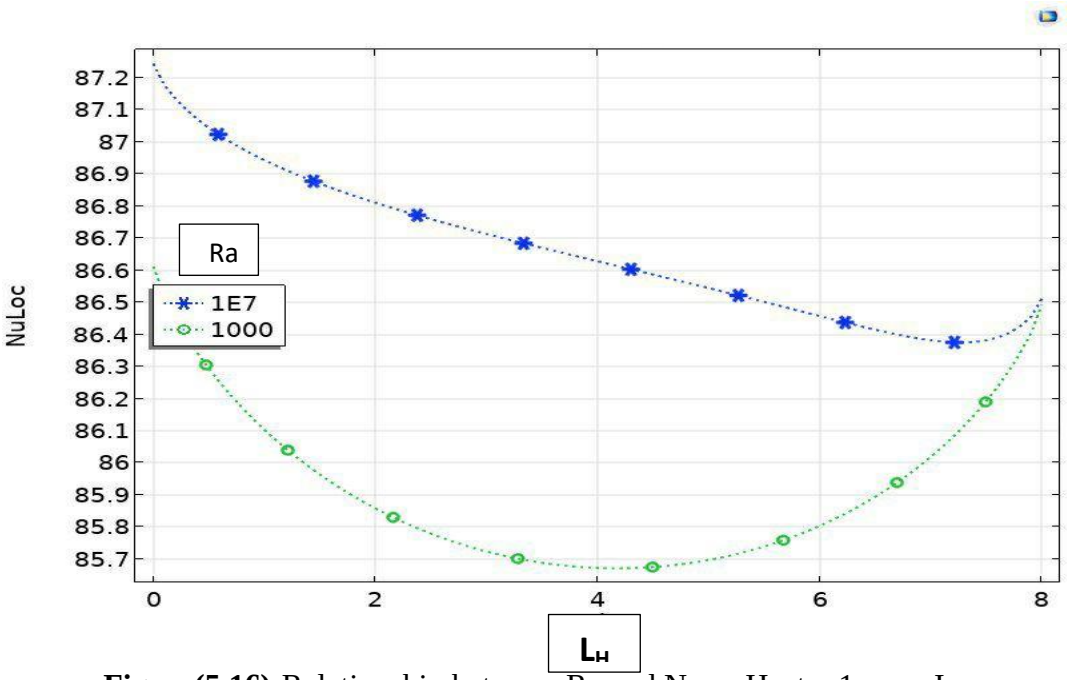

Figure(5.16): Relationship between Ra and Nu $_{loc}$ Heater 1, case I

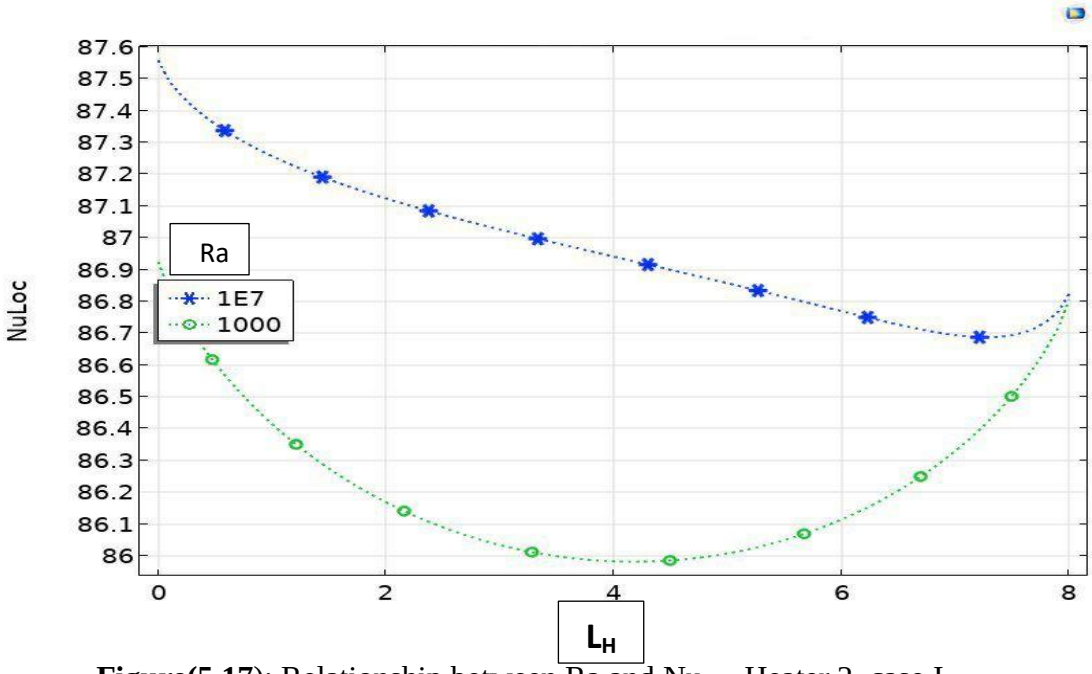

Figure(5.17): Relationship between Ra and Nu $_{loc}$ Heater 2, case I

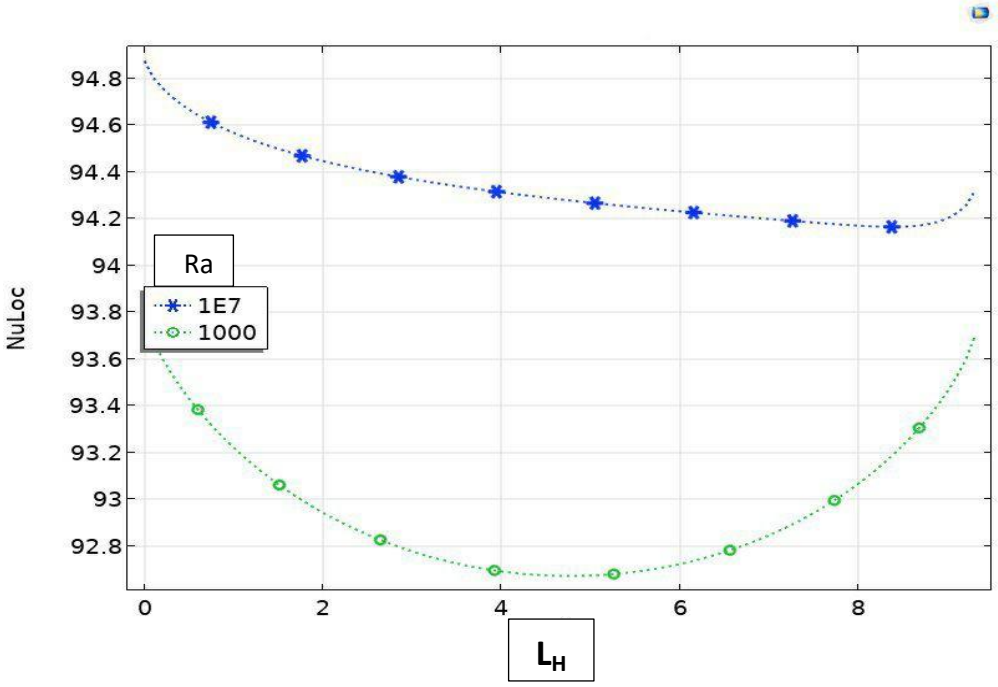

Figure(5.18): Relevance among Ra and Nu $_{loc}$ Heater 3, case I

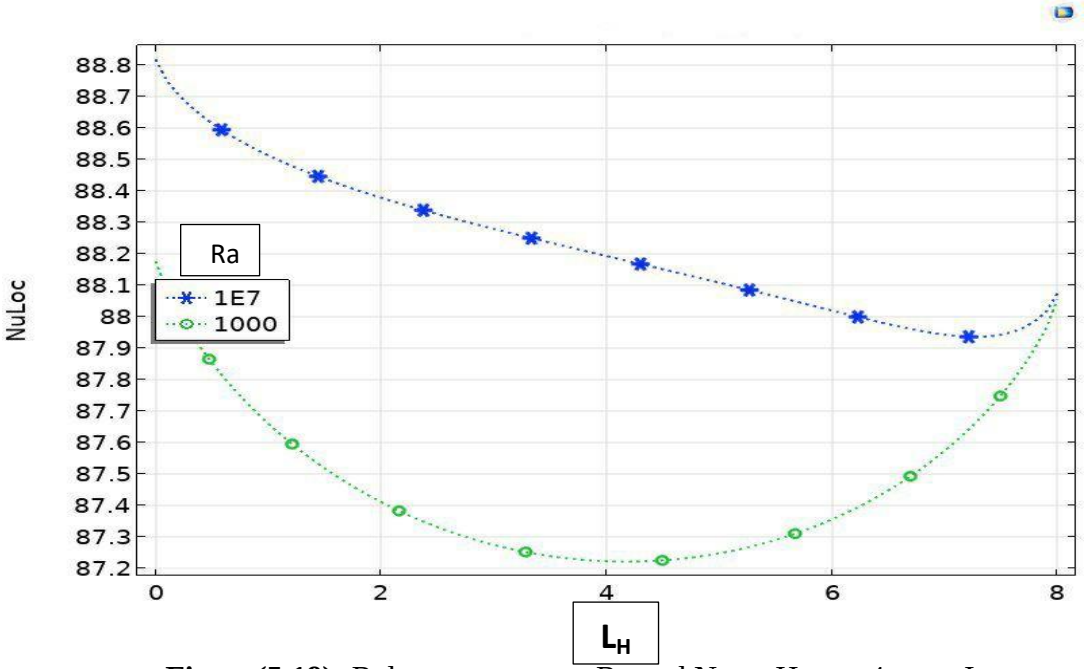

Figure(5.19): Relevance among Ra and Nu $_{loc}$ Heater 4, case I

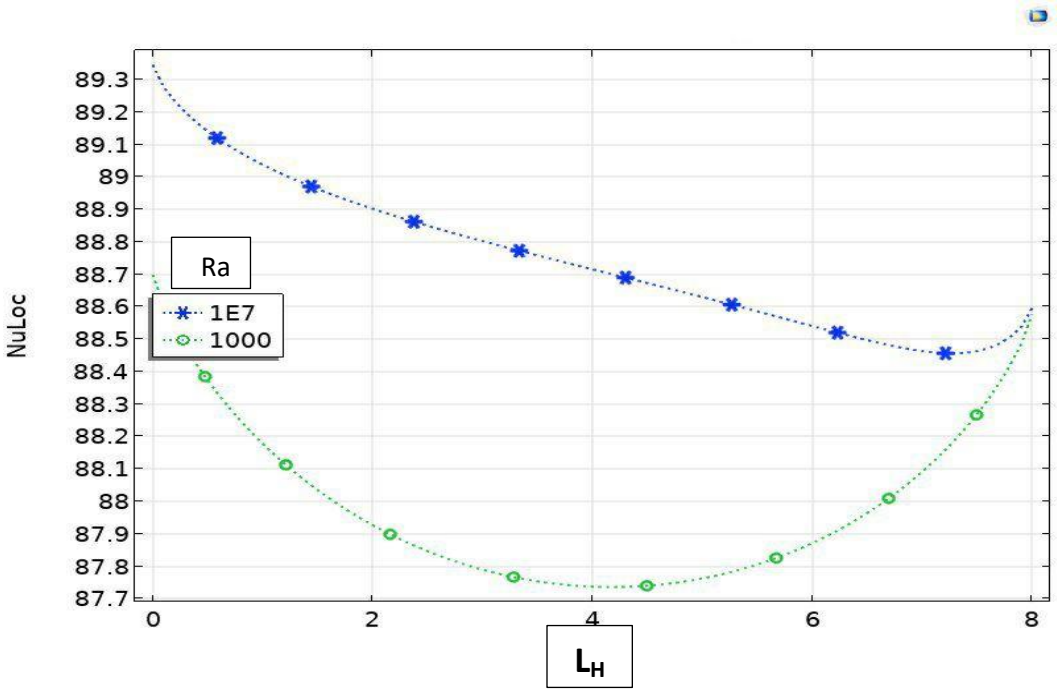

Figure(5.20) : Relationship between Ra and Nu $_{loc}$ Heater 5, case I

The total Nusslet number represents the total amount of thermal transmission which is an indication to the efficiency of heat transfer as illustrated in figure below.

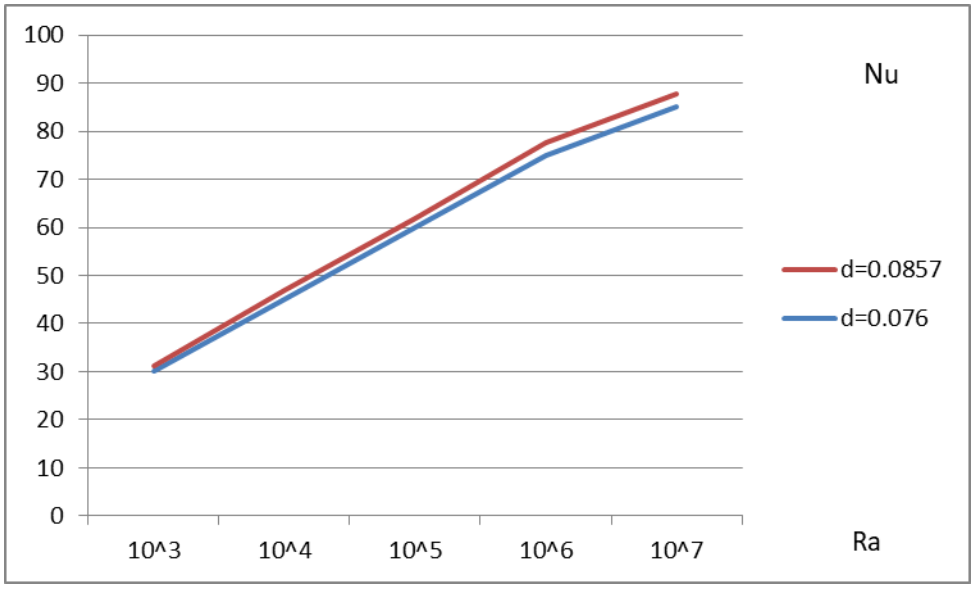

Figure(5.21): Total Nusslet number with Rayleigh number

Figures(5.16),(5.17),(5.18),(5.19),and (5.20) shows the change in the value of the regional Nusslet number according to the location and length of the heat sources.

It was observed that there was a slight change in Nu because of changing the heat source position when using the same length of heat source, while there was a noticeable increase in the value of Nu when using a higher value of heater length.

The highest value of Nu was observed at the third heater(highest length which was illustrated in figure (5.21) that represents the total Nusslet number.

It was also observed that raising the value of Rayliegh number raises the value of Nusslet number. Generally, high values of Nu was estimated since Nu depends mainly on the amount of the applied thermal flux , where a high value of q was applied to reach these results.

5.4 Experimental Results

5.4.1 Results of Case I

Figure (5.22), (5.23), (5.24), (5.25), and (5.26) represents the isothermal contours map on (x-y) plane for case I. In this case five heaters were used. These contours were plotted at different values of Ra. The temperature difference results an increase in Ra magnitude. Here the thermal flux is coming from five sources which leads to increase in the intensity of the heat flux, consequently a large development in the thermal layers will result. The augmentation in the thermal layers will result to boost the buoyancy strength.

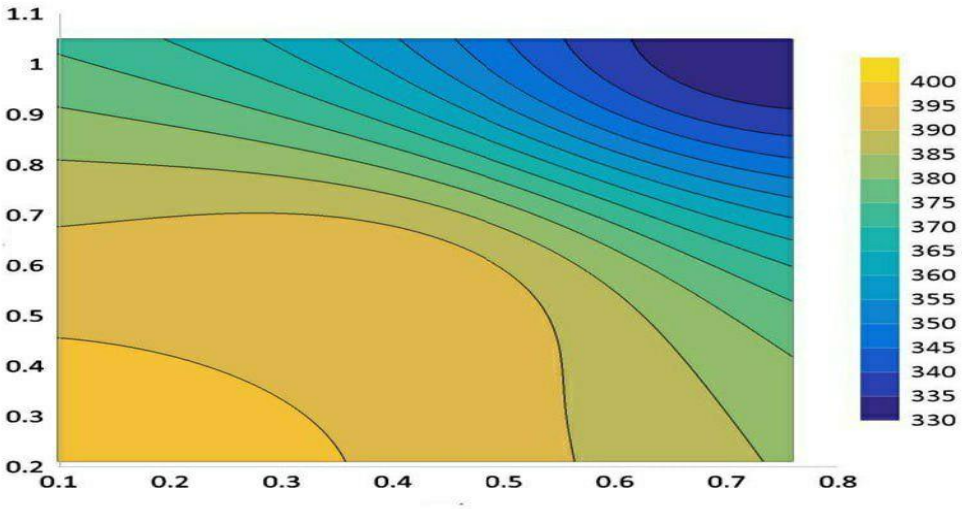

Figure(5.22): x-y Contour map for isothermal lines Ra 10^3

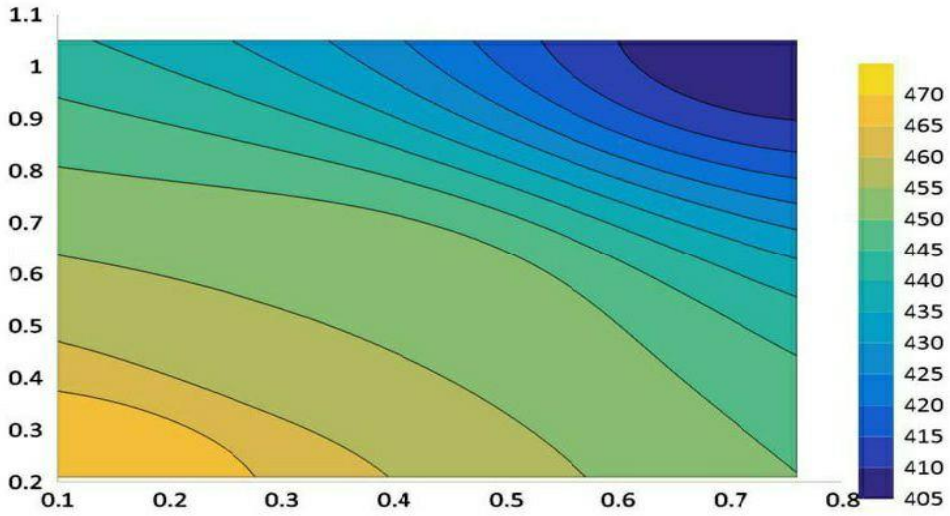

Figure(5.23): x-y Contour map for isothermal lines Ra10^4

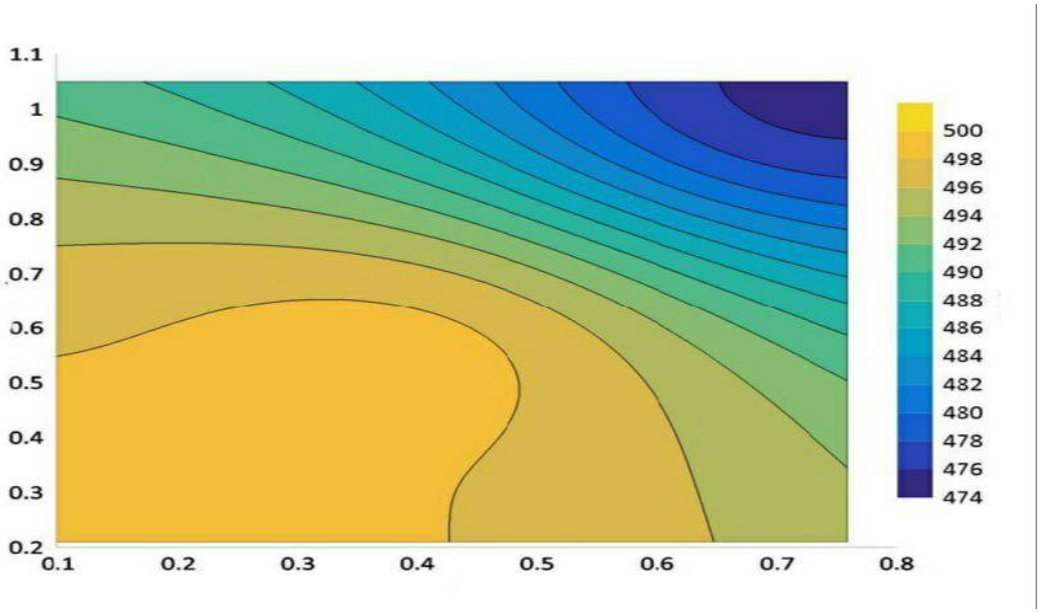

Figure(5.24): x-y Contour map for isothermal lines $Ra10^5$

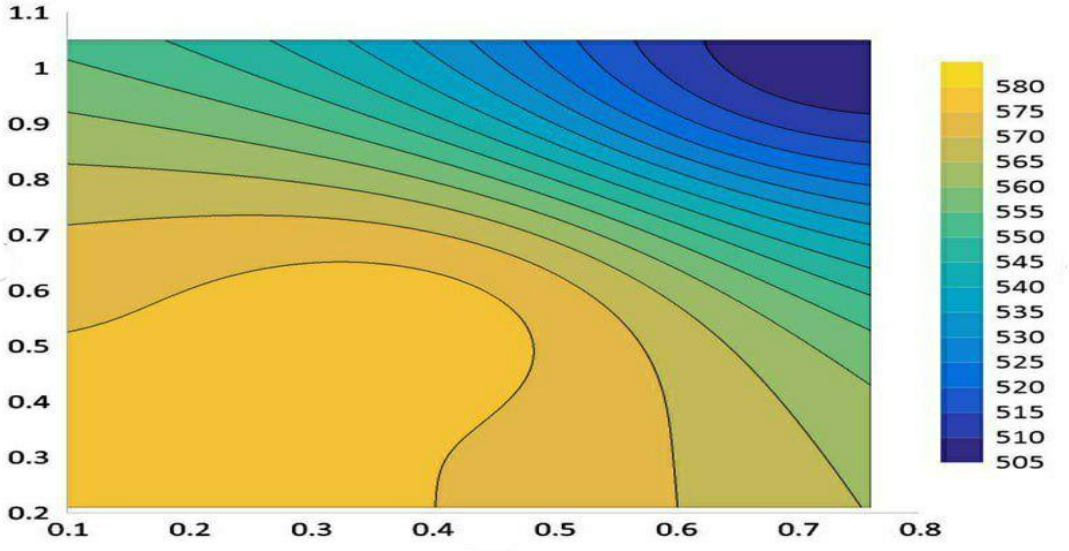

Figure(5.25): x-y Contour map for isothermal lines $Ra10^6$

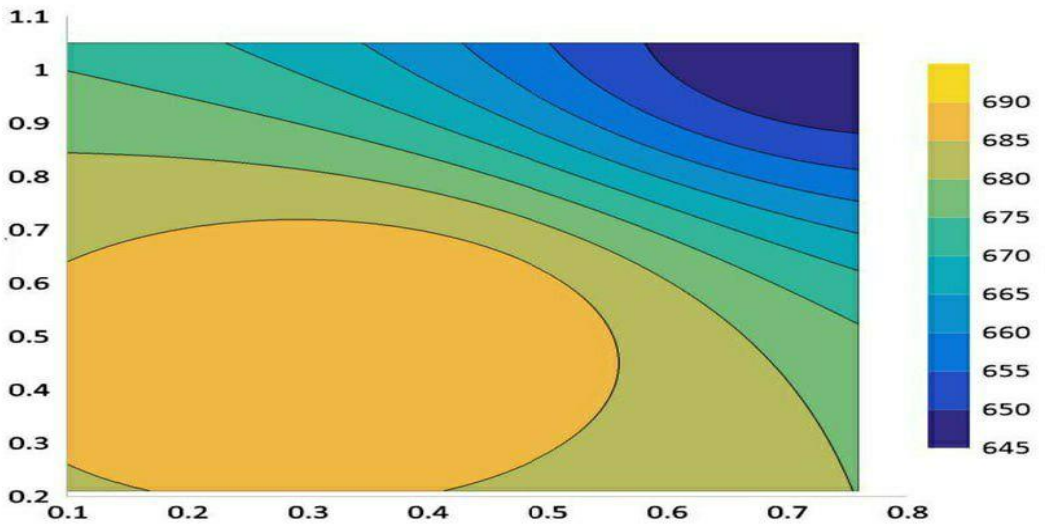

Figure(5.26): x-y Contour map for isothermal lines $Ra10^7$

5.4.2 Results of Case II

Figure (5.27),(5.28),(5.29),(5.30),(5.31) illustrates the isothermal contour map in (x-y) plane. In this case four heaters were used. Different values of temperature differences will produce different values of Ra. The heat flux was supplied by four sources in this case. There is a slight difference between the intensity of the heat flux here and the previous case due to the number of the sources that supplies thermal flux.

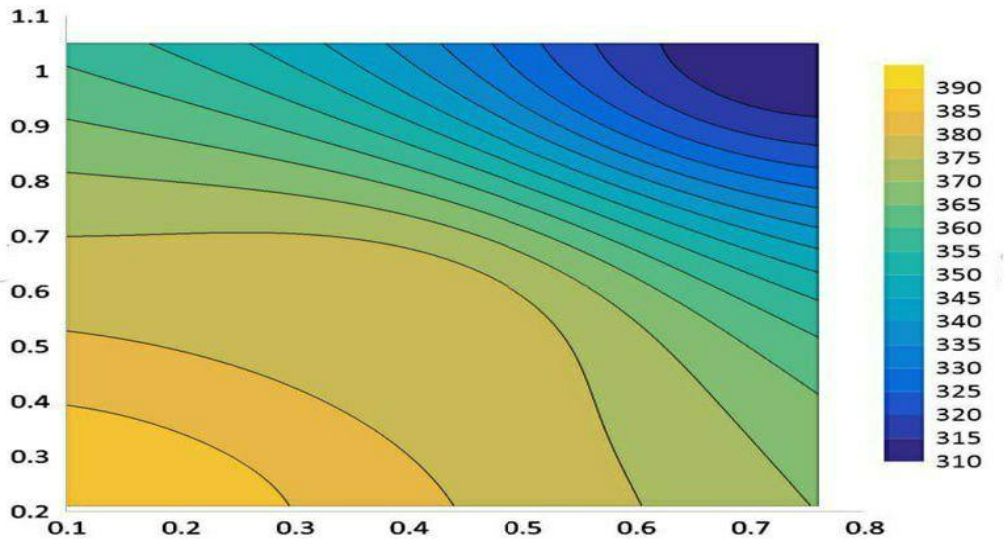

Figure(5.27): x-y Contour map for isothermal lines Ra 10^3

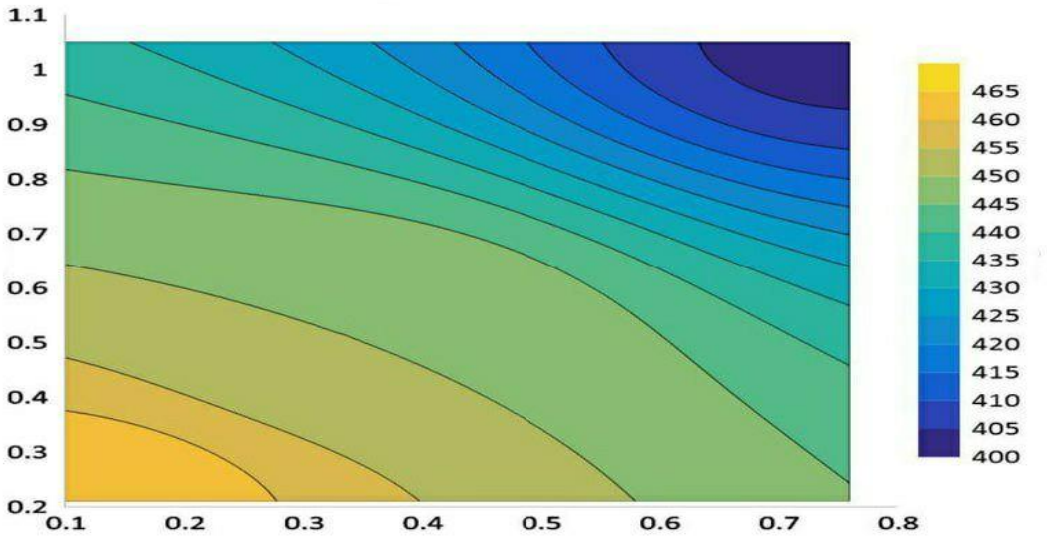

Figure(5.28): x-y Contour map for isothermal lines Ra10^4

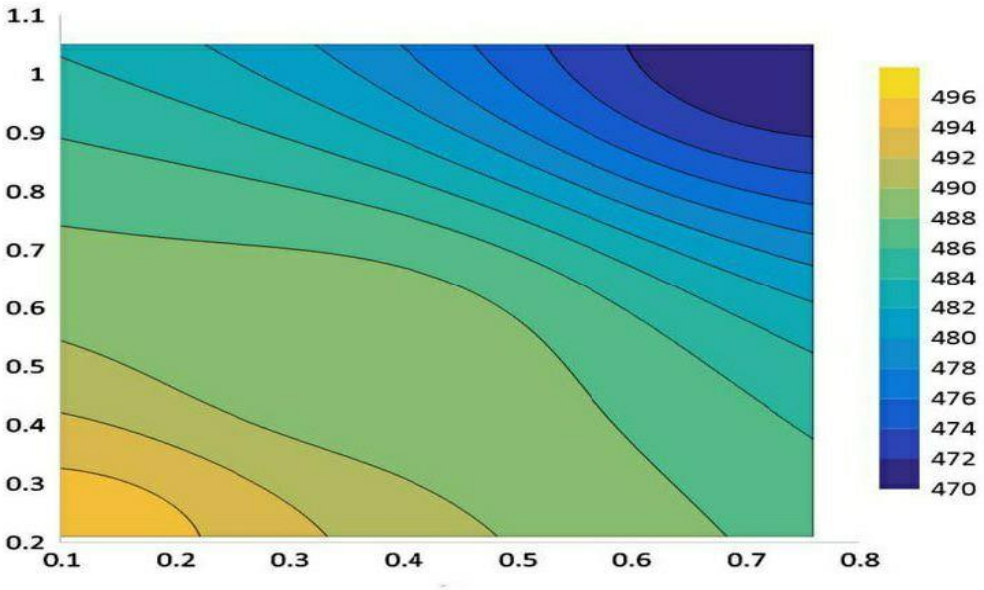

Figure(5.29): x-y Contour map for isothermal lines $Ra10^5$

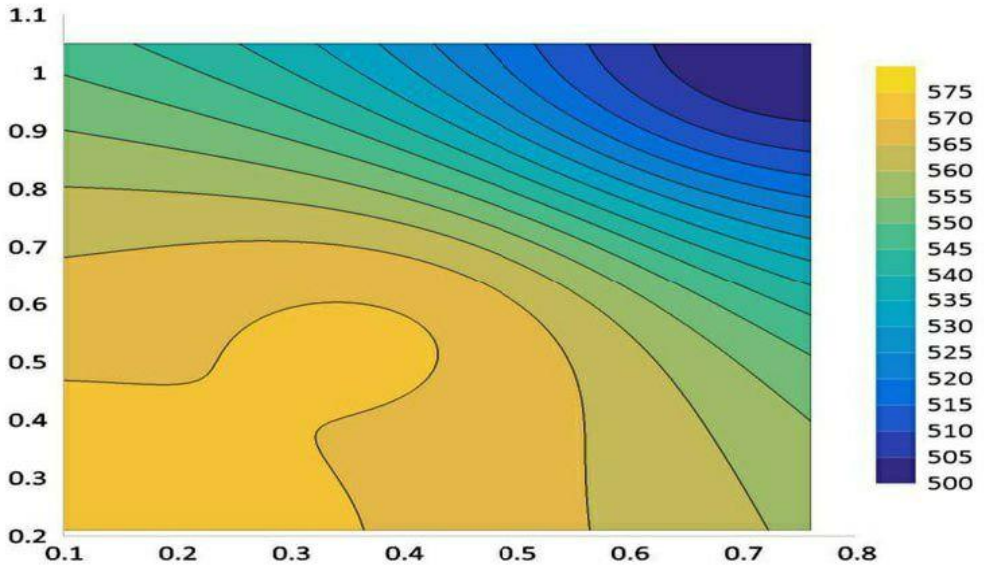

Figure(5.30): x-y Contour map for isothermal lines $Ra10^6$

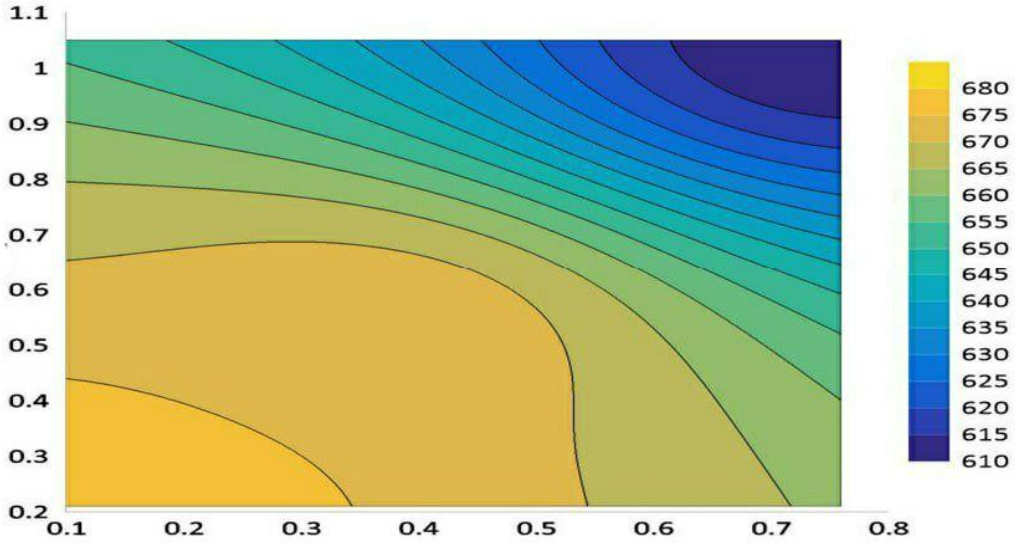

Figure(5.31): x-y Contour map for isothermal lines $Ra10^7$

5.4.3 Results of Case III

Figure(5.32),(5.33),(5.34),(5.35),(5.36) demonstrates the (x-y) plane contour map for the isothermal lines. In this case three heat sources were used, consequently the intensity of the supplied heat flux is less than the two previous cases. In the same way, temperature differences produces changes in the values of Ra. Figure(5.37) represents the relationship between Nu_{avg} with Ra for three distinct cases. It was observed that the highest value of Nu was at caseI due to the large values of temperature differences which leads to a higher value of Ra , consequently achieves a better thermal transmission represented by a huge value of Nu.

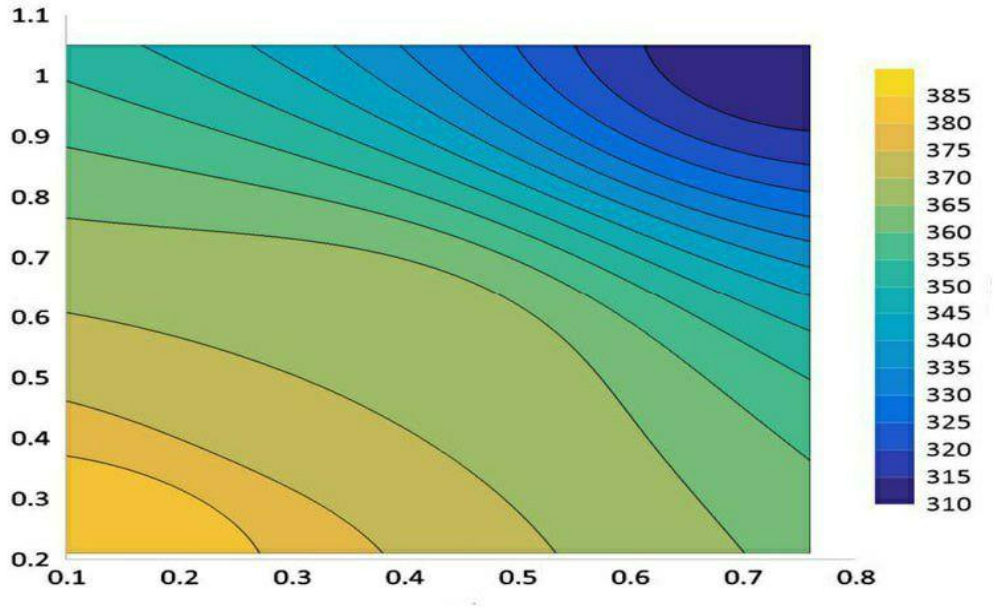

Figure(5.32): x-y Contour map for isothermal lines Ra 10^3

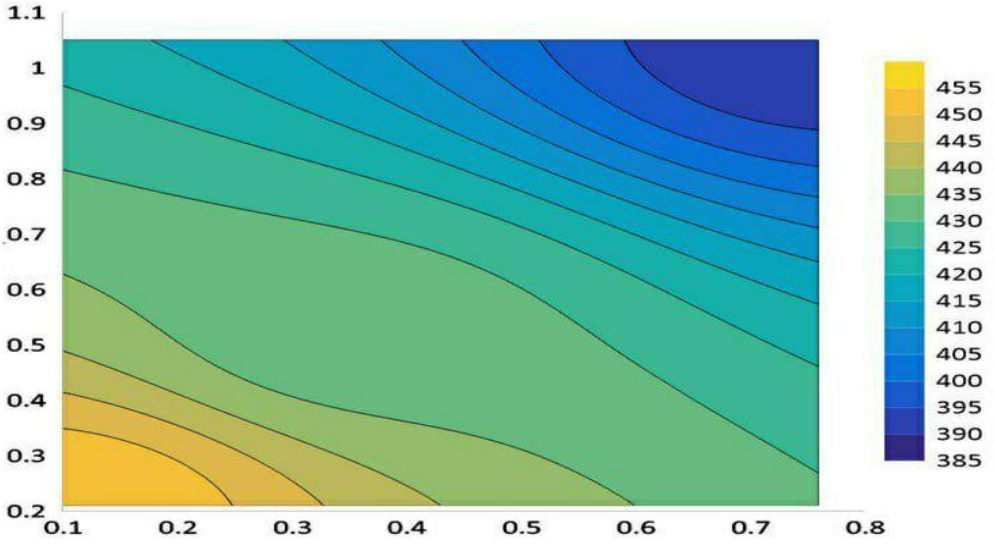

Figure(5.33): x-y Contour map for isothermal lines Ra 10^4

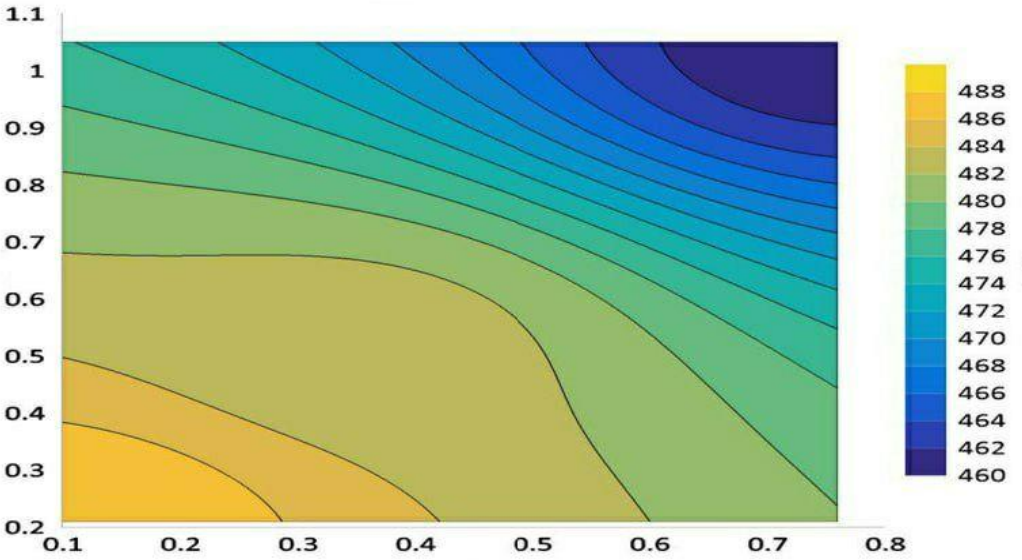

Figure(5.34): x-y Contour map for isothermal lines Ra 10^5

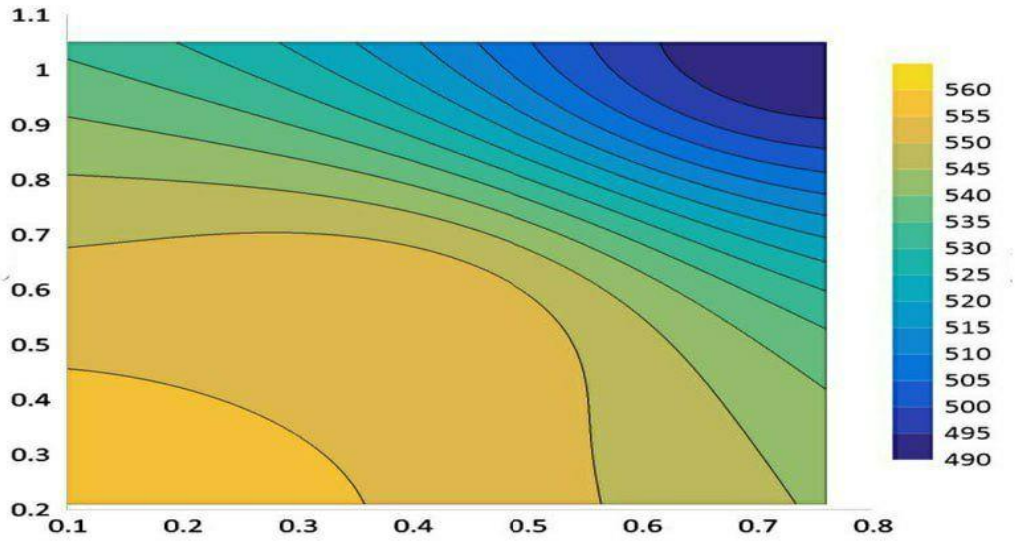

Figure(5.35): x-y Contour map for isothermal lines Ra 10^6

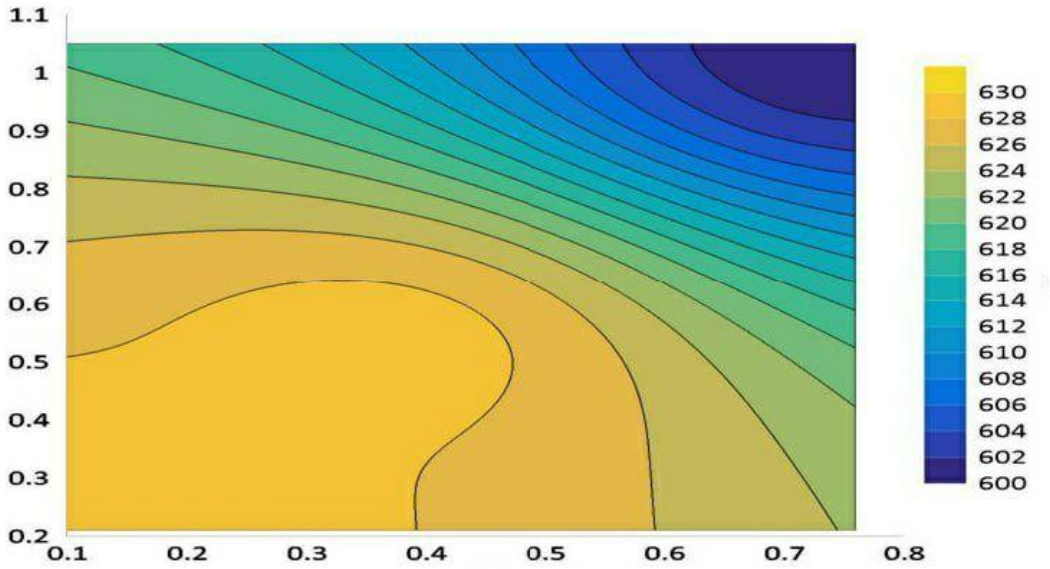

Figure(5.36): x-y Contour map for isothermal lines Ra 10^7

Figure (5.37) shows the relationship between the total Nusslet number with Rayliegh number for three different cases. Obviously, the highest value of Nusslet number was achieved in case(I) which includes the highest nuber of heaters (5heaters). This demonstrates that increasing the number of heaters will raise the average heat transfer. On the other hand, lower rates of thermal transmission occurred in case(II) and case (III) consequently, since a smaller number of heat sources was used in these cases(four heaters for case(II) and three heaters for case(I)).

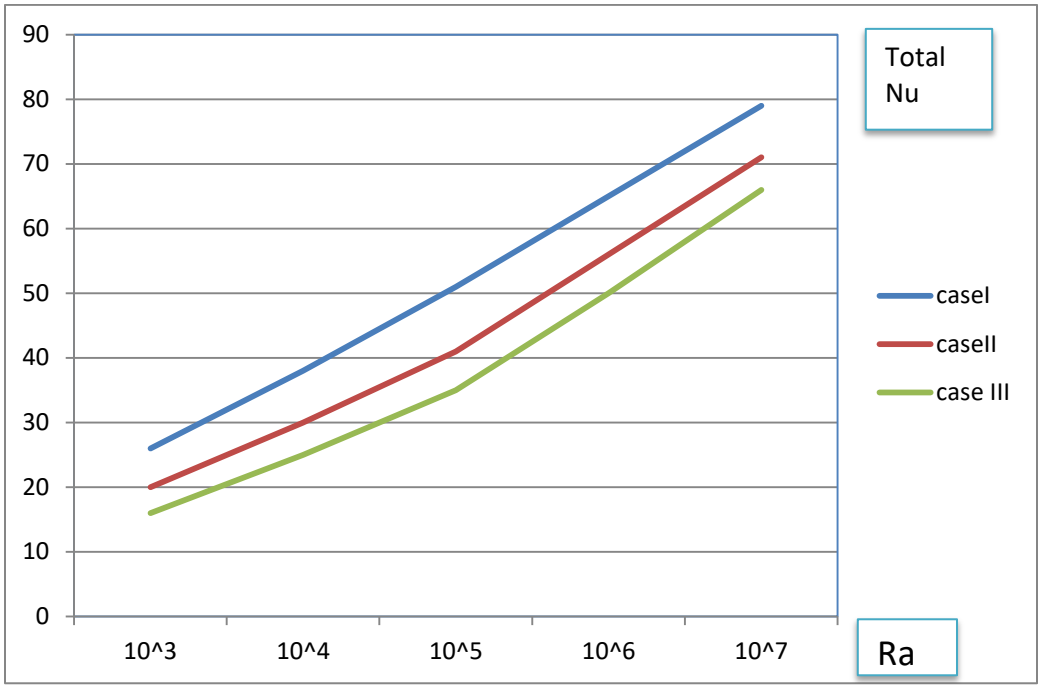

Figure(5.37): Relationship between total Nu and Ra

Figure (5.38) shows the relationship between the numerical and experimental average Nusslet number for case (I).There is a noticeable difference between the numerical and experimental results , this difference due to some errors that may occur during the measuring process .

Figure (5.39) shows the relationship between the numerical and experimental average Nusslet number for case (II).

Figure (5.40) shows the relationship between the numerical and experimental average Nusslet number for case (III).

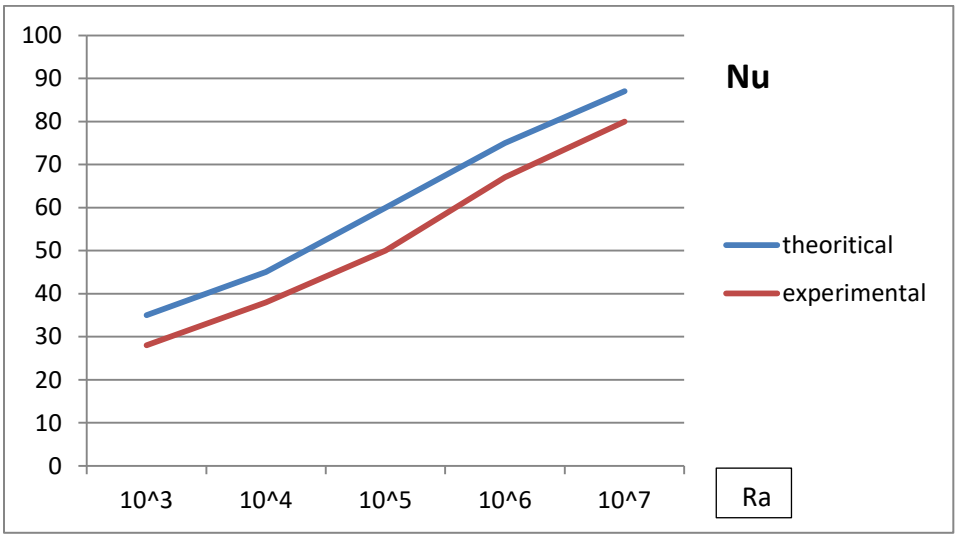

Figure(5.38): Comparison between theoretical & experimental Nu_{avg} for case I

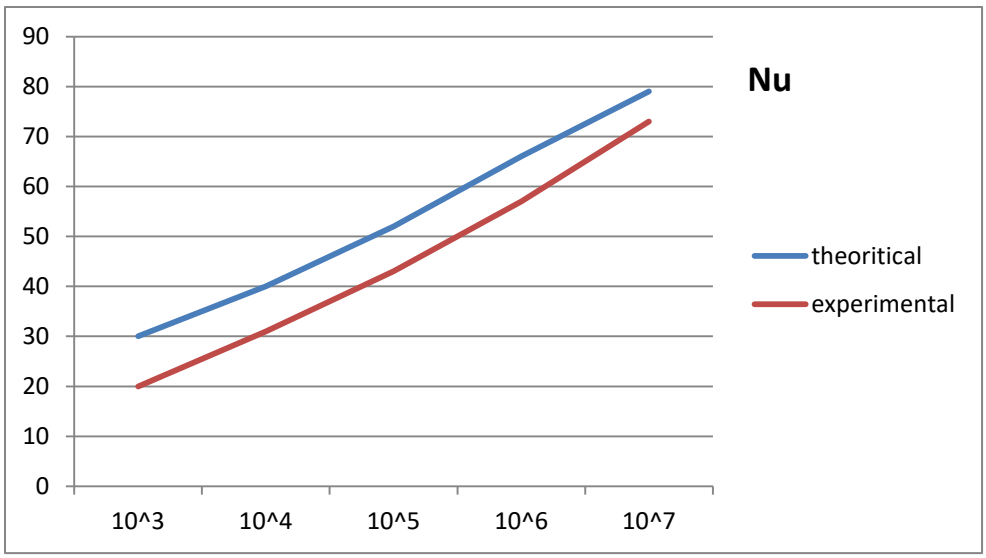

Figure(5.39): Comparison between theoretical & experimental Nuavg for case II

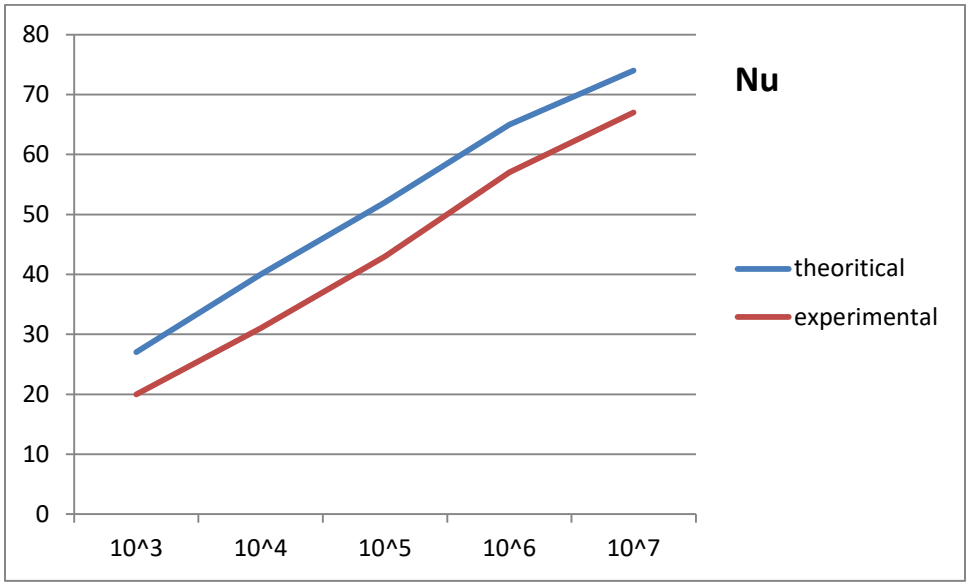

Figure(5.40): Comparison between theoretical & experimental Nuavg for case III

5.5 Comparing Computational & Experimental Results

The numerical results are compared to the experimental results to verify the CFD simulation for the same physical model that was done by COMSOL Multiphysics software package . A correspondence was evaluated from comparing theses outcomes. The percentage error among experimental and theoretical outcomes for case (I) is (18%) , for case(II) is (22%) and for case(III) is (24%). The percentage error formula was applied is [percentage error = [$(\Delta T_{num} - \Delta T_{exp})/\Delta T_{num}$]*100], an average value was taken to estimate the error. The comparisons between the experimental and theoretical results of the temperature difference between the T_h and T_c , where the temperature is estimated to be equal to:

$[\frac{\sum T}{number\ of\ T}]$ **[50].**

The difference among the experimental and computational outcomes occurred due to the following reasons:

1- Instrumental errors due to the inaccuracy of the instrument.

2- Human errors.

3- Procedural errors.

Chapter Six
Conclusion and Suggestions

Chapter Six

Conclusions and Suggestions

6.1 Conclusions

The most important points were concluded from this work can be summarized as following:

1- Increasing the number of heaters leads to an increase in the total Nusslet number values, Consequently enhancing the heat transfer rates.
2- Raising the heat source length improves the flow circulation and the thermal transmission ,this behavior was observed for all considered cases .
3- A significant influence on the local Nusslet number was observed due to changing the location and length of the heaters.
4- A noticeable agreement was observed between theoretical and experimental results.
5- Conduction heat transfer through air occurs when Rayleigh number is less than 10^3, while convection heat transfer (free convection) occurs at Nusselt number is greater than one and Rayleigh greater than 10^3.
6- The velocity raises from zero to the maximum value and at last decreases at the wall of the cylinder to reach zero.
7- It was observed that at highest value of Ra there was merging between the swirls and an increase in the intensity of the stream lines.

6.2 Suggestions

Here are some recommendations to the future work :

1- Investigating this work using different inclination angles to see the effect of inclination on Nu and thermal transmission.
2- Performing an experimental study using forced convection and comparing the results with free convection results.
3- Studying the entropy generation for the same problem.
4- Studying the same problem considered in the present work theoretically as well as experimentally using nano-fluids.
5- Performing the same study using different aspect ratios.
6- Investigating the same problem using more complicated geometries.

References

REFERANCES

[1] Latif M. Jiji , "Heat Convection" book Published by Springer , New York, USA, Second Edition, 2009.

[2] Ammar Abdulkadhim , Khaled Al-Farhany , Azher M. Abed , and Hasan Sh. Majdi, "Comprehensive Review of Natural Convection Heat Transfer in Annulus Complex Enclosures ", AL-QADISIYAH JOURNAL FOR ENGINEERING SCIENCES, vol.13, pp. 80-90, 2020.

[3] Holman J. P, "Heat Transfer" book Published by McGraw-Hill ,USA ,Tenth Edition ,2010.

[4] Rajput Er. R. K, "Heat and Mass Transfer" book Published by S. CHAND& LTD, India ,Fifth Revised Edition ,2012.

[5] A. Chandra and R. P. Chhabra," Effect of Prandtl Number on Natural Convection Heat Transfer from a Heated Semi-Circular Cylinder ",World Academy of Science, Engineering and Technology, vol. 61, 2012.

[6] Hoyt C.Hottel,S.M, "Heat and Mass Transfer" book Published by McGraw-Hill ,USA ,8 Tenth Edition ,2008.

[7] Yunus A. Cengel " Heat Transfer book " Tenth Edition ,2012.

[8] Tahseen A. Al-Hattab , Majid H. Majeed , and Mushtaq F. Abd-Saada, "Heat Transfer by Free Convection between Horizantl Concentric Pipes " , The Iraqi Journal For Mechanical And Material Engineering, Vol.8, No.3, 2008.

[9] J. Mustafaa , M. A. Siddiquib , and S. F. Anwer, "Experimental and Numerical Analysis of Heat Transfer in a Tall Vertical Concentric Annular Thermo-siphon at Constant Heat Flux Condition", Heat Transfer International Journal, VOL. 40, NO. 11,2019.

[10] Mohamed A. Aziz, and Osama A. Gaheen," Effect of the isothermal fins on the natural convection heat transfer and flow profile inside a vertical channel with isothermal parallel walls", Springer Nature Journal,2019.

[11] Xiufeng Yang and Song-Charng Kong, "Numerical study of natural convection states in a horizontal concentric cylindrical annulus using SPH method", the National Science Foundation (Grant No. CBET-133228),2014.

[12] A.K. da Silva, S. Lorente, and A. Bejan , " Optimal distribution of discrete heat sources on a wall with natural convection", International Journal of Heat and Mass Transfer,vol. 47,pp. 203–214, 2003.

[13] A. H. Al-Essa and F. M.S. Al-Hussien , " The effect of orientation of square perforations on the heat transfer enhancement from a fin subjected to natural convection", Heat and Mass Transfer, vol. 40,pp. 509–515, 2003.

[14] T. Dias Jr., and L. F. Milanez , " Natural Convection In High Aspect Ratio ThreeDimensional Enclosure With Uniform Hear Flux On The Heated Wall", Engenharia Térmica (Thermal Engineering), Vol. 3 · No. 2 ·, pp. 96-99, 2004 ·

[15] S. Saha, T.Sultana, G.Saha, and Md.Q.Islam, " Natural convection inside a vee corrugated enclosure:effect of inclination angle and discrete heat source ", Heat Transfer,vol.3, pp.85-99,2005.

[16] Md. Mamun Molla , Md. Anwar Hossain ,and Manosh C. Paul, "Natural convection flow from an isothermal horizontal circular cylinder in presence of heat generation",International Journal of Engineering Science, vol. 44,pp. 949–958, 2006.

[17] B. Pullepu , K. Ekambavanan1 ,and A. J. Chamkha, " Unsteady Laminar Free Convection from a Vertical Cone with Uniform Surface Heat Flux ", Nonlinear Analysis: Modelling and Control, Vol. 13, No. 1,pp. 47–60, 2008.

[18] Jamal A., El-Shaarawi M. A. I., and Mokheimer E. M. A, " Effect Of Eccentricity On Conjugate Natural Convection In Vertical Eccentric Annuli ", 6th International Conference on Heat Transfer, Fluid Mechanics and Thermodynamics, Pretoria, South Africa,pp.345-350,2008.

[19] A. DOGAN, S. BAYSAL and S. BASKAYA, " Numerical Analysis Of Natural Convection Heat Transfer From Partially Open Cavities Heated At One Wall", J. of Thermal Science and Technology, , vol.29, no.1, pp.79-90, 2009.

[20] Xu Xu , Zitao Yu , Yacai Hu , Liwu Fan ,and Kefa Cen, " A numerical study of laminar natural convective heat transfer around a horizontal cylinder inside a concentric air-filled triangular enclosure", International Journal of Heat and Mass Transfer, vol. 53,pp. 345–355, 2009.

[21] S. Sivasankaran , Younghae Do ,and M. Sankar, " Effect of Discrete Heating on Natural Convection in a Rectangular Porous Enclosure",Transp Porous Med,vol. 86,pp. 261–281, 2010.

[22] M. Sankar, Junpyo Park , and Younghae Do, "Natural Convection In A Vertical Annuli With Discrete Heat Sources", Numerical Heat Transfer, Part A, vol.59,pp.594–615, 2011.

[23] M. A. Shoushtari, H.H. Al-Kayiem, A. O. Chikere , and S. Irawan, "On the Natural Convection Heat Transfer in the Tubing-Casing Annulus of Oils Wells",ACSSSR,2011.

[24] A. Andreozzi , B. Buonomo ,and O. Manca, "Numerical investigation of transient natural convection in a vertical channel-chimney system symmetrically heated at uniform heat flux", International Journal of Heat and Mass Transfer,vol. 55,pp. 6077–6089, 2012.

[25] B.Kusammanavar, Dr. K.S.Shashishekar, Dr.K.N.Seetharamu, "Effects Of Heat Source Location On Natural Convection In A Square

Cavity",International Journal of Engineering Research & Technology, Vol. 1,2012.

[26] R. Roslan, H. Saleh, and I. Hashim, ," Natural Convection in a Differentially Heated Square Enclosure with a Solid Polygon", The Scientific World Journal, pp.11,2014.

[27] N.A. Ahamad, H. A. EL Arabawy, and S.I. Ahmed, "Visualization of Natural Convection in a Vertical Annular Cylinder with a Partially Heat Source and Viscous Dissipation", International Journal of Engineering Sciences & Research Technology,2014.

[28] M. N. Kumar, G. Pundarika, K. R. Narasimha, and K. N. Seetharamu, "Effect of Rotation on Natural Convection in Differentially Heated Rotating Enclosure by Numerical Simulation ",Journal of Applied Fluid Mechanics, Vol. 9, No. 3, pp. 1265-1272, 2015.

[29] A. Gupta, M.Nair, H. C. Thakur, and A. Verma, "Study Of Steady Natural Convection With Laminar Flow In The Enclosures Of Diferent Shapes ",17th ISME Conference, Delhi, New Delhi,2015.

[30] M. H. Seraji and H. Khaleghi, "A Numerical Study of the Effect of Aspect Ratio on Heat Transfer in an Annular Flow Through a 270-Degree Curved Pipe", Journal of Chemical and Petroleum engineering,vol.53,No.1, pp101-110.2019.

[31] A. Jamal and E. M. A. Mokheimer, " Conjugate Natural Convection: A Study of Optimum Fluid Flow and Heat Transfer in Eccentric Annular Channels",Hindawi Journal of Engineering,pp.17,2022.

[32] A. O. Elsayed , E. Z. Ibrahim, and S. A. Elsayed," Free convection from a constant heat flux elliptic tube", Energy Conversion and Management, vol. 44, pp.2445–2453,2003.

[33] M. Abd Alsada, " Heat Transfer By Free Convection Between Horizontal Concentric Pipes", M.Sc thesis, collage of Engineering, University of Babylon, 2006.

[34] N. Bianco , O. Manca ,and S. Nardini, ,"Experimental investigation on natural convection in a convergent channel with uniformly heated plates", International Journal of Heat and Mass Transfer,vol. 50,pp.2772-2786, 2007.

[35] Frank M. White, "Viscous Fluid Flow" book Published by McGraw-Hill ,USA ,Third Edition ,2006.

[36] Bruce R. Munson, "Fundamentals of fluid mechanics" book Published by John Wiley & Sons, Inc.,USA ,Sixth Edition,2009.

[37] Amal Abdul Razaq Abdul Hussein, "Effect of the Heat Source Length and Location on the Combined Convection in an Enclosure-Channel Assembly " , M.Sc Thesis, College of Engineering, University of Babylon,2022.

[38] M. Kaviany, "Principles of Convective Heat Transfer", Second Edition, Springer New York, 2001.

[39] Petrovic, Z., and Stupar ,S., "Computational Fluid Dynamic**,**" Book, Eng. Faculty, Belgrade university pres,Mechanical,1996.

[40] C.Multiphysics, "COMSOL Multiphysics 6.0 User's Guide," ed. Canonsburg, PA: COMSOL, Inc., 2020.

[41] W. P. Graebel, "Advanced fluid mechanics" book Published by Elsevier, USA, Third Edition ,2007.

[42] Bakker A., "Applied Computational Fluid Dynamics, Mesh Generation," Computational fluid dynamics lectures 2006, Available: www.bakker.org.

[43] T-O Hågbo, K. E. T Giljarhus, S. Qu, and B H Hjertagerinsulation, "The performance of structured and unstructured grids ",IOP Conf. Series: Materials Science and Engineering 700 012001,Norway, 2019.

[44] Catalog Ceramic Fiber Product specification ISO8541, CE,IEC25523,Specification "Ceramic Fiber Blanket"Model :BTM-4208SD,2012.

[45] UNI-T , UT366A Digital manometer User manual, 2020.

[46] Holman J. P, "Experimental Methods for Engineers" book Published by McGraw-Hill ,USA ,Eigth Edition,2001.

[47] Catalog specification ISO-9001,CE,IEC1010,Specification "12 channel Temp. Recorder,"Model :BTM-4208SD,2008.

[48] Noah M Salih, Sarah B Ezzat, Afnan A Hassan and Qusay K Jasim, " Natural Convection in a Square Cavity Filled with Saturated Porous Media and Partially Heated From Below ", IOP Conf. Series: Materials Science and Engineering vol. 1094 ,2021.

[49] Mebarek-Oudina, H. Laouira, A. Aissa, A. K. Hussein4, and M. El Ganaoui, "Convection Heat Transfer Analysis in a Channel with an Open Trapezoidal Cavity: Heat Source Locations effect", MATEC Web of Conferences 330, 01006 , 2020.

[50] Ruqayah Nassr jawed, " Experimental and Numerical Study of Natural Convection Inside Porous Cavity with Sinusoidal Walls Filled with Fluid " , M.Sc Thesis, College of Engineering, University of Babylon ,2023.

Appendixes A

Free Convection in Annular Flow with Discrete Heat Flux

Abrar Al-hadad[1,a)] and Hussain M. Jassim[2,b)]

[1,2]*University of Babylon-College of Engineering, Mechanical Engineering department*
Babylon-Iraq

Author's E-mails
[a)] *abraralhadad1@gmail*
[b)] *Hussien _m9@yahoo.com*

Abstract. This work uses numerical analysis to examine twodimensional laminar free convection heat transport.Utilizing the COMSOL.Multiphysics 6.0 programme, two concentric vertically constructed cylinders with discrete heat sources wer e examined.By mounting heaters on the wall and maintaining a consistent temperature on the opposite wall, a systematic flow of heat was applied to the left vertical continuous surface.The walls elsewhere were made adiabatic.With the excepti on of the density variation with temperature brought on by buoyancy forces, the parameters of the working fluid were tak en to be constant.The governing equations were solved in the dimensionless form using the finite volumes approach.The Prandtl number for air as the working fluid is 0.71.We looked into how the Rayleigh number affected the Nusselt numbr. Ra was estimated for ranges between 10^3 and 10^7.

INTRODUCTION

The topic of free convection heat transfer has become very substantial in variety of domains. In the last few decades it has received significant attention from researchers due to its influence in number of areas such as cooling electric equipment , nuclear plants , oil drilling equipment , electric cables and electronic devices[1]. Lots of studies considering natural convection in annular flow with heat flux have been performed using different numerical methods , however this work applies FEM which gives more accurate results than the other methods utilized in the previous studies. Moreover, COMSOL 6.0 software was utilized in this study which is considered as a modern version comparing to the other computational programs utilized in the mentioned previous studies. The objective of the present study is to enhance the free convective thermal transmission which will contribute to improve all the cooling systems that depends on free convection in lots of fields such as cooling electronic microchips. The choicest distributive cooling of laminar free convection from separate heaters was studied by (Silva, 2003)[2]. The main goal was to boost the overall degree of thermal conductivity among the solid surface as well as the fluid, alternatively to diminish the heated blot temperatures when the complete rate of the thermal creation including overall system volume are determined. The distances among the heaters were differential ,as well as they depended on the Rayleigh number.The ratio of the thermal source length was taken as H/L=1 and P r = 0.71.Results showed that the best distribution for the heaters leads to a utmost overall performance and a nominal overall thermal resistance between the solid wall and the fluid. Furthermore, the boosted overall conductance raised whenever

Certificate of Paper Acceptance

Dear Abrar Al-hadad and Hussain M. Jassim,

Thank you for your submission to the IRCEAS2023 conference. We are pleased to inform you that your paper entitled "**Free Convection in Annular Flow with Discrete Heat Flux"** has been **accepted as a full paper** for oral presentation at the upcoming International Research Conference on Engineering and Applied Sciences 2023 (IRCEAS2023), which will be held on 9th to 10th October 2023 at College of Engineering building, Al-Iraqia University, Saba'a Abkar Complex, Baghdad, Iraq. Knowing that all accepted papers will be published in **AIP conference proceedings (Scopus-Indexed)**.

Your paper was reviewed by our expert panel of reviewers and was found to be relevant to the conference theme and of high quality. We appreciate the effort and time you have put into your research.

Once again, congratulations for the acceptance, and we look forward to your participation in the conference.

Sincerely,

Prof. Dr. Muwafaq Shyaa Alwan

Chairman of the Conference

College of Engineering, Al-Iraqia University, saba'a Abkar Complex, Baghdad, Iraq
Website: www.irceas.com
Email: conf@irceas.com

IRCEAS

Certificate of Attendance

This is certify that

Abrar Abdulkareem Saeed Alhadad

for the attendance to

International Research Conference On Engineering And Applied Sciences 2023

Organized by College of Engineering, Al-Iraqia University, Baghdad, Iraq in Cooperation with Imam Ja'afar Al-Sadiq University Held on Oct. 16th -17th,2023 at Palestine Hotel, Baghdad - Iraq

Prof. Dr. Muwafaq Shyaa Alwan
Dean of College of Engineering

Numerical Study of Natural Convection in an Annulus

Abrar A. S.Alhadad[1] ,Hussien M.Jassim[2]

1,2University of Babylon-College of Engineering, Mechanical department
E-maile:abraralhadad1@gmail.com

Abstract: In this paper, 2-D laminar free convection thermal transmission has been investigated numerically . Double concentric rectangular enclosures with discrete heaters were studied using COMSOL Multiphysics 6.0 software package. Heat flux was applied using specific number of heaters as well as changing the number and distances of the heaters in each case. Heaters were installed on the left vertical wall of the enclosure the opposite wall was kept at constant temperature. The horizontal walls were considered adiabatic. Air was taken as working fluid and all the features of air were considered constant except the change in density due to buoyancy forces that are driving the fluid. Finite volumes method was chosen for solving the governing equations in the dimensionless formula. The effect of Rayleigh number on Nusselt number was analyzed using the resultant isothermal contours. We attained the results for different values of Rayleigh number. A large enhancement in thermal transmission was achieved in the attained results, it was found that the amount of thermal energy transmitted will increase by increasing the value of Ra.

Keywords: *free convection; heat source; COMSOL; Air.*

1.Introduction

The study of natural convective mode of heat transfer has drawn the attention of researchers during the last decades due to its significance in lots of engineering fields. Convection mode of thermal transmission in rectangular enclosures added to discrete heaters has enormous relevance due to its role in lots of engineering applications such as cooling microchips[1]. The process of thermal energy transmission majorly depends on free convection owing to its straightforwardness , small cost, minimal noise, compact volume, and trustworthiness . The literature review illustrates that the subject of free convective mode of thermal transmission in rectangular geometry has attracted large attention.

Elsayed et al.[2] investigated experimentally the free convection of air around an elliptic tube with fixed thermal flow. For various Rayleigh numbers and tube inclination angles, the local and average Nusselt number distribution was reported. According to the inward thermal flow, the test Rayleigh number varied from 1.1×10^7 to 8×10^7. For the elliptic tube with straight main axis, the total Nusselt number values were assessed as well as associated with Ra values. Constant heat flux elliptic tubes were compared to free convection around isothermal tubes, and it was discovered which at constant state, the constant thermal flow pipe corresponds well with $Ra^{0.25}$, much like the isothermal tube. Regional Nu allocations as well as the total Nu fluctuation against inclination angle have been used to illustrate how tube orientation affects natural convective

Nexo
Revista Científica

Nicaragua, September 15th, 2023

To whom it May concern:

Nexo Scientific Journal, ISSN 1818-6742 (printed version), ISSN 1995-9516 (electronic version), informs by means of the present that the paper: "**Numerical Study of Natural Convection in an Annulus**", written by Abrar A. S. Alhadad and Hussien M. Jassim, has been accepted for publication in Vol. 37, Number 05, December 2023.

Some formatting improvements must be applied to fit the style of the journal. Those comments will be sent directly to the authors.

Thank you very much for your preference of collaboration with our journal.

Sincerely,

Róger E. Sánchez Alonso, Ph.D
Editor
Nexo Revista Científica

Nexo
Revista Científica
Universidad Nacional de Ingeniería
Managua, Nicaragua

Universidad Nacional de Ingeniería, Managua, Nicaragua. Nexo Revista Científica, Tel: (+505) 22701507 ext 122. Email: roger.sanchez@di.uni.edu.ni

الخلاصة

تم اجراء دراسة نظرية و عملية لتحري عملية انتقال الحرارة بطريقة الحمل الحراري الحر خلال اسطوانتين عموديتين متحدتي المركز وكذلك تمت دراسة تأثير طول وموقع المصدر الحراري على عملية انتقال الحرارة. تم اختيار الهواء كمائع العمل. تم اعتبار الجريان ثنائي البعد ثابت مع الزمن و خطي. في النتائج النظرية تم حساب توزيع السرع لجريان المائع وكذلك حساب عدد نسلت الكلي والموضعي . تم ادخال المعادلات وتعويض جميع المتغيرات لحساب النتائج النظرية في برنامج كومسول و تم استخدام طريقة الحجم المحدود(كرانك نيكولسون) لحل المعادلات التفاضلية. القيم الماخوذة لعدد رايلي تتراوح من 10^3 الى 10^7 و نسبة الابعاد تساوي 25.6. تم بناء نموذج فيزيائي مماثل تجريبيا في مختبر الموائع في جامعة بابل. كلتا الاسطوانتين الداخلية والخارجية كانتا مصنوعتين من النحاس ذو موصلية حرارية تساوي 385واط/م^2*كلفن, حيث كان طول الاسطوانة الخارجية 105سم والقطر الخارجي 76ملم وسمكها 3.65 ملم بينما طول الاسطوانة الداخلية 160 سم وقطرها الخارجي 35 ملم وسمكها 2 ملم . تم تثبيت مصادر حرارية على الجدار الخارجي للاسطوانة الخارجية وتم تغيير عدد و موقع المصادر الحرارية لثلاث حالات مختلفة . في الحالة الاولى ثبتت خمس مصادر حرارية بأطوال مختلفة , في الحالة الثانية ثبتت اربع مصادر حرارية باطوال متساوية وفي الحالة الثالثة ثبتت ثلاث مصادر حرارية باطوال مختلفة وتم حساب الفيض الحراري الناتج من هذه المصادر الحرارية. من الجدير بالذكر انه تم استخدام مادة عازلة لتقليل الخسائر الحرارية الى الحد الادنى . تم انشاء لوحة تحكم وربطها بالمصادر الحرارية للتحكم بعملية التشغيل وكذلك لقياس فرق الجهد والتيار المسحوب بواسطة كل مصدر حراري . تم تثبيت مجموعة من متحسسات درجة الحرارة (ثرموكابل) عددها 20 متحسس خلال الحيز الحلقي لقياس تغير درجات الحرارة خلال زمن الاختبار. وكذلك تم استخدام جهاز رقمي لقياس الضغط خلال التجربة . النتائج النظرية عرضت على شكل خطوط الجريان وعدد نسلت الموضعي. اظهرت النتائج ان زيادة طول المصدر الحراري يؤدي الى زيادة عدد نسلت الموضعي ويحسن

من الجريان. بالاضافة الى ذلك زيادة عدد المصادر الحرارية يؤدي الى تحسين انتقال الحرارة الكلي وبالتالي اعلى معدل انتقال حرارة تم تحقيقه في الحالة الاولى والتي تتضمن اعلى عدد من المصادر الحرارية(5). واخيرا تمت مقارنة النتائج النظرية مع النتائج العملية لاختبار مدى التقارب . تم تحقيق تقارب ملحوظ حيث حققت الحالة الاولى 82% وحققت الحالة الثانية تقارب يصل ل 78% بينما حققت الحالة الثالثة تقارب يصل ل 76%.

وزارة التعليم العالي والبحث العلمي
جامعة بابل
كلية الهندسة
قسم الهندسة الميكانيكية

تأثير الفيض الحراري المنفصل و المتناوب على الحمل الحراري الحر في الجريان الحلقي

رسالة

مقدمة الى كلية الهندسة جامعة بابل كجزء من متطلبات نيل شهادة الماجستير في علوم الهندسة/ الهندسة الميكانيكية/ قدرة

اعدت من قبل

ابرار عبد الكريم سعيد الحداد
بكالوريوس في الهندسة الميكانيكية 2019

بإشراف

الأستاذ المساعد الدكتور حسين محمود جاسم

1445هـ - 2024 م